ANALYSIS OF UNSTEADY GAS FLOW IN A PLAIN PIPE EXHAUST SYSTEM OF A FIRING ENGINE AND ITS EFFECT UPON THE PERFORMANCE OF A NATURALLY ASPIRATED TWO-STROKE OIL ENGINE

By

E. H. WRIGHT, B.Sc., A.M.I.Mech.E.

Thesis submitted for an Official Degree.

Department of Mechanical Engineering,
University of Birmingham.

MAY, 1961.

SYNOPSIS

The present investigation is part of a long term research programme dealing with the wave action in the exhaust and induction pipes of a two-stroke oil engine and their effect upon the cylinder scavenge process.

As a development of fundamental researches carried out at the University Laboratories using simulated cylinder release pressures in a motored engine, the present investigation seeks to extend the established data to the practical problem of the engine under firing conditions.

In this report, the theoretical analysis of unsteady one-dimensional gas flow, allowing for the effects of wall friction, heat exchange with the surroundings, and temperature discontinuities is developed, and the Method of Characteristics is applied to effect a solution. Theoretical exhaust pipe and cylinder indicator diagrams are evaluated using this theory, and compared with the experimental diagrams from the firing engine.

From performance trials, the measured air consumption using a constant air/fuel ratio, but different exhaust pipe lengths and engine speeds, is evaluated and plotted on a dimensionless basis for comparison with the previous simulated work.

CONTENTS

Acknowledgements

The following investigations were carried out in the Department of Mechanical Engineering of the University of Birmingham.

The author is deeply indebted, initially to Professor G. F. Mucklow, D.Sc., M.I.Mech.E., and latterly to Professor S. A. Tobias, D.Sc., Ph.D., A.M.I.Mech.E., for their permission to use the facilities of the Department, and for their interest and encouragement.

Thanks are also due to the late Mr. L. Hone, the present Steward Mr. G. Wallace, and other members of the Departmental workshop and laboratory staff for their assistance in the construction and maintainance of the apparatus.

Original Work

As far as is known by the author, no published work is available in which wave action in the exhaust pipe system of a firing engine is analysed in terms of the Theory of Characteristics.

The application of this method to effect the solution of the problem has necessitated the new sections of theory and techniques dealt with in Sections 3.7(b), 3.7(c), 3.8(b), and 3.8(d).

1. Introduction

The potential advantage of the two-stroke cycle engine over the four-stroke cycle engine of equal swept volume is substantial. The output torque is more uniform and for the same speed of rotation, the power developed is theoretically doubled giving a much improved power-weight ratio. In addition, the number of moving parts is reduced, simplifying maintainance and giving improved reliability. In practice, however, considerable difficulty has been encountered in attempting to realise the potentially high specific output, due primarily to the problem of efficient scavenging.

Success of the two-stroke cycle engine depends upon the efficiency of the air exchange process in the cylinder, since both the power developed per unit of swept-volume and the fuel consumption are closely related to the efficiency of the scavenge process. In the high speed engine, the time available for scavenging the cylinder is very small. Hence, to achieve any measure of success, the scavenge air must be supplied under pressure, or an appreciable pressure difference must be maintained between the air duct and the cylinder. The method of achieving this is usually to use either crankcase compression or an external air blower or pump driven by the engine. Thus scavenging is achieved at the expense of the power developed, a reduction in the power-weight ratio, and increased fuel consumption and

capital cost.

One of the most significant contributions in the development of the two-stroke cycle engine was due to M. Kadenacy[1], who, in 1936, patented certain features of port timing and design. His specifications were concerned with the means of improving the air exchange process in the cylinder, and engines converted to his designs showed a considerable improvement in performance. Evidence in support of his theoretical concept of Ballistic Discharge, accompanied by supersonic gas velocities, was published by Davies[2] in 1940.

Davies's conclusions were contested by Mucklow, who held the opinion that the results were not due to high discharge velocities, but to pressure waves in the exhaust pipe. Extensive theoretical and practical research on the sudden release of compressed air from a cylinder into a pipe was published by Mucklow and Bannister[3] in 1948. This showed conclusively that the depression in the cylinder following release, the Kadenacy effect, was due solely to wave action in the pipe, and that the observed phenomena could be explained satisfactorily by the laws of thermodynamics and on the basis of a theory of waves of finite amplitude due to Earnshaw and Riemann.

The work of Mucklow and Bannister was extended by Wallace and Mitchell[4] who examined the discharge of compressed air from a ported cylinder liner into pipes

of variable length. The research yielded valuable information on the variation of the coefficient of discharge of the exhaust ports with port opening, cylinder pressure and over a limited temperature range. It also showed the influence of wave effects in the exhaust pipe on the duration and magnitude of the depression in the cylinder following release.

Further work was carried out by Wallace[5] using a motored opposed piston two-stroke cycle engine, in which cylinder release pressures, comparable with the firing engine, were simulated, and a full analysis made.

The present work is an extension of the research carried out by Wallace, using the same engine but under firing conditions and the Method of Characteristics is employed for the solution of the flow equations.

The Method of Characteristics is due to Prandtl and Busemann (1929) who used it in the solution of plane supersonic steady flow problems. The method was developed to include one dimensional non-steady flow by Sauer (1942) and Schultz-Grunon (1942) and a variant of this was developed by de Haller in 1945. It is on this latter method that the present work is based.

The work of Jenny[6], who used the Method of Characteristics to investigate wave action in a pipe following the discharge of compressed air from a cylinder, constituted a great help in the development of the theory upon which this thesis is based.

(a)

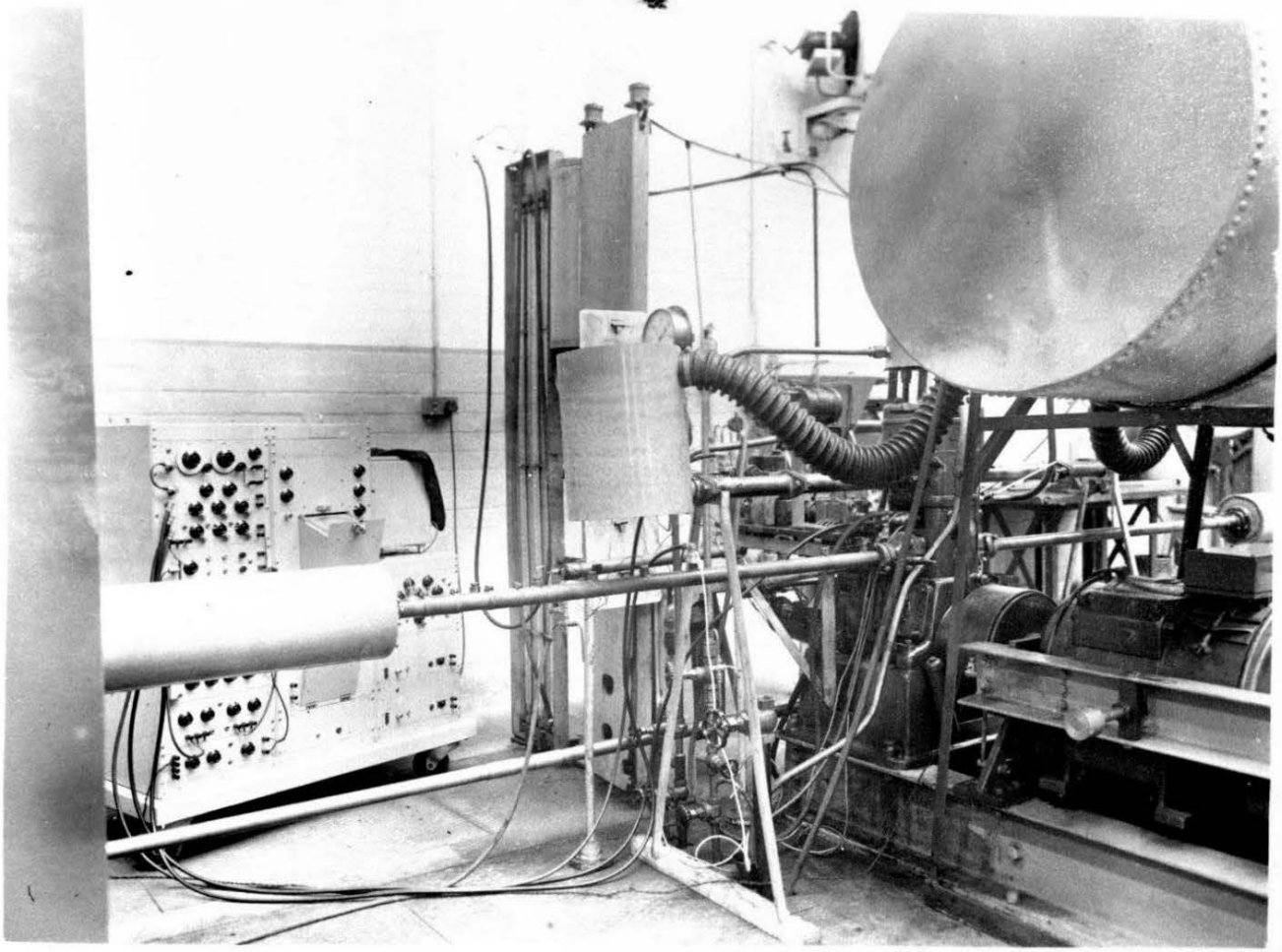

(b)

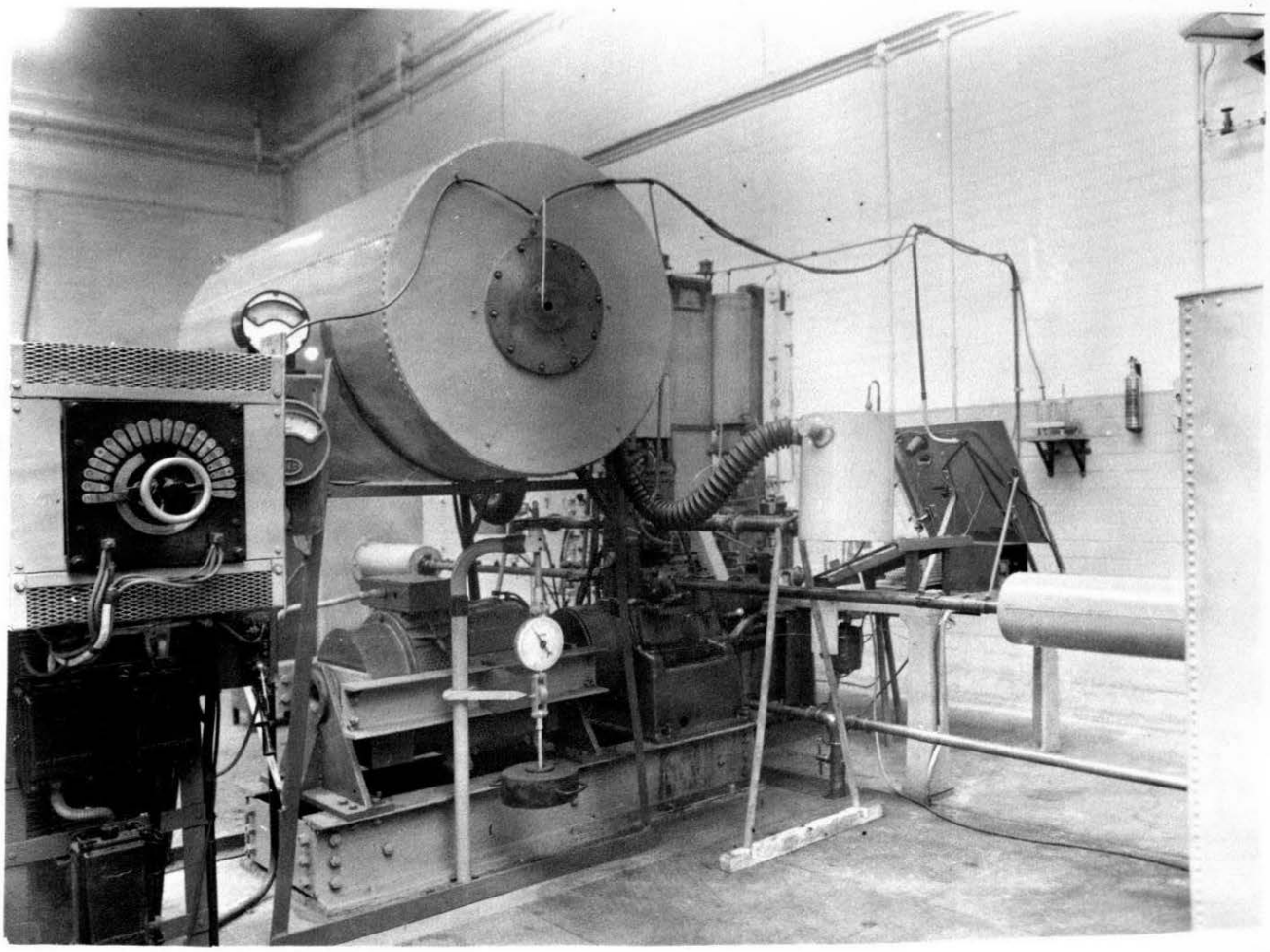

Plate 1.

2. Apparatus

2.1. General Layout.

Two views of the apparatus are shown in Plate 1 and the layout is shown diagrammatically in Fig.1. Plate 1, however, shows induction pipes fitted to the engine, but these are not used for the present investigation.

The vertical opposed piston two-stroke cycle engine is flexibly coupled to a swinging field electrical dynamometer, and the combined unit is rigidly mounted on a bed plate consisting of two longitudinal R.S.J. sections bolted to a concrete plinth set in the laboratory floor.

An auxiliary drive shaft, driven by the engine crankshaft, carries sprockets which provide chain drives for the fuel injection pump, the revolution counter, and a three phase A.C. tachometer.

The fuel injection pump is gravity fed from the fuel tank via a filter, and its rack is accurately positioned by means of a micrometer attachment. The fuel line is connected via cocks to two measuring pipettes of capacities 66 cc and 22 cc arranged in parallel for accurate monitoring of the fuel consumption.

The expansion chambers bolted to the induction pipes, are linked by large bore rubber hoses to the air measuring box, and the latter is mounted in a cradle straddling the dynamometer. To this air box is connected the laboratory compressed air supply which is used for starting the engine.

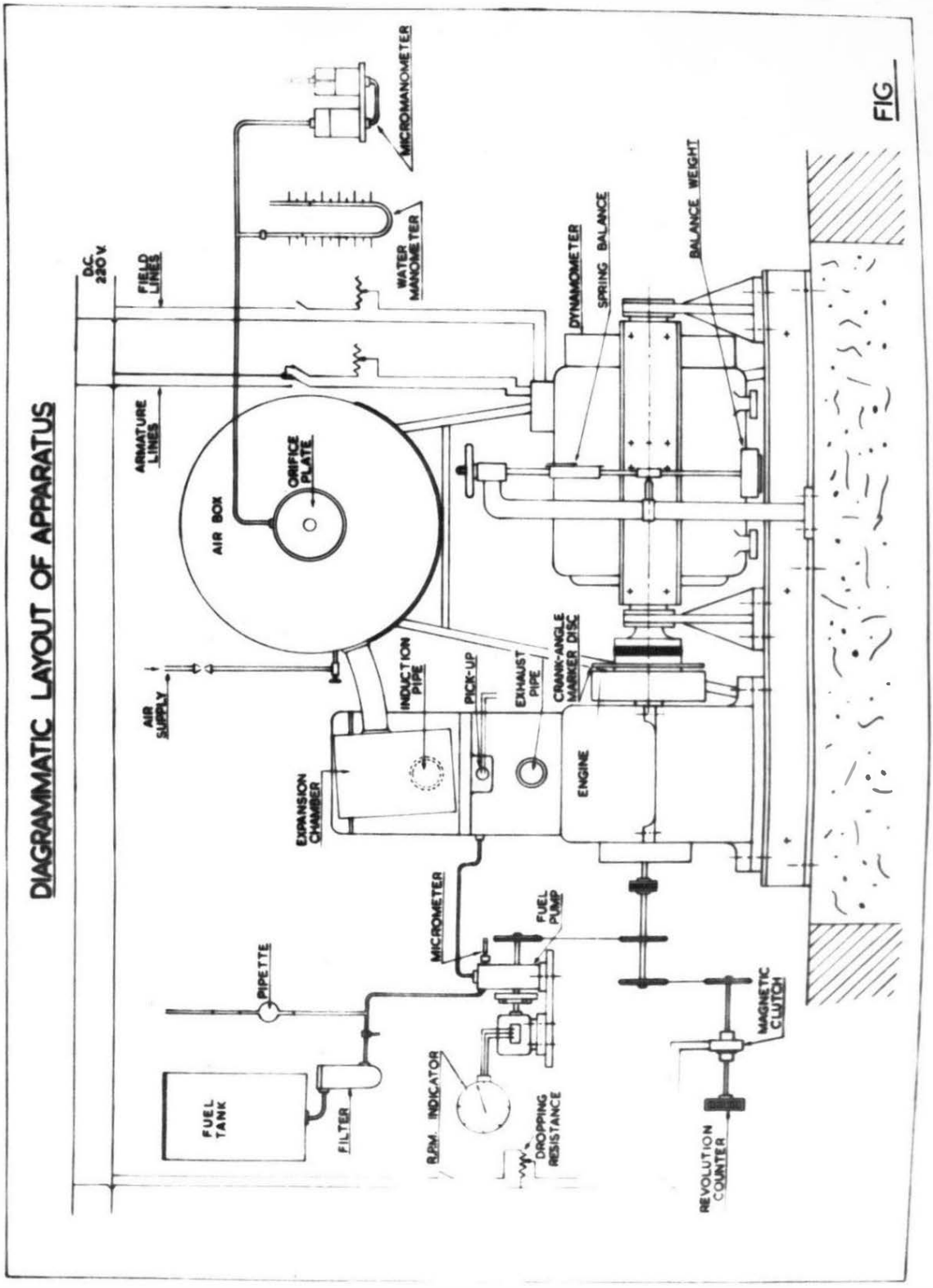
DIAGRAMMATIC LAYOUT OF APPARATUS
FIG
D.C. 220 V.
FIELD LINES
ARMATURE LINES
MICROMANOMETER
WATER MANOMETER
DYNAMOMETER
SPRING BALANCE
BALANCE WEIGHT
ORIFICE PLATE
AIR BOX
AIR SUPPLY
INDUCTION PIPE
PICK-UP
EXHAUST PIPE
CRANK-ANGLE MARKER DISC
EXPANSION CHAMBER
ENGINE
MICROMETER
FUEL PUMP
PIPETTE
FUEL TANK
FILTER
R.P.M. INDICATOR
DROPPING RESISTANCE
MAGNETIC CLUTCH
REVOLUTION COUNTER

Fig.1.

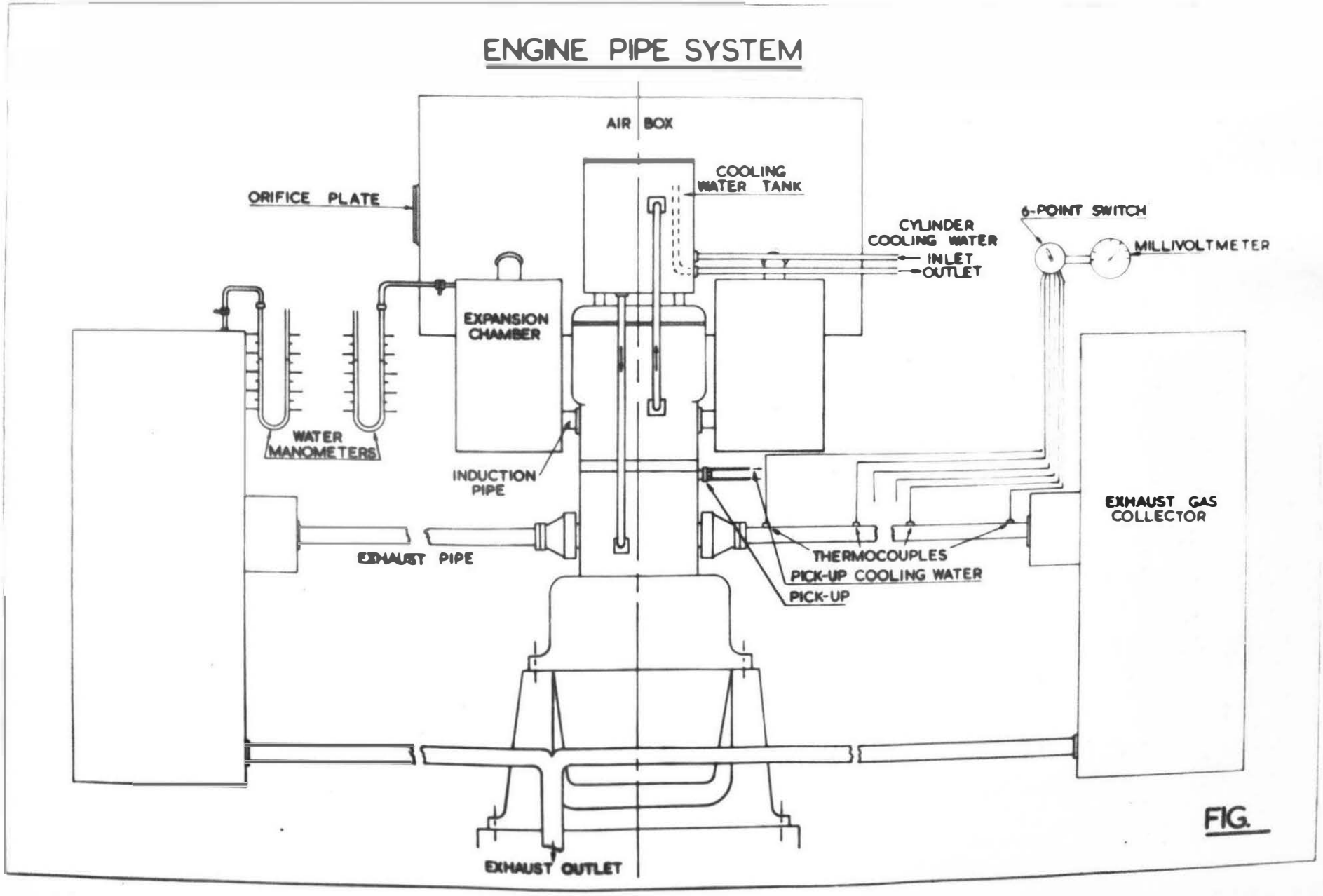
ENGINE PIPE SYSTEM
AIR BOX
COOLING WATER TANK
ORIFICE PLATE
6-POINT SWITCH
MILLIVOLTMETER
CYLINDER COOLING WATER
INLET
OUTLET
EXPANSION CHAMBER
WATER MANOMETERS
INDUCTION PIPE
EXHAUST GAS COLLECTOR
EXHAUST PIPE
THERMOCOUPLES
PICK-UP COOLING WATER
PICK-UP
EXHAUST OUTLET
FIG.

Fig. 2.

The exhaust pipes terminate in large expansion tanks which are mounted on castors to facilitate their movement, see Fig.2. These tanks also serve as exhaust gas collectors and are connected to the laboratory fan extraction system.

One air expansion chamber and one exhaust gas collector are connected to water manometers mounted on the control panel.

2.2. Engine and exhaust pipe system.

The opposed piston two-stroke cycle compression ignition engine is of Junkers design, and the cross-sectional arrangement is shown in Fig.3.

The engine has a bore of 65 mm., a combined stroke of 210 mm., and a trapped volume of 609.7 cc. The upper or air piston controls the air ports, and is carried on a 'crosshead'. Two connecting rods attached one on either side of this crosshead, are coupled to cranks on either side of the crank controlling the lower or exhaust piston.

The air piston has a stroke of 90 mm., the exhaust piston a stroke of 120 mm., and their respective cranks are asymmetrically opposed, the angle between them being 165 degrees. This arrangement gives an exhaust lead of 16 degrees, with an air port closure at 14 degrees after the exhaust ports. The pistons have detachable crowns and are fitted with 'fire-rings', the edges of which are flush with the flat piston tops.

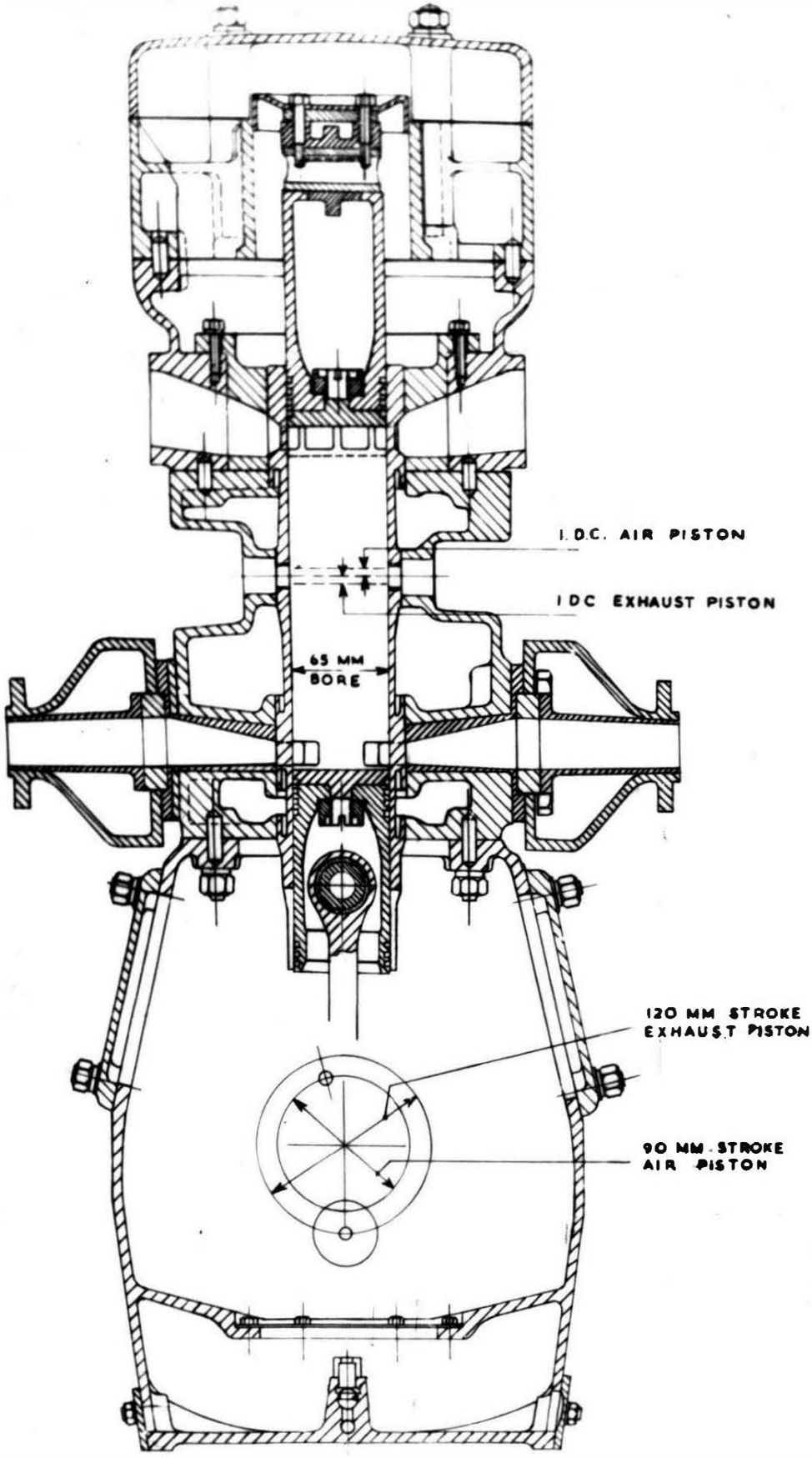

SECTIONAL ARRANGEMENT OF ENGINE

Fig. 3.

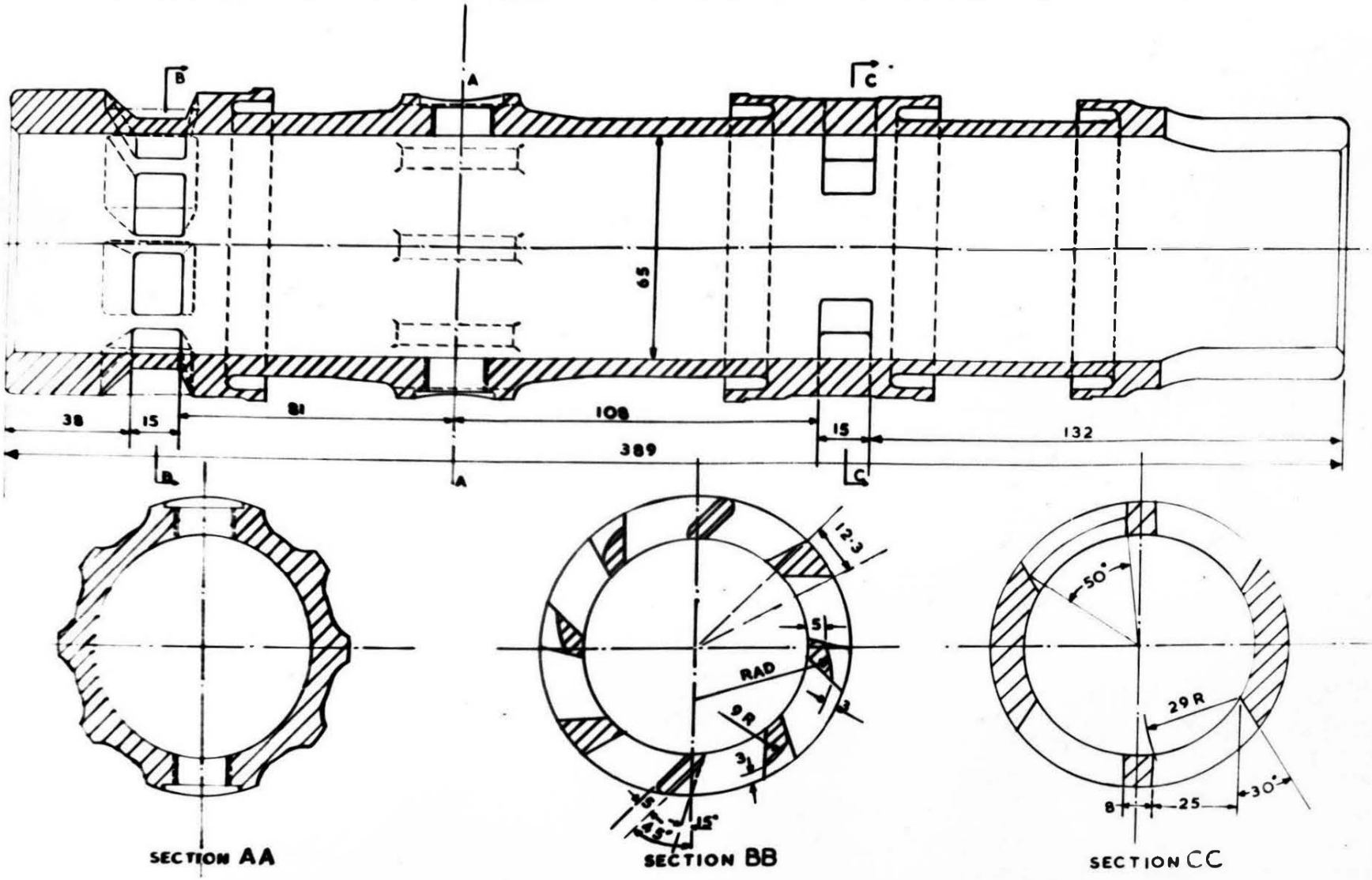

CYLINDER LINER

DIMENSIONS IN MM

MATERIAL : CLOSE GRAINED CAST IRON

Fig. 4.

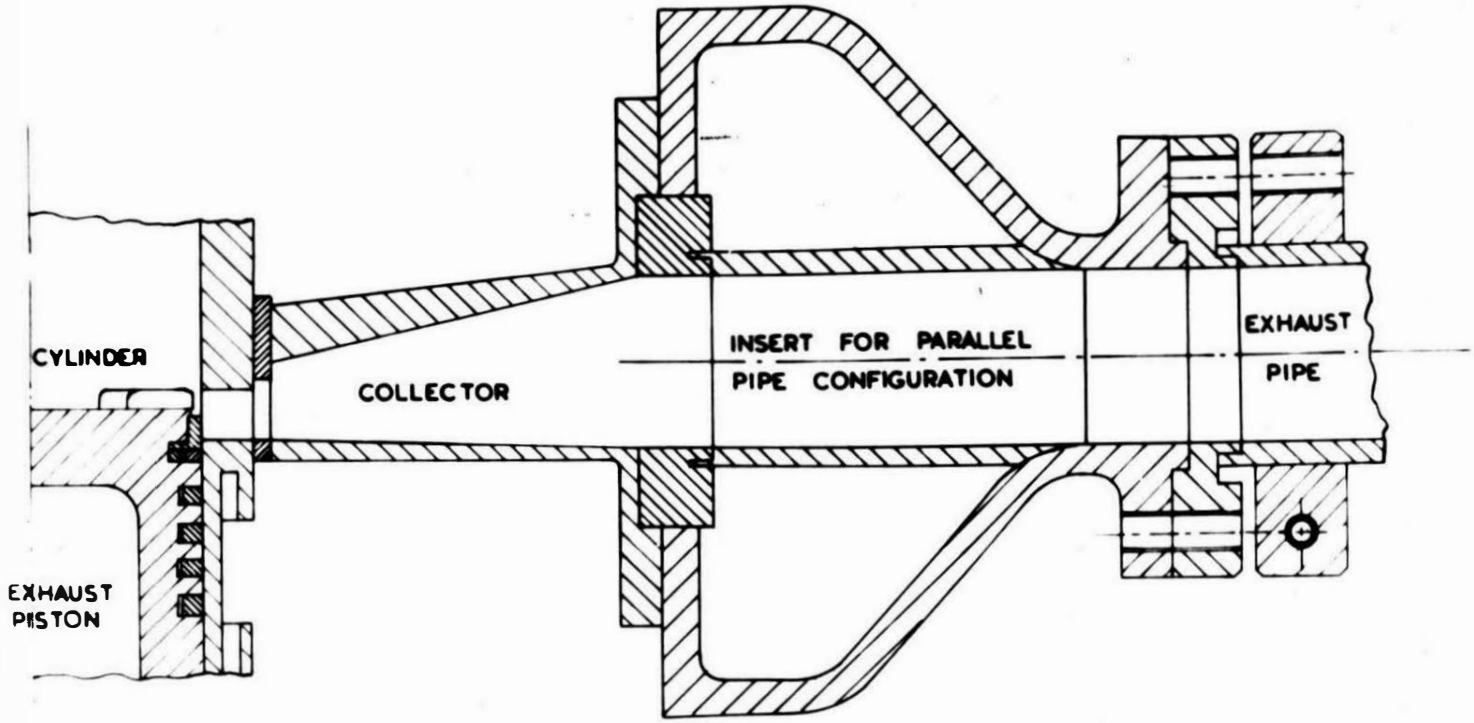

LAYOUT OF EXHAUST PASSAGE FIG. 5

Fig.5.

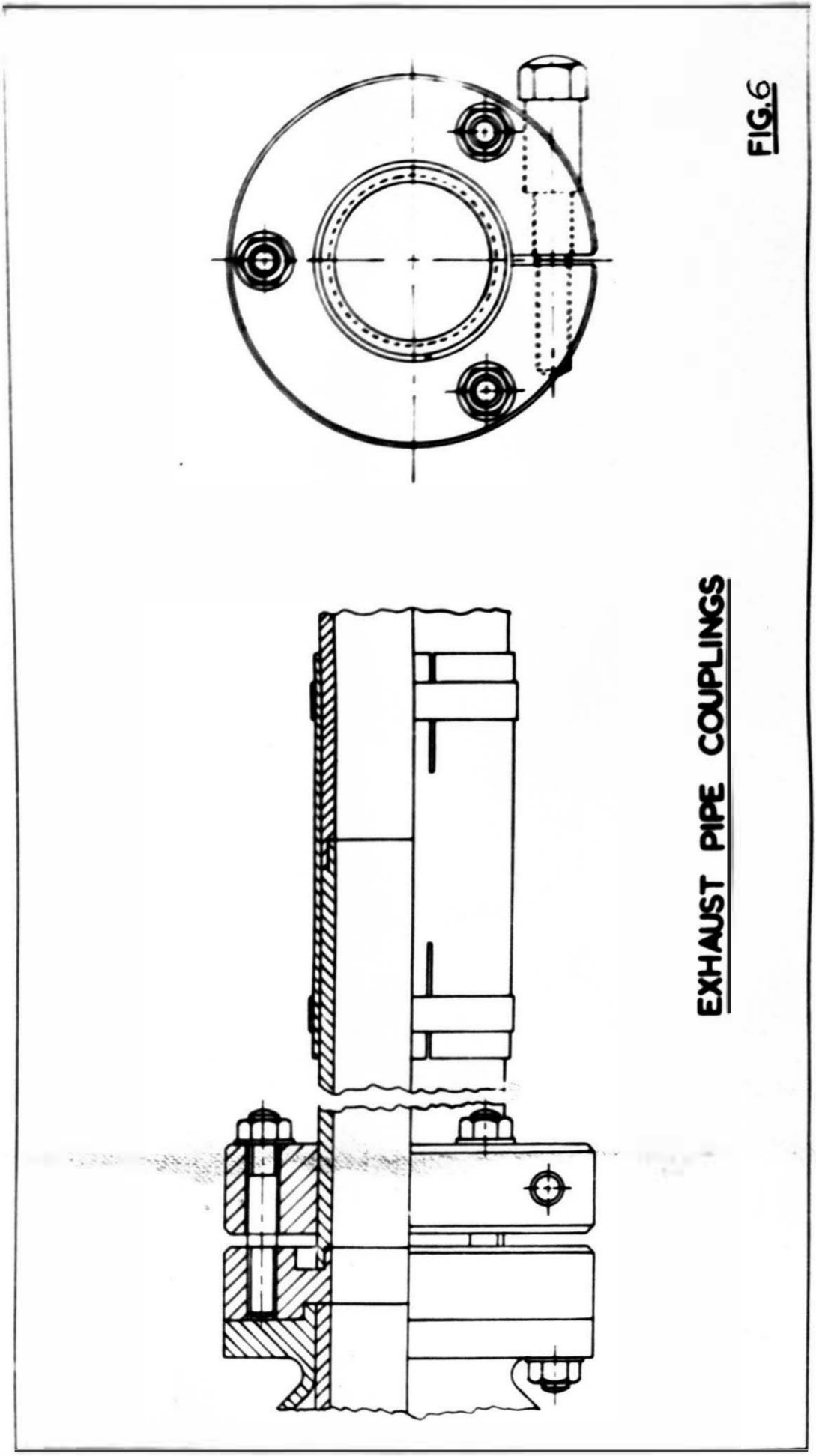

Fig.6.

The combustion chamber, formed by the cylinder and the piston crowns, normally has two fuel injector nozzles diametrically opposed, see Section AA, Fig.4. For the present research, however, only one injector is used and the other cylinder boss houses a pressure transducer.

Both the air and exhaust ports are arranged symmetrically around the periphery of the cylinder liner, see Sections BB and CC respectively, Fig.4. The air ports communicate with the air expansion boxes through two ducts, 180 degrees apart, each having a constant cross-sectional flow area equivalent to that of the 2" bore induction pipes. The total distance from the air ports to the air boxes is approximately 5".

The exhaust system is similarly disposed to the air system, and incorporates exhaust ejectors designed to the original Kadenacy specifications. These are, however, rendered inoperative by the insertion of short lengths of pipe, see Fig.5. The collector ducts between the exhaust ports and the $1\frac{3}{8}$" bore exhaust pipes each have a constant cross-sectional area equivalent to that of the pipe.

The exhaust pipes are built up in sections and can be varied in length from zero to 11 feet in 6 inch steps. The fixing arrangements for pipe to pipe connection and pipe to engine connection are shown in Fig.6.

2.3. Dynamometer.

The dynamometer, shown in Fig.7, is constructed from

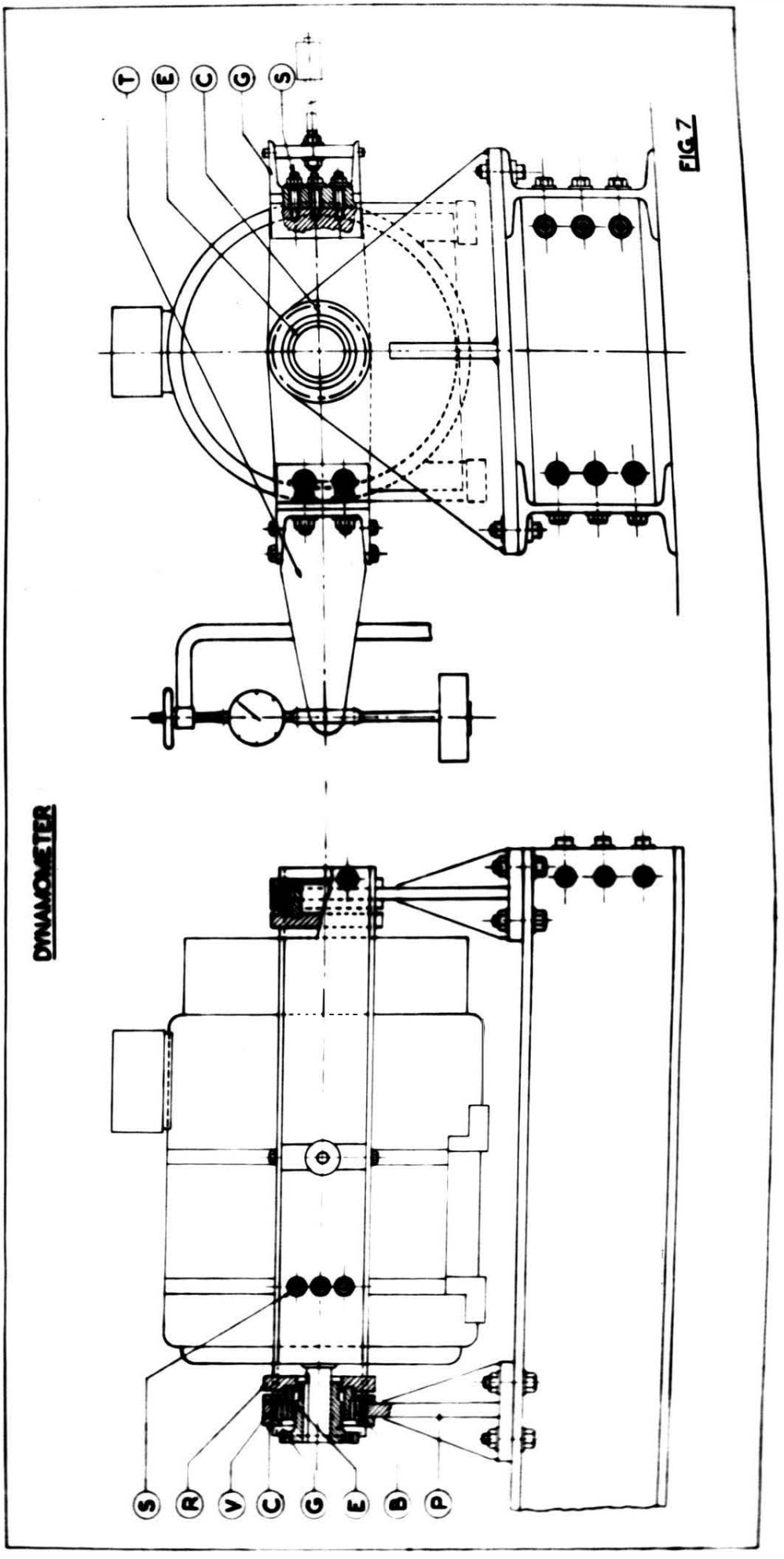

Fig.7.

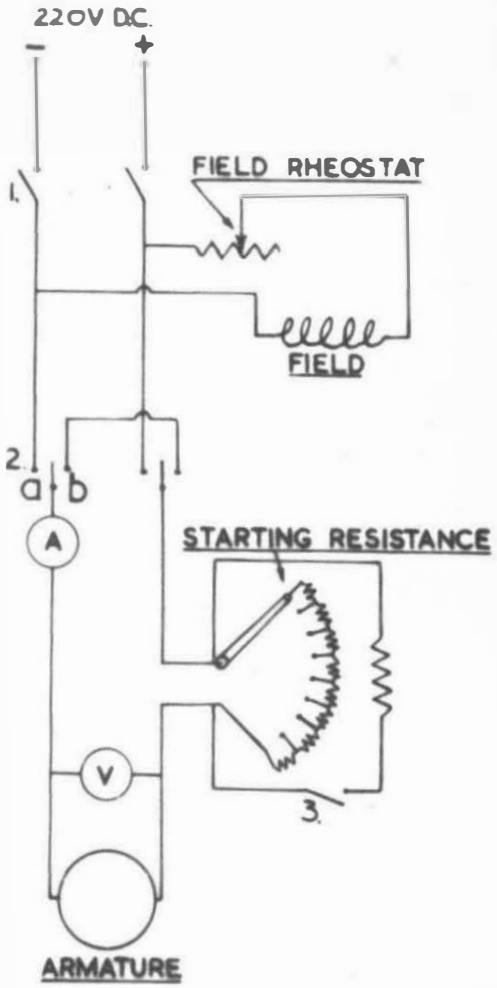

ELECTRICAL CIRCUIT

FIG. 8

Fig. 8.

a 220 volt. D.C. shunt wound motor and is arranged to swing freely in a cradle which is bolted to the motor frame. The cradle is supported at either end on trunnions which are mounted in needle roller bearings (B).

A torque arm, of effective length 2 feet, is produced by the bracket (T)bolted to one channel of the motor cradle. To the other end of this bracket is attached the balance weight, opposed by the spring balance. See also Plate 1(b). A balance weight is attached to the other channel of the motor cradle.

The armature and field circuit for the dynamometer is shown diagrammatically in Fig.8. When motoring or starting the engine, switch (2) is closed in position (a) and the engine is brought up to speed by means of the starting resistance. When the engine is firing, switch (2) is thrown to position (b). Speed control is then effected by using the starting resistance and the field reostat for coarse and fine adjustments respectively. The starting resistance is shunted by a 7 ohm. resistance which may be dispensed with by opening switch (3) for engine running under light load.

2.4. Air Circuit.

The air box used for air flow measurement consists of a fabricated steel drum 6 feet in length and 3 feet overall diameter. This is connected to the two expansion chambers, which are attached to the engine induction pipes

by two 3 inch bore flexible rubber hoses, see Figs. 1 and 2.

Air flow is measured by means of a range of sharp-edged orifice plates constructed in accordance with the B.S.S. recommendations on flow measurement. Each plate is used for a limited range of air flow such that the maximum pressure differential across the metering orifice does not exceed one inch head of alcohol.

The orifice, Fig.9, consists of a steel carrier plate (A) bolted to the air box (G) by set screws. The bronze orifice plate (B) is located in a recess in the carrier and the approach to the orifice is unobstructed. The patent rubber rings (C) and (D) ensure perfect sealing of the orifice plate and carrier respectively. The downstream pressure tapping (E) is drilled through the carrier plate and leads to the nipple (F).

The pressure differential across the metering orifice is measured by a micromanometer, Fig.1 and Plate 1 (b), connected to nipple (F) by a long length of thick walled rubber tubing. The latter provides heavy damping and ensures a steady flow reading. The water manometer connected in this circuit, Fig.1, is provided to give a reading of the pressure in the air box when supplying the compressed air for starting. During the starting period the rubber connecting tube to the micromanometer is clamped to prevent the alcohol from being blown out, and the orifice plate is sealed by a rubber plug.

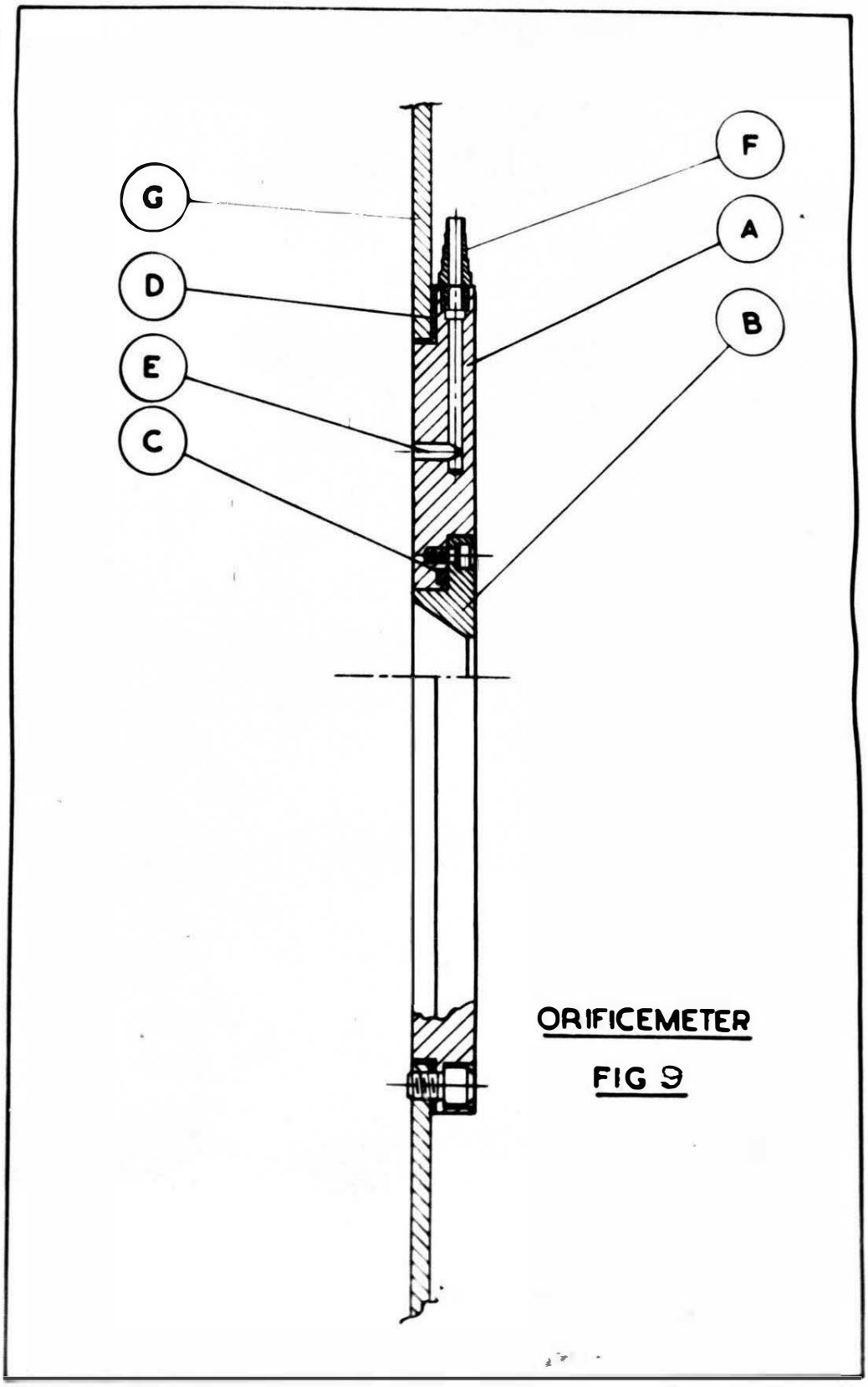

ORIFICEMETER

FIG 9

Fig. 9.

2.5. Instrumentation.

(a) Engine speed measurement.

Nominal engine speed is recorded by means of a three phase A.C. tachometer. Accurate measurement of the mean engine speed is obtained by a revolution counter and a stop watch.

The revolution counter is mounted coaxially with a magnetic clutch which is chain driven from the engine crankshaft, Fig.1. The spring loaded sleeve of this clutch carries three dowels, one of which engages with the crank on the counter. Engagement is achieved by energizing the coil surrounding the sleeve, and disengagement is effected by the spring behind the sleeve when the electric supply is switched off.

(b) Exhaust gas temperature measurement.

The exhaust gas temperature is measured by thermocouples mounted in thin walled, small diameter stainless steel tubes. The tubes have one end sealed and are flanged so that they locate in the pick-up bosses which are provided at 6 inch intervals along the exhaust pipe.

The six iron-constantan thermocouples are connected via a six way selector switch to a previously calibrated millivoltmeter, Fig.2.

(c) Cylinder and exhaust pipe pressure measurement.

Pressure variations in the engine cylinder and

exhaust pipe are recorded by means of a Southern Instruments Type Me 112 Engine Indicator, Plate 1(a). This is a switched three channel cathode ray oscillograph recorder incorporating a two beam cathode ray tube. The tube is viewed through a lens system by a rotating drum camera which has built in beam suppression contacts. The camera drum is driven by a D.C. electric motor, the speed of which is controlled by the battery voltage applied.

Southern Instruments Type G 204 water cooled pressure transducers with a range of 0 to 15 p.s.i. are used for measurement of the pressure in the exhaust pipe. A similar G 204 transducer with a range of 0 to 75 p.s.i. is used to obtain the continuous light spring cylinder pressure record. The cylinder pressure at exhaust port opening is accurately determined by using a Standard Sunbury Electronic Engine Indicator in conjunction with a balanced disc cylinder pressure calibrating unit.

A 'marker disc' bolted to the engine flywheel, Fig.1, provides signal pulses at 20 degrees interval of crank angle for superimposition on the Me 112 Indicator pressure records. A Sunbury Time Base Unit, driven from the auxiliary drive shaft of the engine, provides correlation between pressure and crank angle when using the Sunbury Indicator. This unit gives a signal pulse every 2 degrees with identification pulses every 10 and 90 degrees of crank angle.

A small two-way cock, interposed between the G2O4 transducers and the measuring point, enables the pressure records to be calibrated by applying known values of air pressure directly onto the transducer diaphragm.

The calibrating compressed air supply, which is also used with the Sunbury balanced disc pick-up, is controlled by an air potentiometer circuit, Fig.10. This consists of a small presssure vessel equipped with high and low pressure gauges for cylinder and pipe calibrations respectively, and it is connected to the two-way cock. The pressure within the vessel is read on the appropriate gauge and regulated by the combined use of the air supply valve and the blow-off valve.

Sub-atmospheric pressures are obtained by extracting air from the vessel by means of the water ejector, the vacuum obtained being regulated by controlling the rate of water flow and using the blow-off valve as an air bleed.

A system of valves is used to isolate the various sections and pressure gauges when they are not in use.

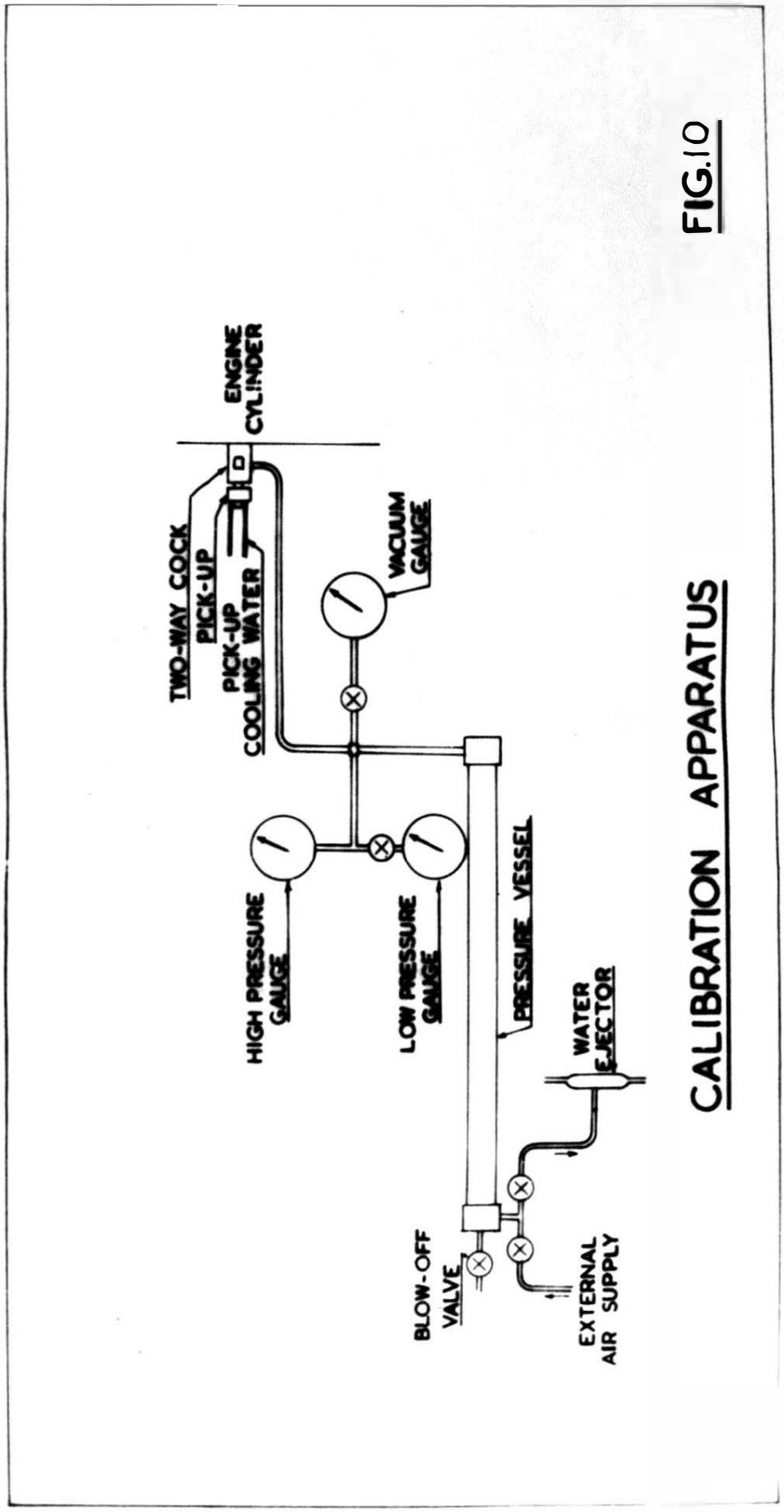
ENGINE CYLINDER
TWO-WAY COCK
PICK-UP
PICK-UP COOLING WATER
VACUUM GAUGE
HIGH PRESSURE GAUGE
LOW PRESSURE GAUGE
PRESSURE VESSEL
WATER EJECTOR
BLOW-OFF VALVE
EXTERNAL AIR SUPPLY
CALIBRATION APPARATUS
FIG.10

Fig. 10.

3. Theory

3.1. NOMENCLATURE

A - cross-sectional area (ft^2)

a - acoustic velocity (ft/sec.)

C_d - coefficient of discharge.

C_p - specific heat at constant pressure (ft.pdls/lb.°C)

C_v - specific heat at constant volume (ft.pdls/lb.°C)

d - pipe diameter (ft.)

F - wall friction term (pdls/lb.)

f - coefficient of friction.

H - enthalpy. (ft.pdls/lb.)

k - effective area ratio, defined as

$$\frac{\text{geometrical port area}}{\text{total pipe area}} \times C_d$$

K - degrees centigrade absolute.

L - total exhaust pipe length (ft.)

m - mass (lb.)

M - dimensionless mass flow.

n - engine speed (r.p.m.)

P - pressure ($pdls/ft^2$)

q - rate of heat transfer ($ft.pdls/ft^3 sec.$)

R - gas constant.

R_e - Reynolds number.

R_m - modified Reynolds number.

r - hydraulic radius.

S - entropy

T - absolute temperature (°C)

t - time (secs.)

U - internal energy (ft.pdls/lb.)

$\bar{U}$ - dimensionless particle velocity.

u - particle velocity (ft./sec.)

V - volume (ft^3)

W - work (ft.pdls)

$\bar{X}$ - dimensionless pressure ratio.

x - distance along pipe (ft.)

γ - ratio of specific heats ($\frac{C_p}{C_v}$)

Δ - finite change.

θ - temperature difference (°C)

I - characteristic co-ordinate, rightward wave.

μ - absolute viscosity (centipoises)

II - characteristic co-ordinate, leftward wave.

ρ - density ($lb./ft^3$)

ϕ - velocity potential.

Suffixes.

o - datum state parameters

1 - cylinder state parameters

2 - pipe state parameters

os - state parameters referred isentropically to datum isobar.

c - state parameters at cylinder port vena contracta.

a - state parameters of air in the cylinder.

e - state parameters of exhaust gas in the cylinder.

3.2 Scope of Theoretical Treatment

Discharge of exhaust products from the cylinder of a two-stroke cycle engine results in the propagation of a steep fronted compression wave to the open end of the exhaust pipe. Here it is reflected as a rarefaction wave which travels back to the exhaust port where it is partially reflected and partially transmitted. The latter produces a depression in the engine cylinder which draws in the fresh charge for the next cycle.

Wall friction, due to the presence of carbon deposits in the exhaust system, and heat loss to the surroundings through the pipe walls make the flow process irreversible, and their effect is sufficient to warrant consideration. Further, temperature discontinuities exist in the flow since there is a considerable difference in temperature between the exhaust gases just leaving the cylinder and those discharged by the previous cycle. Hence the flow problem to be solved is one of unsteady motion in a pipe with wall friction, heat transfer and temperature discontinuities taken into account.

The flow is assumed to be one-dimensional since, due to its nature, a developed velocity profile will not exist; and although the affect of wall friction and heat transfer are not strictly one-dimensional, to simplify the analysis a one-dimensional model using the appropriate

mean quantities is employed.

The equations defining the flow are derived from consideration of mass continuity, momentum and energy, (Section 3.3), and the three resulting simultaneous equations are solved by a finite difference calculation procedure developed from the Method of Characteristics (Section 3.6). Wall friction and heat transfer results in an entropy gradient in the pipe and allowance for this is made by applying a correction to the local acoustic velocity referred isentropically to the ambient pressure (Section 3.4). This permits evaluation of the changes in fluid properties from one region of state to the next by following two reversible paths connecting the end states. Thus characteristic nets can be constructed which give the solution at any point and time in the exhaust pipe for all the fluid properties. The true curvilinear characteristic net is, however, replaced by a net of straight line chords which are closely spaced so that linear interpolation is permissible.

Passage of a wave point through a temperature discontinuity can be taken into account analytically providing the position of the discontinuity in the pipe at any instant is known. The method of solution is discussed for various conditions of flow in Section 3.7. For simplicity, it is assumed that the temperature discontinuity is a plane at right angles to the flow and that no diffusion or heat conduction occurs across the interface.

The flow conditions at entry to and exit from the exhaust pipe are determined by the boundary conditions which define the flow behaviour for the varying physical configurations (Section 3.8). Theoretical relationships are derived in a framework of dimensionless co-ordinates of pressure and particle velocity from which boundary curves are drawn. Isentropic conditions are assumed for the cylinder contents and the boundary curves are used for relating cylinder to pipe conditions. At the open end of the exhaust pipe it is assumed that, for outflow, equalisation with ambient pressure occurs in the plane of the open end, and for inflow, the end of the pipe behaves as a Borda mouthpiece.

The theoretical section is concluded by a summary of all the theoretical expressions necessary for the solution of one-dimensional unsteady flow in a plain exhaust pipe (Section 3.9).

The Appendices (Section 9), contain the mathematical theory for the solution of two and three partial differential equations from which the characteristic equations are derived, and the application of the Method of Characteristics to the simpler case of isentropic flow.

3.3 Unsteady one-dimensional flow equations in a constant cross-sectional area duct.

Consideration of the three basic equations of fluid flow viz. continuity of mass, momentum and energy, gives analytical expressions which define the variation in the state parameters for a fluid flowing in a duct.

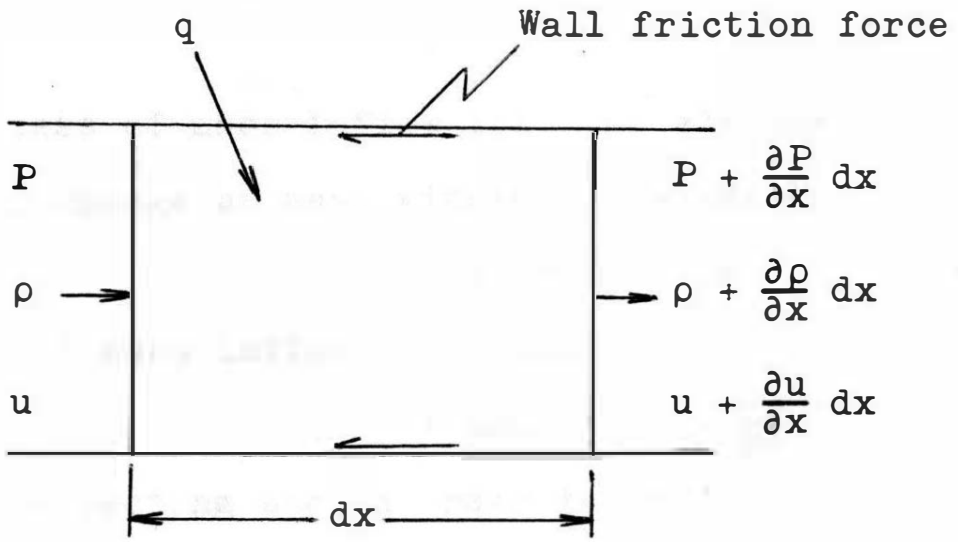

Fig. 11

Consider the instantaneous flow of gas in an element of pipe, length dx, of constant cross-sectional area A. Assume that the pressure, density and particle velocity change from P, ρ and u to $P + \frac{\partial P}{\partial x} dx$, $\rho + \frac{\partial \rho}{\partial x} dx$ and $u + \frac{\partial u}{\partial x} dx$, respectively, see Fig. 11 .

Since the flow to be examined is of an unsteady nature, a plane velocity profile can be assumed to exist across the pipe at any section, hence viscous shearing forces within the fluid can be neglected.

At any arbitrary instant of time, t, the fundamental equations of flow are derived as follows:

(a) Mass Continuity

The rate of change of mass within the element

=

the excess of mass inflow into the element.

Rate of change of mass within the element

$$= A\,dx\,\frac{\partial \rho}{\partial t}\,.\,dt$$

Excess of mass inflow into element

$$= A\rho u - A\left(\rho + \frac{\partial \rho}{\partial x}\,dx\right)\left(u + \frac{\partial u}{\partial x}\,dx\right)$$

which neglecting second order terms

$$= -\rho A \frac{\partial u}{\partial x}\,dx - u\,A\,\frac{\partial \rho}{\partial x}\,dx$$

Equating these two results gives:

$$\rho \frac{\partial u}{\partial x} + u \frac{\partial \rho}{\partial x} + \frac{\partial \rho}{\partial t} = 0 \qquad (3.3\text{-}1)$$

(b) Continuity of Momentum

The net force acting on the element

=

the mass acceleration of the fluid within the element.

The net force acting on the element

$$= PA - A\left(P + \frac{\partial P.dx}{\partial x}\right) - \Delta P.A$$

where ΔP = the pressure drop due to wall friction.

Assuming that the pressure drop due to wall friction is given by the equation for steady flow and can be applied instantaneously to the case of unsteady flow without undue error,

$$\text{then } \frac{dP}{dx} = \frac{f}{2d} \frac{u}{|u|} u^2 \rho$$

$$= F \rho$$

where F = the frictional resistance.

The factor $\frac{u}{|u|}$ is introduced to ensure that the frictional force always acts in a direction opposite to that of particle motion.

Then the net force on the element

$$= PA - A \left(P + \frac{\partial P}{\partial x} dx\right) - AF\rho dx$$

Inertia force on the element

$$= \rho A dx \frac{Du}{Dt}$$

where the symbol $\frac{D}{Dt}$ = the substantial derivative with respect to time and denotes that the differentiation is to be carried out while following a particular fluid particle.

Euler's equation of motion gives:

$$\frac{Du}{Dt} = \frac{\partial u}{\partial t} + u \frac{\partial u}{\partial x}$$

Hence, the inertia force on the element

$$= \rho A dx \left(\frac{\partial u}{\partial t} + u \frac{\partial u}{\partial x}\right)$$

Equating the net force and the inertia force, and simplifying, yields

$$\frac{\partial u}{\partial t} + u \frac{\partial u}{\partial x} + \frac{1}{\rho} \frac{\partial P}{\partial x} + F = 0 \qquad (3.3\text{-}2)$$

(c) Continuity of Energy

No external mechanical work is done by the elemental system in the surroundings and there is no change of potential energy of the system, thus the energy balance between the system and the surroundings becomes:

Rate of heat transfer into the system

=

rate of change of internal energy of the system

+

rate of net flow work done by the system

+

rate of change of kinetic energy within the system.

Rate of heat transfer into the system

$$= q.A.dx$$

Rate of change of internal energy of the system

$$= \rho A \, dx \frac{dU}{dt}$$

Rate of net flow work done by the system

$$= (P + \frac{\partial P}{\partial x} dx)A(u + \frac{\partial u}{\partial x} dx) - PAu$$

which neglecting second order terms

$$= A \, dx \, (P \frac{\partial u}{\partial x} + u \frac{\partial P}{\partial x})$$

Rate of change of kinetic energy within the system

$$= \rho A\, dx \frac{d}{dt}\left(\frac{u^2}{2}\right)$$

$$= \rho A u\, dx \frac{du}{dt}$$

The energy balance can therefore be written as:

$$q A\, dx = \rho A\, dx \frac{dU}{dt} + A\, dx \left(P \frac{\partial u}{\partial x} + u \frac{\partial P}{\partial x}\right) + \rho A u\, dx \frac{du}{dt}$$

Substituting $\frac{du}{dt} = \frac{\partial u}{\partial t} + u \frac{\partial u}{\partial x}$, dividing throughout by A dx and rearranging gives:

$$\rho \frac{dU}{dt} + P \frac{\partial u}{\partial x} + \rho u \left(\frac{\partial u}{\partial t} + u \frac{\partial u}{\partial x} + \frac{1}{\rho} \frac{\partial P}{\partial x}\right) - q = 0 \qquad (3.3\text{-}3)$$

Substitution of the momentum equation (3.3-2) and the continuity equation (3.3-1) in equation (3.3-3) gives:

$$\rho \frac{dU}{dt} - \frac{P}{\rho}\left(u \frac{\partial \rho}{\partial x} + \frac{\partial \rho}{\partial t}\right) - \rho u F - q = 0 \qquad (3.3\text{-}4)$$

$$\text{Now } \rho \frac{dU}{dt} = \rho \frac{d}{dt}\left(C_v T\right)$$

$$= \frac{\rho}{\gamma - 1} \frac{d}{dt}\left(\frac{P}{\rho}\right)$$

$$= \frac{1}{\rho(\gamma - 1)}\left(\rho \frac{dP}{dt} - P \frac{d\rho}{dt}\right)$$

$$\text{Also } \frac{dP}{dt} = \frac{\partial P}{\partial t} + u \frac{\partial P}{\partial x}$$

$$\text{and } \frac{d\rho}{dt} = \frac{\partial \rho}{\partial t} + u \frac{\partial \rho}{\partial t}$$

$$\text{hence } \rho \frac{dU}{dt} = \frac{1}{\gamma - 1}\left[\frac{\partial P}{\partial t} + u \frac{\partial P}{\partial x} - \frac{P}{\rho}\left(\frac{\partial \rho}{\partial t} + u \frac{\partial \rho}{\partial x}\right)\right]$$

which on substitution in equation (3.3-4) and simplifying gives:

$$\frac{\partial P}{\partial t} + u \frac{\partial P}{\partial x} - \frac{\gamma P}{\rho} \left(\frac{\partial \rho}{\partial t} + u \frac{\partial \rho}{\partial x}\right) - (\gamma-1)(\rho u F + q) = 0$$

Writing $a^2 = \frac{\gamma P}{\rho}$ gives:

$$\frac{\partial P}{\partial t} + u \frac{\partial P}{\partial x} - a^2 \left(\frac{\partial \rho}{\partial t} + u \frac{\partial \rho}{\partial x}\right) - (\gamma-1)(\rho u F + q) = 0 \qquad (3.3\text{-}5)$$

Isentropic Flow

For isentropic flow, both F and q are equal to zero. Further, the energy equation (3.3-5) becomes redundant and is replaced by the isentropic state relationship:

$$\frac{P}{\rho^{\gamma}} = \text{constant}$$

$$\text{i.e. } \frac{\partial P}{\partial x} \propto \gamma \rho^{\gamma-1} \frac{\partial \rho}{\partial x} = \frac{\gamma P}{\rho} \frac{\partial \rho}{\partial x}$$

$$= a^2 \frac{\partial \rho}{\partial x} \qquad (3.3\text{-}6)$$

The momentum equation (3.3-2) becomes:

$$\frac{\partial u}{\partial t} + u \frac{\partial u}{\partial x} + \frac{1}{\rho} \frac{\partial P}{\partial x} = 0$$

Substituting equation (3.3-6) then gives:

$$\rho \frac{\partial u}{\partial t} + \rho u \frac{\partial u}{\partial x} + a^2 \frac{\partial \rho}{\partial x} = 0 \qquad (3.3\text{-}7)$$

(3.3-7) and the mass continuity equation (3.3-1) completely define the flow under isentropic conditions.

3.4 Characteristic Quantity for the Entropy of a Gas Layer.

As a result of wall friction and heat transfer to the surroundings, the flow process in the pipe is irreversible. Thus changes of state from instant to instant in the pipe can only be determined by following two reversible paths connecting the end states of the fluid particle under consideration. The most convenient reversible paths to use are those of constant pressure and constant entropy, see Fig.12 .

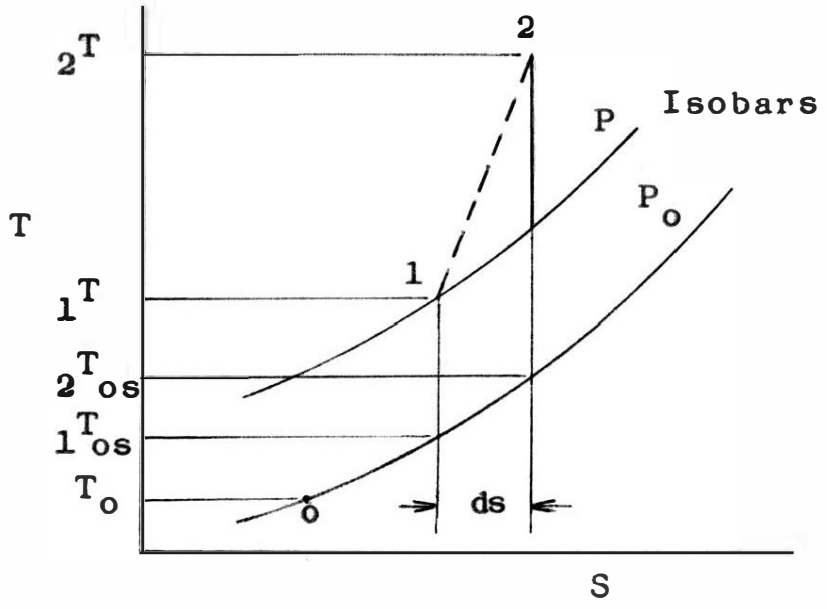

Fig. 12

In the application of the Method of Characteristics to the theory (see Section 3.5), it is desirable to relate all state points isentropically to the reference datum pressure P_o, and to a_{os} and T_{os} appropriate to the state under consideration, see Fig. 12 .

Thus the change of entropy ds in the process from state 1 to state 2 can be accounted for by determining the change in a_{os} from ${}_1a_{os}$ to ${}_2a_{os}$.

For a reversible process:

$$ds = \frac{dQ}{T}$$

therefore, for a finite change along the isobar P_o

$$\delta s = \frac{\delta Q}{T}$$

$$= C_p \frac{\delta T_{os}}{T_{os}}$$

and as δT_{os} approaches zero,

$$\text{then } ds = C_p \, d(\log_e T_{os}) \qquad (3.4\text{-}1)$$

$$\text{Now } a_{os}^2 = \gamma R T_{os}$$

$$\text{i.e. } d(\log_e T_{os}) = 2 \, d(\log_e a_{os})$$

which substituted in equation (3.4-1) gives:

$$ds = 2 C_p \, d(\log_e a_{os}) \qquad (3.4\text{-}2)$$

For any reversible process:

$$ds = \frac{dQ}{T}$$

$$= C_v \frac{dT}{T} + \frac{P}{T} dV$$

$$= C_v \frac{dT}{T} + R \frac{dV}{V} \qquad (3.4\text{-}3)$$

For a quasi-perfect gas, i.e. one that obeys the characteristic equation for a perfect gas but has specific heats which are a function of temperature,

$$PV = RT$$

Taking logs and differentiating:

$$\frac{dP}{P} + \frac{dV}{V} = \frac{dT}{T}$$

$$\text{Also } R = C_p - C_v$$

Substitution of these two equations in (3.4-3) then gives

$$ds = C_v \frac{dP}{P} + C_p \frac{dV}{V}$$

$$= C_v \frac{dP}{P} - C_p \frac{d\rho}{\rho}$$

which can be written as:

$$\frac{P}{C_v} \frac{ds}{dt} = \frac{dP}{dt} - \frac{\gamma P}{\rho} \frac{d\rho}{dt}$$

$$= \frac{dP}{dt} - a^2 \frac{d\rho}{dt} \qquad (3.4\text{-}4)$$

$$\text{Writing } \frac{dP}{dt} = \frac{\partial P}{\partial t} + u \frac{\partial P}{\partial x}$$

$$\frac{d\rho}{dt} = \frac{\partial \rho}{\partial t} + u \frac{\partial \rho}{\partial x}$$

and substituting in equation (3.4-4) gives:

$$\frac{P}{C_v} \frac{ds}{dt} = \frac{\partial P}{\partial t} + u \frac{\partial P}{\partial x} - a^2 \left(\frac{\partial \rho}{\partial t} + u \frac{\partial \rho}{\partial x}\right)$$

which from the energy equation (3.3-5)

$$= (\gamma-1)(\rho u F + q)$$

$$\text{Whence } ds = (\gamma-1) \frac{C_v}{P} (\rho u F + q) dt \qquad (3.4\text{-}5)$$

Equating equations (3.4-2) and (3.4-5) gives:

$$d(\log_e a_{os}) = \frac{(\gamma-1)}{2\gamma} \frac{1}{P} (\rho u F + q)\, dt$$

which on integration gives:

$$\frac{2^{a}os}{1^{a}os} = \exp. \sum_{t=t_1}^{t=t_2} \frac{(\gamma-1)}{2\gamma} \frac{1}{P} (\rho u F + q)\, dt \qquad (3.4\text{-}6)$$

The exponential of equation (3.4-6) can be expanded, and if in the step by step evaluation small intervals of time are considered, then second and higher order terms can be neglected without error, hence

$$\frac{2^{a}os}{1^{a}os} = 1 + \frac{(\gamma-1)}{2\gamma} \frac{1}{P} (\rho u F + q)\, \Delta t$$

Substituting: $\frac{\rho}{P} = \frac{\gamma}{a^2}$

$$a^2 = a_{os}{}^2 \left(\frac{P}{P_o}\right)^{\frac{\gamma-1}{\gamma}}$$

and $F = \frac{f}{2d} \frac{u}{|u|} u^2$ gives:

$$\frac{2^{a}os}{1^{a}os} = 1 + \frac{(\gamma-1)}{2} \frac{f}{2d} \frac{u}{|u|} \left(\frac{u}{a_{os}}\right)^2 \frac{\Delta t}{(P/P_o)^{\frac{\gamma-1}{\gamma}}}$$

$$+ \frac{(\gamma-1)}{2\gamma} \frac{q}{P} \Delta t \qquad (3.4\text{-}7)$$

where Δt is the particle time from state 1 to state 2 and the variables are the means between states 1 and 2.

Equation (3.4-7) is the required equation denoting the change of entropy along the particle path from state 1 to state 2.

3.5 Application of the Method of Characteristics.

For characteristics to be found, heat conduction and viscous friction within the fluid must be negligible since higher derivatives and squares of the first derivative cannot be taken into account in the theory. The assumption that these effects are negligible was made in Section 3.3 when developing the three basic equations given below which define the flow parameters.

$$\rho \frac{\partial u}{\partial x} + u \frac{\partial \rho}{\partial x} + \frac{\partial \rho}{\partial t} = 0 \qquad (3.3\text{-}1)$$

$$u \frac{\partial u}{\partial x} + \frac{\partial u}{\partial t} + \frac{1}{\rho} \frac{\partial P}{\partial x} + F = 0 \qquad (3.3\text{-}2)$$

$$u \frac{\partial P}{\partial x} + \frac{\partial P}{\partial t} - a^2 u \frac{\partial \rho}{\partial x} - a^2 \frac{\partial \rho}{\partial t} - (\gamma - 1)(\rho u F + q) = 0 \qquad (3.3\text{-}5)$$

The general solution of three partial differential equations of this form is given in Section 9.1. The equations solved therein are of the form:

$$\left.\begin{aligned} A_1 \frac{\partial v}{\partial x} + B_1 \frac{\partial v}{\partial y} + C_1 \frac{\partial w}{\partial x} + D_1 \frac{\partial w}{\partial y} + E_1 \frac{\partial z}{\partial x} + F_1 \frac{\partial z}{\partial y} + G_1 = 0 \\ A_2 \frac{\partial v}{\partial x} + B_2 \frac{\partial v}{\partial y} + C_2 \frac{\partial w}{\partial x} + D_2 \frac{\partial w}{\partial y} + E_2 \frac{\partial z}{\partial x} + F_2 \frac{\partial z}{\partial y} + G_2 = 0 \\ A_3 \frac{\partial v}{\partial x} + B_3 \frac{\partial v}{\partial y} + C_3 \frac{\partial w}{\partial x} + D_3 \frac{\partial w}{\partial y} + E_3 \frac{\partial z}{\partial x} + F_3 \frac{\partial z}{\partial y} + G_3 = 0 \end{aligned}\right\} \qquad (3.5\text{-}1)$$

It is established Section 9.1. that the partial differential equations (3.5-1) can be transformed into total differentials along three paths, the slopes of which are given by:

$$\begin{vmatrix} A_1 \phi - B_1 & A_2 \phi - B_2 & A_3 \phi - B_3 \\ C_1 \phi - D_1 & C_2 \phi - D_2 & C_3 \phi - D_3 \\ E_1 \phi - F_1 & E_2 \phi - F_2 & E_3 \phi - F_3 \end{vmatrix} = 0 \quad (3.5\text{-}2)$$

where $\phi = \frac{dy}{dx}$

Comparison of equations (3.3-1), (3.3-2), and (3.3-5) with equations (3.5-1) yields the following identities:

A_1	B_1	C_1	D_1	E_1	F_1	G_1
ρ	0	u	1	0	0	0
A_2	B_2	C_2	D_2	E_2	F_2	G_2
u	1	0	0	$\frac{1}{\rho}$	0	F
A_3	B_3	C_3	D_3	E_3	F_3	G_3
0	0	$-a^2 u$	$-a^2$	u	1	$(\gamma-1)(\rho u F+q)$

(3.5-3)

where $v \equiv u$; $w \equiv \rho$; $z \equiv P$; $x \equiv x$; $y \equiv t$.

Substitution of these identities in equation (3.5-2) gives the determinant:

$$\begin{vmatrix} \rho\,\emptyset & u\,\emptyset - 1 & 0 \\ u\emptyset - 1 & 0 & -a^2(u\emptyset - 1) \\ 0 & \frac{1}{\rho}\,\emptyset & u\,\emptyset - 1 \end{vmatrix} = 0 \qquad (3.5\text{-}4)$$

where $\emptyset = \frac{dt}{dx}$

Expansion of this determinant gives:

$$(u\,\emptyset - 1)^3 - a^2(u\,\emptyset - 1)\,\emptyset^2 = 0$$

which has the following roots:

$$\left(\frac{dx}{dt}\right)_{I,\,II} = u \pm a \quad \text{(Mach lines)} \qquad (3.5\text{-}5)$$

$$\frac{dx}{dt} = u \quad \text{(Path lines)} \qquad (3.5\text{-}6)$$

Equation (3.5-5) signifies that disturbances are propagated either rightward or leftward with the local acoustic velocity relative to the fluid and that wall friction, heat exchange with the surroundings and entropy gradients have no influence on the propagation velocity of a wave point.

Equation (3.5-6) represents the path lines or loci of the fluid particles and shows that they are characteristic curves along which the entropy or temperature gradients may have discontinuities.

The general solution obtained in Section 9.1 gives the differential equations of the Mach lines in terms of

the state parameters on substitution of the identities given by (3.5-3).

From Section 9.1:

$$(m_1 A_1 + m_2 A_2 + A_3)dv + (m_1 C_1 + m_2 C_2 + C_3)dw + (m_1 E_1 + m_2 E_2 + E_3)dz + (m_1 G_1 + m_2 G_2 + G_3)dx = 0 \tag{3.5-7}$$

where $$m_1 = \frac{(A_2 \phi - B_2)(C_3 \phi - D_3) - (A_3 \phi - B_3)(C_2 \phi - D_2)}{(A_1 \phi - B_1)(C_2 \phi - D_2) - (A_2 \phi - B_2)(C_1 \phi - D_1)} \tag{3.5-8}$$

and $$m_2 = \frac{(A_3 \phi - B_3)(C_1 \phi - D_1) - (A_1 \phi - B_1)(C_3 \phi - D_3)}{(A_1 \phi - B_1)(C_2 \phi - D_2) - (A_2 \phi - B_2)(C_1 \phi - D_1)} \tag{3.5-9}$$

Substitution of the values for the coefficients given by (3.5-3) in equations (3.5-8) and (3.5-9) yields the result:

$$m_1 = a^2 \tag{3.5-10}$$

$$m_2 = -\frac{a^2 \rho \phi}{u \phi - 1} \tag{3.5-11}$$

Hence, using equations (3.5-3), (3.5-10) and (3.5-11), equation (3.5-7) becomes:

$$\left[a^2 \rho - \frac{a^2 \rho u \phi}{u \phi - 1} \right] du + \left[\frac{-a^2 \phi}{u \phi - 1} + u \right] dP + \left[-\frac{F a^2 \rho \phi}{u \phi - 1} - (\gamma - 1)(\rho u F + q) \right] dx = 0$$

from which,

$$du = \left[- \emptyset + \frac{u}{a^2} (u\emptyset - 1) \right] \frac{dP}{\rho} + \left[- F\emptyset - \frac{(\gamma-1)}{a^2 \rho} (\rho u F + q)(u\emptyset - 1) \right] dx$$

Replacing $\emptyset = \frac{dt}{dx}$ gives:

$$du = \frac{1}{\rho} \frac{dP}{dx} \left[\frac{u}{a^2} (u\,dt - dx) - dt \right] - F\,dt - \frac{\gamma-1}{a^2 \rho} (\rho u F + q)(u\,dt - dx)$$

and substituting $u\,dt - dx = \mp a\,dt$ from equation (3.5-5) then gives:

$$du = \frac{dP}{\rho} \cdot \frac{dt}{dx} \left(\mp \frac{u}{a} - 1 \right) - F\,dt \pm \frac{(\gamma-1)}{a\,\rho} (\rho\, u\, F + q)\, dt$$

which after putting $\frac{dt}{dx} = \frac{1}{u \pm a}$ becomes:

$$du = \mp \frac{dP}{a\rho} - F \left[1 \mp (\gamma-1) \frac{u}{a} \right] dt \pm \frac{(\gamma-1)}{a\,\rho}\, q\, dt$$

Replacing F by $\frac{f}{2d} \cdot \frac{u}{|u|} \cdot u^2$ and eliminating ρ by writing $\frac{1}{a\,\rho} = \frac{a}{\gamma P}$, then

$$du = \mp \frac{a}{\gamma} \frac{dP}{P} - \frac{f}{2d} \frac{u}{|u|} u^2 \left[1 \mp (\gamma-1) \frac{u}{a} \right] dt$$

$$\pm \frac{(\gamma-1)}{\gamma} \frac{a\,q}{P}\, dt \qquad (3.5\text{-}12)$$

Equation (3.5-12) can be made dimensionless by dividing throughout by a_o, the datum level for the system,

thus becoming:

$$d\left(\frac{u}{a_o}\right) = \mp \frac{1}{\gamma}\frac{a}{a_o}\frac{d\left(\frac{P}{P_o}\right)}{\left(\frac{P}{P_o}\right)} - \frac{f}{2d}\frac{u}{|u|}\frac{u^2}{a_o}\left[1 \mp (\gamma-1)\frac{u}{a}\right] dt$$

$$\pm \frac{(\gamma-1)}{\gamma}\frac{a\,q}{a_o P}\,dt \qquad (3.5\text{-}13)$$

Now $\frac{a}{a_{os}} = \left(\frac{P}{P_o}\right)^{\frac{\gamma-1}{2\gamma}}$ (see Section 3.4)

Therefore

$$\frac{a}{a_{os}}\frac{d\left(\frac{P}{P_o}\right)}{\frac{P}{P_o}} = \left(\frac{P}{P_o}\right)^{\frac{\gamma-1}{2\gamma}-1} . d\left(\frac{P}{P_o}\right)$$

$$= \frac{2\gamma}{\gamma-1}\, d\left[\left(\frac{P}{P_o}\right)^{\frac{\gamma-1}{2\gamma}}\right]$$

$$\text{or} \quad a\frac{d\left(\frac{P}{P_o}\right)}{\left(\frac{P}{P_o}\right)} = \frac{2\gamma}{\gamma-1}\, a_{os}\, d\left[\left(\frac{P}{P_o}\right)^{\frac{\gamma-1}{2\gamma}}\right] \qquad (3.5\text{-}14)$$

Hence writing $\bar{U}$ for $\left(\frac{u}{a_o}\right)$, $\bar{X}$ for $\left(\frac{P}{P_o}\right)^{\frac{\gamma-1}{2\gamma}}$ and substituting equation (3.5-14), equation (3.5-13) becomes:

$$(d\bar{U})_{I,II} = \mp \frac{2}{\gamma-1}\frac{a_{os}}{a_o}(d\bar{X})_{I,II} - \frac{f}{2d}\frac{u}{|u|}\frac{u^2}{a_o}\left[1 \mp (\gamma-1)\frac{u}{a}\right](dt)_{I,II}$$

$$\pm \frac{\gamma-1}{\gamma}\frac{aq}{a_o P}(dt)_{I,II} \qquad (3.5\text{-}15)$$

This is the final equation denoting the change in state and particle velocity along a characteristic in the physical plane.

Equation (3.5-15) may be written as:

$$(d\,\bar{U})_{I,\,II} = \mp \frac{2}{\gamma-1} \frac{a_{os}}{a_o} (d\,\bar{X})_{I,\,II} - (d\,\bar{U}_f)_{I,\,II} + (d\,\bar{U}_q)_{I,\,II}$$

the last two terms representing the influence of wall friction and heat transfer with the surroundings. Neglecting these correction terms and assuming isentropic flow conditions gives the result:

$$(d\,\bar{U})_{I,\,II} = \mp \frac{2}{\gamma-1} (d\,\bar{X})_{I,\,II} \qquad (3.5\text{-}16)$$

which is identical with that obtained by initially assuming isentropic flow. (see Section 9.3)

3.6 Solution of Flow Equations Using the Method of Characteristics.

The graphical solution of the flow equations using the equations of the characteristics requires the construction of a position diagram and a state diagram. The former has Mach lines which represent changes in position with time of points on the pressure wave under consideration, and the latter has lines along which the change of state is defined. The Mach lines on the position diagram enclose regions in the pipe whose states are defined by the appropriate points in the state diagram.

The solution of the flow equations for isentropic conditions in a constant cross-sectional area pipe is described in Section 9.4. This method has to be modified for the solution of the flow equations allowing for the effects of wall friction and heat transfer from the surroundings. Since the process is now irreversible, lines cannot be drawn on the state diagram, as in the isentropic case, which describe the changes of state from region to region in the pipe.

The equations required for the construction of the characteristic net are developed in Section 3.5. These are repeated below for convenience, the characteristic state equation (3.5-15) being written in finite difference form.

$$(\Delta \bar{U})_{I,II} = \mp \frac{2}{\gamma-1} \frac{a_{os}}{a_o} (\Delta \bar{X})_{I,II} - \frac{f}{2d} \frac{u}{|u|} \frac{u^2}{a_o} \left[1 \mp (\gamma-1)\frac{u}{a}\right](\Delta t)_{I,II}$$

$$\pm \frac{\gamma-1}{\gamma} \frac{a}{a_o} \frac{q}{P} (\Delta t)_{I,II} \qquad (3.5\text{-}15)$$

$$\left(\frac{dx}{dt}\right)_{I,II} = u \pm a \qquad (3.5\text{-}5)$$

$$\frac{dx}{dt} = u \qquad (3.5\text{-}6)$$

Consider the position and state diagrams, Fig. 13 and Fig. 14 respectively. Given that the state parameters of regions 6.4 and 5.5 are known and that those of region 6.5 are required to be found, the modified method of solution is summarized below.

1. A provisional state point 6.5' is found by constructing the characteristics through 5.5 and 6.4, the slopes used being those obtained by neglecting friction and heat transfer effects, i.e. from:

$$(\Delta \bar{U})_{I,II} = \mp \frac{2}{\gamma-1} \frac{a_{os}}{a_o} (\Delta \bar{X})_{I,II}$$

The values used for a_{os} in this equation are those of the regions 6.4 and 5.5 for the slopes from 6.4 to 6.5' and from 5.5 to 6.5' respectively, and the value of γ is that appropriate to the region in which the network is constructed.

Position Diagram

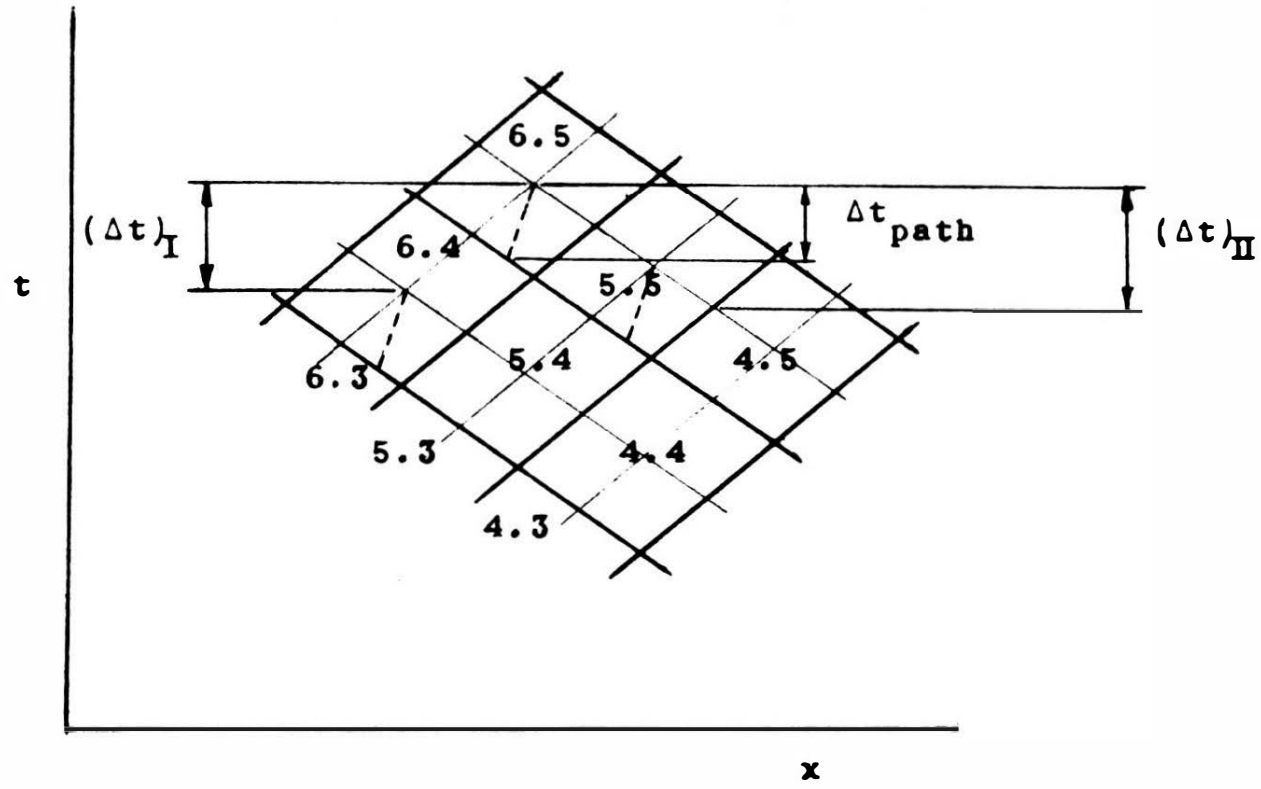

Fig.13.

State Diagram

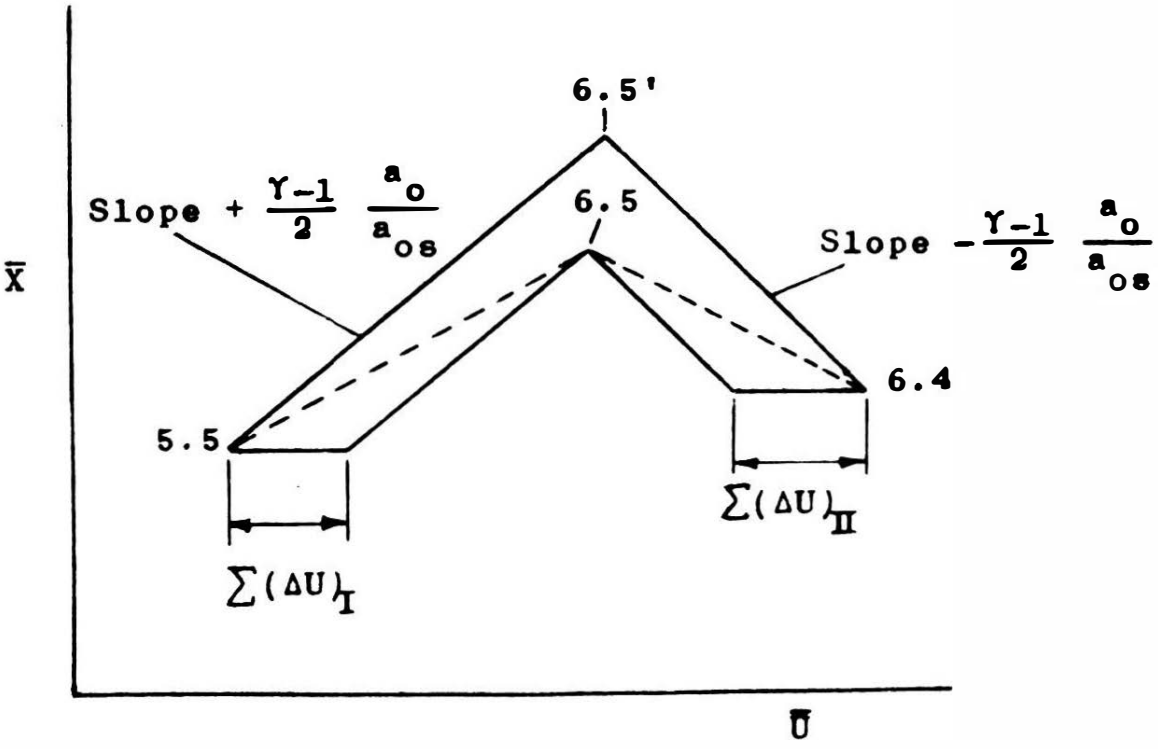

Fig. 14.

2. Using the approximate state 6.5', the mean values of u, a, P, f and q between the states 6.4 and 6.5' can be determined. Hence, in the position diagram, the approximate Mach lines which complete the field boundaries of region 6.5 can be drawn using equation (3.5-5), and the path line (shown dotted) can be drawn using equation (3.5-6).

The approximate mean time (Δt path) for particles arriving in region 6.5 from region 6.4 can be obtained from the position diagram by direct measurement. Substitution of this, together with the mean values for the other variables in equation (3.4-7) gives the first approximate value of a_{os} for the region 6.5.

3. The wave times $(\Delta t)_{I, II}$ can be obtained by direct measurement from the position diagram and substituted in the characteristic state equation (3.5-15) together with the mean values between 6.4 and 6.5' and 5.5 and 6.5' for the variables a_{os}, u, a, P, f and q. The state equations are then solved giving the first approximation for $\bar{U}$ and $\bar{X}$ in the region 6.5.

4. The first approximation to state 6.5 can be plotted in the state diagram and the procedure outlined in paragraphs 2 and 3 above repeated until satisfactory convergence of the values of $\bar{U}$ and $\bar{X}$ are obtained.

3.7. Solution with temperature discontinuity.

A temperature discontinuity in the gas flow is established at the surface of separation of the hot gases being discharged from the cylinder and the cooler residual gases from the previous cycle. This interface will be swept along the exhaust pipe with the local particle velocity and is thus a path line. In general, the volume of the exhaust pipe is in excess of the volume of gases discharged from the cylinder, and several discontinuities will exist in the pipe at any instant. A pressure wave encountering a discontinuity of this nature undergoes a change of state due to partial reflection. The transmitted wave is propagated in the next gas region at a velocity appropriate to the fluid temperature.

To analyse the conditions at the interface, it is necessary to assume that no diffusion or heat conduction occurs between the hot and cold regions and that the discontinuity is a definite plane fluid boundary. Also, the fluid pressure and particle velocity immediately adjacent to both sides of the interface must have the same values.

In order to clarify the method of solution, the problem is considered below in three stages, viz: (a) solution for isentropic flow with constant specific heats; (b) solution for isentropic flow with variable

specific heats; (c) solution for irreversible flow with variable specific heats. The latter is the method of solution required for the firing engine analysis.

In all three cases, the parameters referring to the hot and cold regions associated with the discontinuity are identified by the index marks ' and " respectively.

(a) Solution for isentropic flow with constant specific heats.

From the state characteristic equation (3.5-16), written in finite difference form:

$$(\Delta \bar{U}')_I = -\frac{2}{\gamma-1}\left(\Delta \frac{a'}{a_o}\right)_I$$

$$(\Delta \bar{U}")_{II} = +\frac{2}{\gamma-1}\left(\Delta \frac{a"}{a_o}\right)_{II} \qquad (3.7\text{-}1)$$

On either side of the temperature discontinuity the following isentropic relationships hold:

$$\frac{a'}{a_o} = \frac{a'_{os}}{a_o}\left(\frac{P'}{P_o}\right)^{\frac{\gamma-1}{2\gamma}}$$

$$\frac{a"}{a_o} = \frac{a"_{os}}{a_o}\left(\frac{P"}{P_o}\right)^{\frac{\gamma-1}{2\gamma}} \qquad (3.7\text{-}2)$$

If the region of state associated with the discontinuity is small, then the pressure and particle

velocity will be the same for the whole region, thus:

$$\frac{u'}{a_o} = \frac{u''}{a_o} \qquad (3.7\text{-}3)$$

$$\text{and} \quad \frac{P'}{P_o} = \frac{P''}{P_o}$$

From equations (3.7-1), (3.7-2) and (3.7-3) it follows that:

$$(\Delta \bar{U})_I = -\frac{2}{\gamma-1} \frac{a_{os}'}{a_o} (\Delta \bar{X})_I \qquad (3.7\text{-}4)$$

$$(\Delta \bar{U})_{II} = +\frac{2}{\gamma-1} \frac{a_{os}''}{a_o} (\Delta \bar{X})_{II}$$

where $\Delta \bar{U} = \Delta \bar{U}' = \Delta \bar{U}''$

$\Delta \bar{X} = \Delta \bar{X}' = \Delta \bar{X}''$

Thus the characteristics for the rightward and leftward moving waves have slopes $(-\frac{2}{\gamma-1} \frac{a_{os}'}{a_o})_I$ and $(+\frac{2}{\gamma-1} \frac{a_{os}''}{a_o})_{II}$ respectively.

Consider the beginning of blowdown with exhaust gas entering the pipe at a temperature T'. The stagnant gas at ambient pressure P_o in the exhaust pipe is assumed to exist in two distinct temperature regions T" and T"' as shown in Fig. 15.

At the instant of port opening, the acoustic wave

Position Diagram

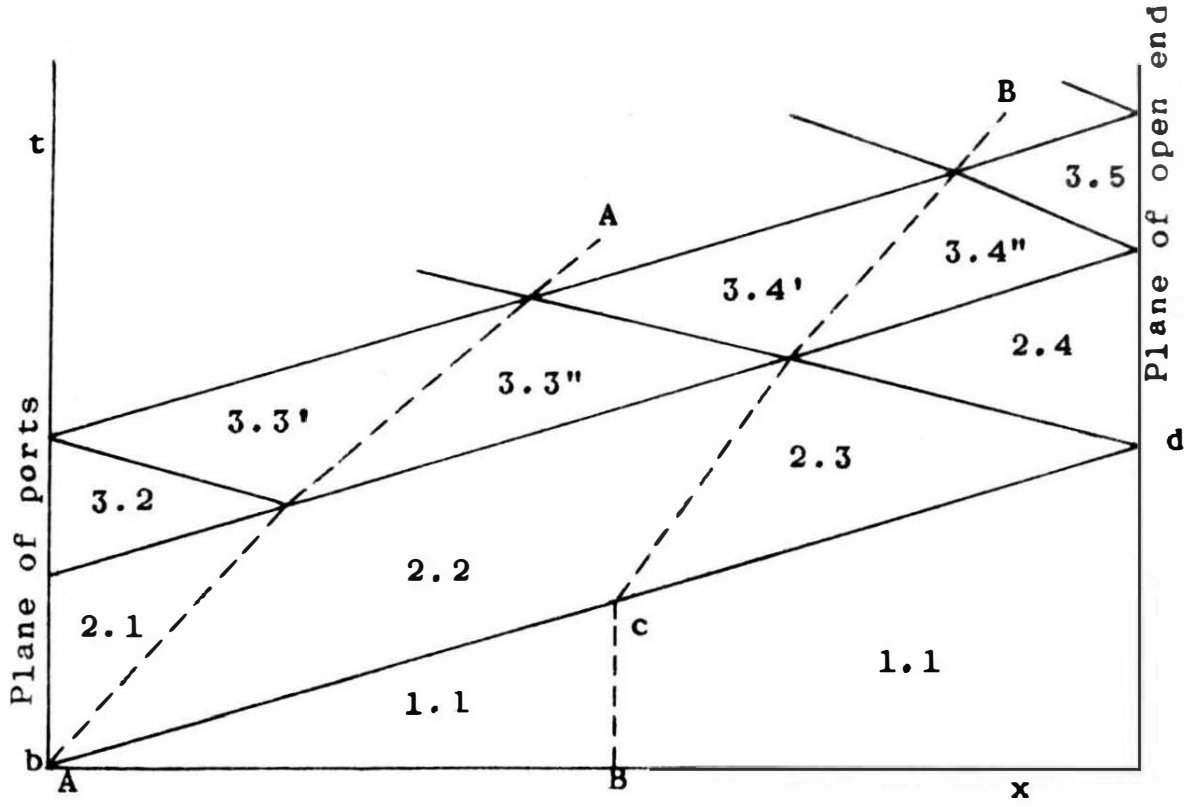

Initial Temperature Plot.

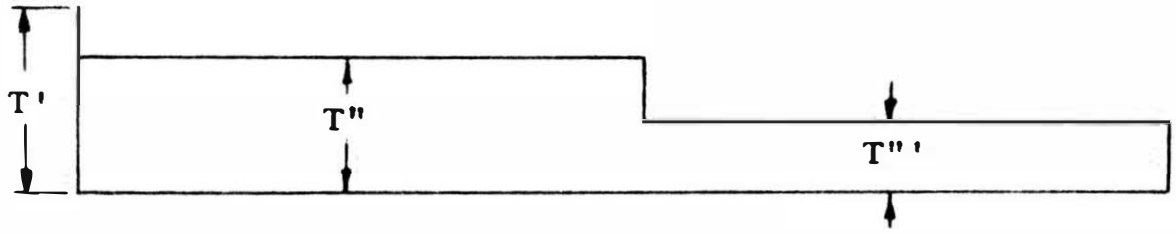

State Diagram

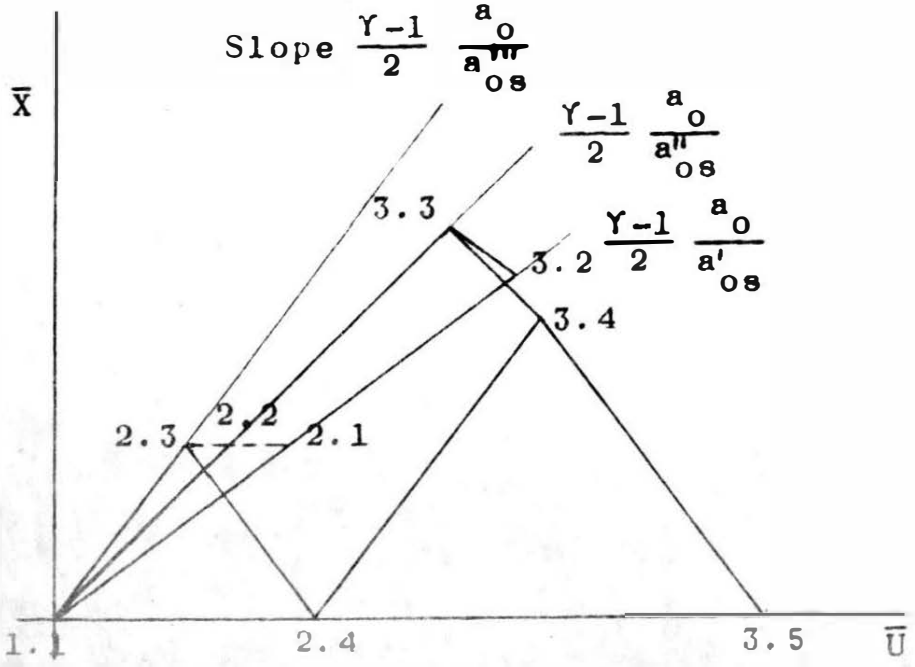

Fig.15.

b c d will travel along the pipe, its propagation velocity depending upon the temperature of the gas regions through which it successively passes.

The initial wave 2 is then propagated along the pipe, the amplitude and particle velocity of region 2.1 being known from the boundary conditions. Thus state point 2.1 lies on a characteristic of slope $+\frac{\gamma-1}{2}\frac{a_o}{a_{os}'}$ through 1.1 in the state diagram.

On reaching the discontinuity AA, partial reflection of the wave 2 occurs. The partially transmitted wave moving to the right must now satisfy the state conditions of the next region at temperature T" and thus state point 2.2 lies on a characteristic of slope $+\frac{\gamma-1}{2}\frac{a_o}{a_{os}''}$ through 1.1.

The mean pressures of regions 2.1 and 2.2 must have the same value since no mechanism exists in these regions to produce any change. It should be noted, however, that although no discontinuity in pressure and particle velocity exists on either side of and immediately adjacent to the temperature interface, a variation in particle velocity can exist between regions 2.1 and 2.2 when considering the mean states, since these regions are comparatively large.

Since γ is constant, $\bar{X}$ for state 2.2 will have

the same value as $\bar{X}$ for state 2.1, and thus the intersection of a horizontal line drawn through 2.1 with the $+\frac{\gamma-1}{2}\frac{a_o}{a_{os}}$ characteristic locates state point 2.2. The path of the temperature discontinuity in the position diagram can now be plotted using equation (3.5-6) and the mean value of u between states 2.1 and 2.2.

The rightward moving wave 2 will continue along the pipe with uniform velocity until it encounters the temperature discontinuity BB. If it is assumed that this discontinuity is small, then reflections from this interface can be neglected without undue error, and the state point 2.3 and the discontinuity path line between regions 2.2 and 2.3 can be plotted in a similar manner to that given above.

The partial reflection of wave 2 at the discontinuity AA travels back to the engine ports and, for convenience, the duration of region 3.2 is made to coincide with this reflection. The state point 3.2 must lie on a characteristic of slope $-\frac{\gamma-1}{2}\frac{a_o}{a_{os}}$ through 2.1 and the state is determined by transferring this characteristic to the boundary diagram and satisfying the boundary conditions (see Section 3.8).

The state point 3.3 is determined by the intersection of the two characteristics of slope $-\frac{\gamma-1}{2}\frac{a_o}{a_{os}}$ and

$+ \frac{\gamma-1}{2} \frac{a_o}{a_{os}''}$ through state points 3.2 and 2.2 respectively. State point 3.3 represents the state of the whole region since the means of the two portions 3.3' and 3.3" lie close to the temperature discontinuity.

The solution for further regions associated with the temperature discontinuity is similar to that for region 3.3.

(b) Solution for isentropic flow with variable specific heats.

The ratio of the specific heats, γ, is now a function of temperature and $\gamma' \neq \gamma''$. Therefore, although the pressure on either side of the discontinuity in any particular region must be the same, $\bar{X}' \neq \bar{X}''$ for the hot and cold parts of the region respectively.

Consider the superimposition of two waves in a region in which a temperature discontinuity exists, see Fig. 16.

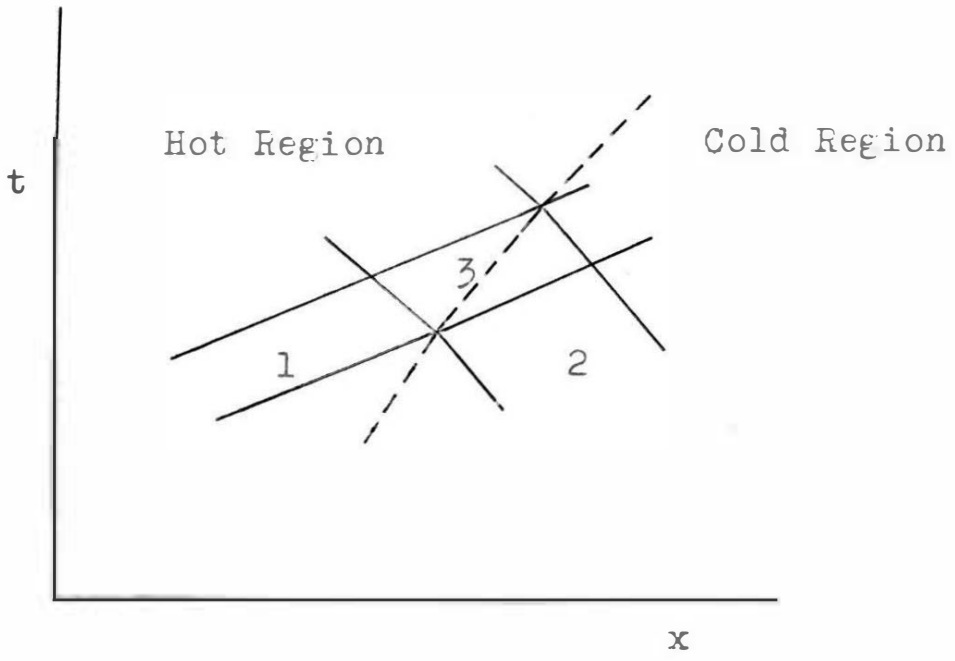

Position Diagram

Fig. 16.

From the state characteristic equation (3.5-16) written in finite difference form:

$$(\Delta \bar{U}')_I = -\frac{2}{\gamma'-1}(\Delta \frac{a'}{a_o})_I$$

$$(\Delta \bar{U}'')_{II} = +\frac{2}{\gamma''-1}(\Delta \frac{a''}{a_o})_{II} \qquad (3.7\text{-}5)$$

If the region of state associated with the discontinuity is small, then the pressure and particle velocity will be the same for the whole region, thus:

$$\bar{U}_3' = \frac{u_3'}{a_o} = \frac{u_3''}{a_o} = \bar{U}_3'' \qquad (3.7\text{-}6)$$

and $\frac{P_3'}{P_o} = \frac{P_3''}{P_o}$ which may be written as:

$$(\frac{a_3'}{a_{os}'})^{\frac{2\gamma'}{\gamma'-1}} = (\frac{a_3''}{a_{os}''})^{\frac{2\gamma''}{\gamma''-1}} \qquad (3.7\text{-}7)$$

From equation (3.7-5)

$$\left.\begin{aligned} \bar{U}_3' - \bar{U}_1 &= -\frac{2}{\gamma'-1}\frac{1}{a_o}(a_3' - a_1) \\ \bar{U}_3'' - \bar{U}_2 &= +\frac{2}{\gamma''-1}\frac{1}{a_o}(a_3'' - a_2) \end{aligned}\right\} \qquad (3.7\text{-}8)$$

Using the equality given by equation (3.7-6) and subtracting equations (3.7-8) gives:

$$\bar{U}_2 - \bar{U}_1 = -\frac{2}{\gamma'-1}\frac{1}{a_o}(a_3' - a_1) - \frac{2}{\gamma''-1}\frac{1}{a_o}(a_3'' - a_2) \qquad (3.7\text{-}9)$$

From equation (3.7-7):

$$a_3' = a_{os}' \left(\frac{a_3''}{a_{os}''}\right)^{\frac{\gamma'-1}{\gamma''-1}\cdot\frac{\gamma''}{\gamma'}}$$

which on substitution in equation (3.7-9) and rearranging gives:

$$\frac{a_3''}{a_{os}''} = \left[\frac{(\gamma'-1)}{2}\frac{a_o}{a_{os}'}\left(\bar{U}_1-\bar{U}_2-\frac{2}{\gamma''-1}\frac{a_3''}{a_{os}''}\frac{a_{os}''}{a_o}+\frac{2}{\gamma''-1}\frac{a_2}{a_o}+\frac{2}{\gamma'-1}\frac{a_1}{a_o}\right)\right]^{\frac{\gamma''-1}{\gamma'-1}\cdot\frac{\gamma'}{\gamma''}}$$

$$= \left\{\frac{(\gamma'-1)}{2}\frac{a_o}{a_{os}'}\left(\bar{U}_1-\bar{U}_2+\frac{2}{\gamma''-1}\frac{a_2}{a_o}+\frac{2}{\gamma'-1}\frac{a_1}{a_o}\right)x\right.$$

$$\left.\left[1-\frac{2}{\gamma''-1}\frac{a_3''}{a_{os}''}\frac{a_{os}''}{a_o}\frac{1}{\left(\bar{U}_1-\bar{U}_2+\frac{2}{\gamma''-1}\frac{a_2}{a_o}+\frac{2}{\gamma'-1}\frac{a_1}{a_o}\right)}\right]\right\}^{\frac{\gamma''-1}{\gamma'-1}\cdot\frac{\gamma'}{\gamma''}}$$

$$= \left[\frac{(\gamma'-1)}{2}\frac{a_o}{a_{os}'}K\left(1-\frac{2}{\gamma''-1}\frac{a_3''}{a_{os}''}\frac{a_{os}''}{a_o}\frac{1}{K}\right)\right]^{\frac{\gamma''-1}{\gamma'-1}\cdot\frac{\gamma'}{\gamma''}}$$

where $K = \bar{U}_1-\bar{U}_2+\frac{2}{\gamma''-1}\frac{a_2}{a_o}+\frac{2}{\gamma'-1}\frac{a_1}{a_o}$,

Therefore:

$$\frac{a_3''}{a_{os}''} = K_1\left(1-K'\frac{a_3''}{a_{os}''}\right)^{\frac{\gamma''-1}{\gamma'-1}\cdot\frac{\gamma'}{\gamma''}} \qquad (3.7\text{-}10)$$

where $K' = \frac{2}{\gamma'' - 1} \frac{a_{os}''}{a_o} \frac{1}{K}$

and $K_1 = \left[\frac{(\gamma'-1)}{2} \frac{a_o}{a_{os}'} K \right]^{\frac{\gamma''-1}{\gamma'-1} \cdot \frac{\gamma'}{\gamma''}}$

K' and K_1 are unique constants for the step under consideration since for small changes, the change in γ' and γ'' will be infinitesimally small.

Expanding equation (3.7-10) by the binomial theorem and neglecting second and higher orders gives:

$$\frac{a_2''}{a_{os}''} = K_1 \left(1 - \frac{\gamma''-1}{\gamma'-1} \cdot \frac{\gamma'}{\gamma''} K' \frac{a_2''}{a_{os}''}\right)$$

$$= K_1 \left(1 - K_2 \frac{a_2''}{a_{os}''}\right)$$

where $K_2 = \frac{\gamma''-1}{\gamma'-1} \cdot \frac{\gamma'}{\gamma''} \cdot K'$

Hence $$\frac{a_2''}{a_{os}''} = \frac{K_1}{1+K_1 \cdot K_2} \qquad (3.7\text{-}11)$$

where $$K_1 = \left[\frac{(\gamma'-1)(\bar{U}_1-\bar{U}_2)}{2} \frac{a_o}{a_{os}'} + \frac{(\gamma' - 1)a_2 + (\gamma'' - 1)a_1}{(\gamma''-1)\, a_{os}'} \right]^{\frac{\gamma''-1}{\gamma'-1} \frac{\gamma'}{\gamma''}}$$

and $$K_2 = \frac{2\gamma'}{\gamma''(\gamma'-1)} \frac{a_{os}''}{a_o} \frac{1}{(\bar{U}_1 - \bar{U}_2 + \frac{2}{\gamma''-1} \frac{a_2}{a_o} + \frac{2}{\gamma'-1} \frac{a_1}{a_o})}$$

To solve a region of state such as region 3, Fig.16, $\frac{a_2''}{a_{os}''} = X_3''$ is obtained from equation (3.7-11) using the

known values for the state parameters of regions 1 and 2. Substitution in equation (3.7-7) then gives $\frac{a'_3}{a_{os}} = \bar{X}'_3$.

Use of the characteristic state equation (3.5-16) will then yield the value of $\bar{U}_3$, and hence the state of region 3 is completely defined.

(c) Solution for irreversible flow with variable specific heats.

The method of solution for a region in which a temperature discontinuity is present when the effects of friction and heat transfer are included, is similar to the previous case (b) with the additional complication of determining the change in a_{os} for both the hot and cold parts of the region.

From the characteristic state equation (3.5-15), written in finite difference form:

$$\left.\begin{aligned} (\Delta \bar{U}')_I &= -\frac{2}{\gamma'-1}\left(\Delta \frac{a'}{a_o}\right)_I - (\Delta \bar{U}'_{f+q})_I \\ (\Delta \bar{U}'')_{II} &= +\frac{2}{\gamma''-1}\left(\Delta \frac{a''}{a_o}\right)_{II} + (\Delta \bar{U}''_{f+q})_{II} \end{aligned}\right\} \qquad (3.7\text{-}12)$$

where $(\Delta \bar{U}_{f+q})_{I,\,II}$ represents the combined effect of friction and heat transfer.

Following the same argument as given in case (b), but using equation (3.7-12) instead of equation (3.7-5) gives the result:

$$\frac{a''_3}{a''_{os}} = \frac{K_3}{1 + K_3 K_4} \qquad (3.7\text{-}13)$$

where:

$$K_3 = \left\{ \frac{(\gamma'-1)}{2}(\bar{U}_1-\bar{U}_2)\frac{a_o}{a_{os}'} + \frac{(\gamma'-1)a_2 + (\gamma''-1)a_1}{(\gamma''-1)\,a_{os}'} - \frac{(\gamma'-1)}{2}\frac{a_o}{a_{os}'}\left[(\Delta\bar{U}'_{f+q})_I + (\Delta\bar{U}''_{f+q})_{II}\right]\right\}^{\frac{\gamma''-1}{\gamma'-1}\cdot\frac{\gamma'}{\gamma''}}$$

and

$$K_4 = \frac{2\gamma'}{\gamma''(\gamma'-1)}\frac{a_{os}''}{a_o}\cdot\frac{1}{(\bar{U}_1-\bar{U}_2)+\frac{2}{\gamma''-1}\frac{a_2}{a_o}+\frac{2}{\gamma'-1}\frac{a_1}{a_o}-\left[(\Delta\bar{U}'_{f+q})_I + (\Delta\bar{U}''_{f+q})_{II}\right]}$$

Consider Fig.17 in which it is assumed that regions 3.5, 3.6, and 4.5 are known, and region 4.6 is required to be found. The method of solution is summarized below.

1. The approximate state point (~4.6) is first determined neglecting the effects of friction and heat transfer, i.e. isentropic flow with variable specific heats, using the method outlined in (b).

2. Using the approximate state point (~4.6), the mean values of u, a, P, f and q between the states 4.5 and 4.6', and 3.6 and 4.6" can be determined. Hence in the position diagram, the approximate Mach lines which complete the field boundary of region 4.6 can be drawn using equation (3.5-5), and the path line drawn using equation (3.5-6).

3. The approximate mean time (Δt path) for particles arriving in region 4.6 from region 3.5 can be obtained

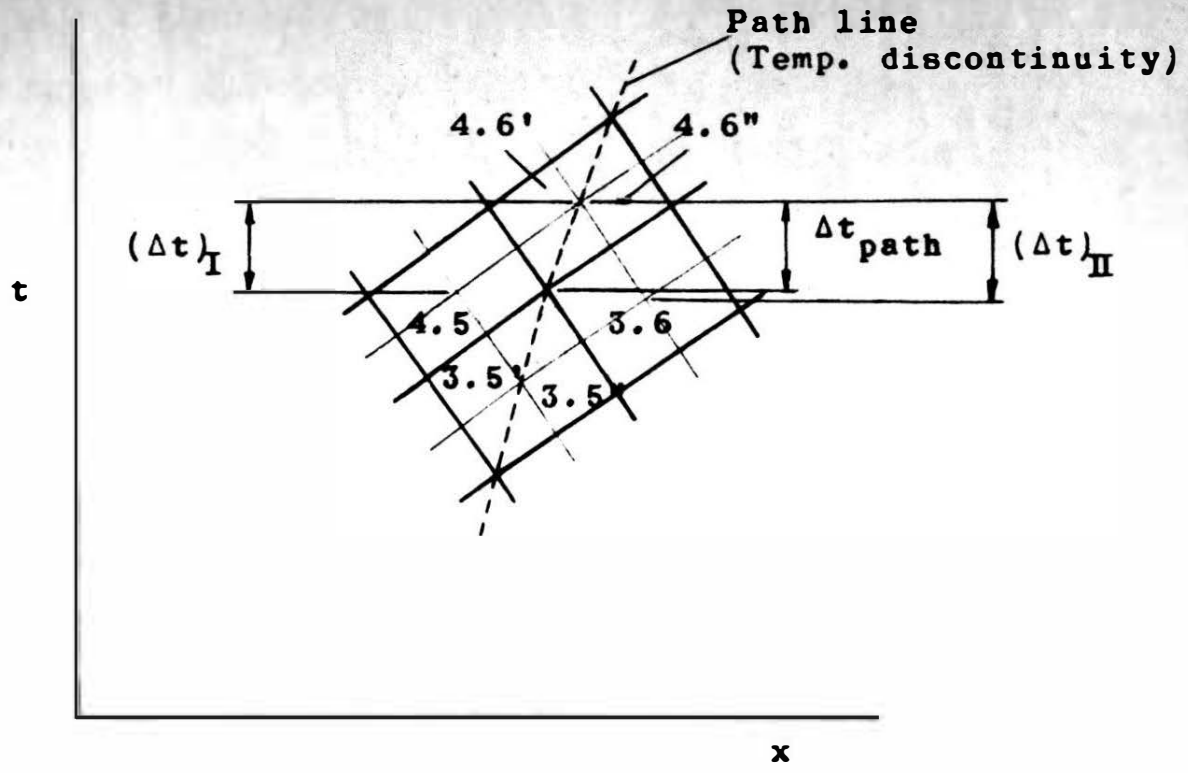

Position Diagram

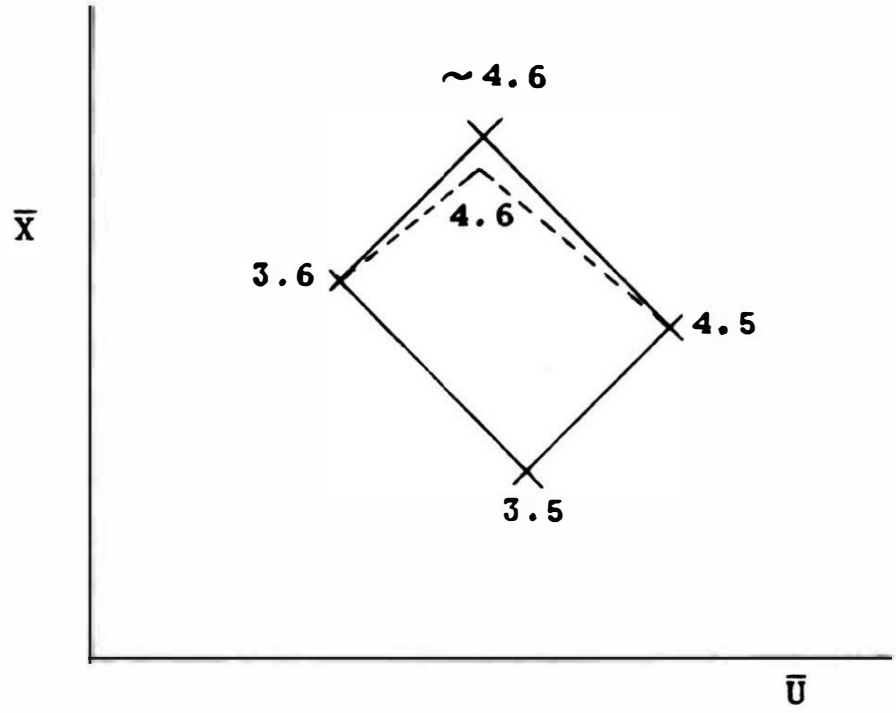

State Diagram

Fig. 17.

from the position diagram by direct measurement. Substitution of this, together with the mean values for the other variables in equation (3.4-7) evaluated for both sides of the discontinuity gives the first approximate values of a_{os}' and a_{os}'' for region 4.6.

4. The approximate wave times $(\Delta t)_{I, II}$ can be obtained by direct measurement from the position diagram and substituted with the mean values between states 4.5 and 4.6' and states 3.6 and 4.6" for the variables a_{os}, u, a, P, f and q to obtain the value of $\left[(\Delta \bar{U}'_{f+q})_I + (\Delta \bar{U}''_{f+q})_{II}\right]$.

5. Equation (3.7-13) is then used to obtain a closer approximation for $\frac{a_2''}{a_{os}''}$ and a closer approximation to state 4.6 evaluated.

6. The procedure outlined in paragraphs 2, 3, 4 and 5 above are now repeated until satisfactory convergence of the values of $\bar{U}_{4.6}$ and $P_{4.6}$ are obtained.

3.8. Boundary conditions.

The solution of the unsteady one-dimensional flow equations in the exhaust pipe by the construction of characteristic nets in the physical and state planes is developed in Section 3.6. At the engine ports and at the open end of the pipe, however, the boundary regions are determined from the boundary conditions. In this Section, the boundary conditions are developed and the application of the boundary chart described.

An exact analysis of the flow process must take account of unsteady motion in the boundary regions. This is, however, extremely difficult, and plausible approximations can be made to simplify the analysis without introducing undue error.

The assumptions made in the development of the flow equations and the analysis for changes occurring in the cylinder are listed below.

1. Adiabatic quasi-steady flow through the air and exhaust ports, and at the open end of the pipe. This implies that the steady flow adiabatic energy equation applies instantaneously across the engine ports and at the open end of the pipe. Further, the flow condition that is valid for steady flow through a restriction where the effective flow area is small in comparison with the upstream and downstream areas holds. This is

equivalent to assuming that the change in flow pattern with respect to time may be neglected in comparison with the change with respect to distance.

2. The effect of wave action in the cylinder on the process of discharge decreases so rapidly with increase in the ratio of cylinder area to pipe area that it may be neglected for the problem under consideration.

3. The cylinder ports are regarded as a sharp edged orifice, the coefficient of discharge depending upon the pressure ratio across them and Reynolds Number (see Fig. 28).

4. The ratio of the specific heats, γ, across the ports and at the pipe open end is taken as the upstream value in each case.

5. There is no mixing of the products of combustion from the previous cycle with the fresh air charge drawn in during the scavenge process. This means that during the scavenge process, the cylinder is assumed to contain two distinct gas regions separated by a plane fluid boundary.

6. The fluid in the cylinder is regarded as quasi-perfect, the appropriate mean value of γ being used for each step in the process.

7. The temperature of the air in the cylinder is taken to be the temperature of the air upstream of the air ports, i.e. no heat energy is absorbed by the air

after its admission into the cylinder.

8. The pressure throughout the cylinder is uniform instantaneously.

9. All processes, excluding the cylinder constents, are adiabatic and not necessarily isentropic.

10. The cylinder process is isentropic.

11. For fluid flow from pipe into cylinder, there is no pressure recovery after the vena contracta, i.e. the pressure in the cylinder equals the pressure at the vena contracta.

12. For fluid flow from cylinder to pipe, pressure recovery occurs after the vena contracta.

13. For inflow at the open end of the exhaust pipe, the pipe end behaves as a Borda mouthpiece.

Assumptions 1, 2, 3, 8, 9, 10, 11, 12, and 13 have been shown by earlier research to be valid approximations.

(a) Boundary diagrams for the cylinder.

The assumption of quasi-steady flow through the cylinder ports enables theoretical relationships to be established between the pressures on either side of the cylinder ports, the mass flow through the ports, and the associated particle velocity in the pipe. These relationships can be expressed in the form:

$$\frac{P_2}{P_1} = f'\left(k, \frac{u_2}{a_1}\right)$$

$$\frac{P_2}{P_1} = f''\left(M, \frac{u_2}{a_1}\right)$$

Using these relationships, curves showing the dependence of $\frac{u_2}{a_1}$ on $\frac{P_2}{P_1}$ for constant values of effective flow area k, and mass flow number M, are shown in Figs. 18, 19, 20 and 21 for values of $\gamma = 1.3$ and $\gamma = 1.4$, and for both inflow into, and outflow from, the cylinder.

Strictly, the outflow charts relate to conditions at a plane in the pipe some distance from the ports. However, this distance is very small in comparison with the pipe length and can be ignored.

Outflow from the cylinder.

The equations describing outflow are as follows:

1. Cylinder to vena contracta

Energy equation:

$$u_c^2 = \frac{2}{\gamma-1}(a_1^2 - a_c^2)$$

Isentropic state equation:

$$\frac{P_c}{P_1} = \left(\frac{a_c}{a_1}\right)^{\frac{2\gamma}{\gamma-1}}$$

Characteristic gas equation:

$$\rho_c = \frac{\gamma P_c}{a_c^2}$$

2. Vena contracta to pipe entry section:

Energy equation:

$$u_2^2 - u_c^2 = \frac{2}{\gamma-1}(a_c^2 - a_2^2)$$

Continuity equation:

$$u_c \rho_c A_c = u_2 \rho_2 A_2$$

which on putting $k = \frac{A_c}{A_2}$ becomes

$$u_c \rho_c k = u_2 \rho_2$$

Characteristic gas equation:

$$\rho_2 = \frac{\gamma P_2}{a_2^2}$$

For subsonic flow through the ports, the pressure existing at the centre of the vena contracta may be assumed to hold, not only in the gas stream, but also in the stagnant region surrounding the fluid stream in the pipe entry section. Hence the momentum equation can be applied from the vena contracta to the pipe.

i.e. $P_2 - P_c = k \rho_c u_c^2 - \rho_2 u_2^2$

Solving the above system of equations gives the result:

$$\left(\frac{P_2}{P_1}\right)^{\frac{\gamma-1}{2\gamma}} = k\left(\frac{a_1}{u_2}\right)\sqrt{\frac{2}{\gamma-1}\left[\left(\frac{P_2}{P_1}\right)^{\frac{1-\gamma}{\gamma}} - 1\right]\left[1 - \frac{\gamma-1}{2}\left(\frac{u_2}{a_1}\right)^2\right]} \qquad (3.8\text{-}1)$$

For sonic flow through the ports, the particle velocity u_c at the vena contracta is equal to the local acoustic velocity a_c. Using this criterion instead of the momentum equation, and solving, gives the result:

$$\frac{P_2}{P_1} = k\left(\frac{a_1}{u_2}\right)\left(\frac{2}{\gamma+1}\right)^{\frac{\gamma+1}{2(\gamma-1)}}\left[1 - \frac{(\gamma-1)}{2}\left(\frac{u_2}{a_1}\right)^2\right] \qquad (3.8\text{-}2)$$

To determine the mass flow relationship, it is sufficient to consider the conditions in the cylinder and the pipe only. This obviates the assumption of sonic or subsonic velocities at the vena contracta and the resulting relationship is valid for all conditions. Further, it is convenient to introduce a dimensionless mass flow parameter M, defined as:

$$M = \frac{A_2 \rho_2 u_2}{A_2 \rho_1 a_1} = \frac{\rho_2 u_2}{\rho_1 a_1}$$

The flow equations from cylinder to pipe are:

Energy equation:

$$u_2^2 = \frac{2\gamma}{\gamma-1} \left(\frac{P_1}{\rho_1} - \frac{P_2}{\rho_2}\right)$$

Characteristic gas equation:

$$\frac{\gamma P}{\rho} = a^2$$

which on rearranging and solving gives:

$$\frac{\rho_2}{\rho_1} = \frac{\frac{P_2}{P_1}}{1 - \frac{\gamma-1}{2} \left(\frac{u_2}{a_1}\right)^2}$$

Eliminating $\frac{\rho_2}{\rho_1}$ by means of the mass flow parameter M gives the result:

$$\frac{P_2}{P_1} = M \left(\frac{a_1}{u_2}\right) \left[1 - \frac{\gamma-1}{2} \left(\frac{u_2}{a_1}\right)^2\right] \qquad (3.8\text{-}3)$$

Equations (3.8-1), (3.8-2) and (3.8-3) plotted for constant values of k and M, are termed 'boundary diagrams'.

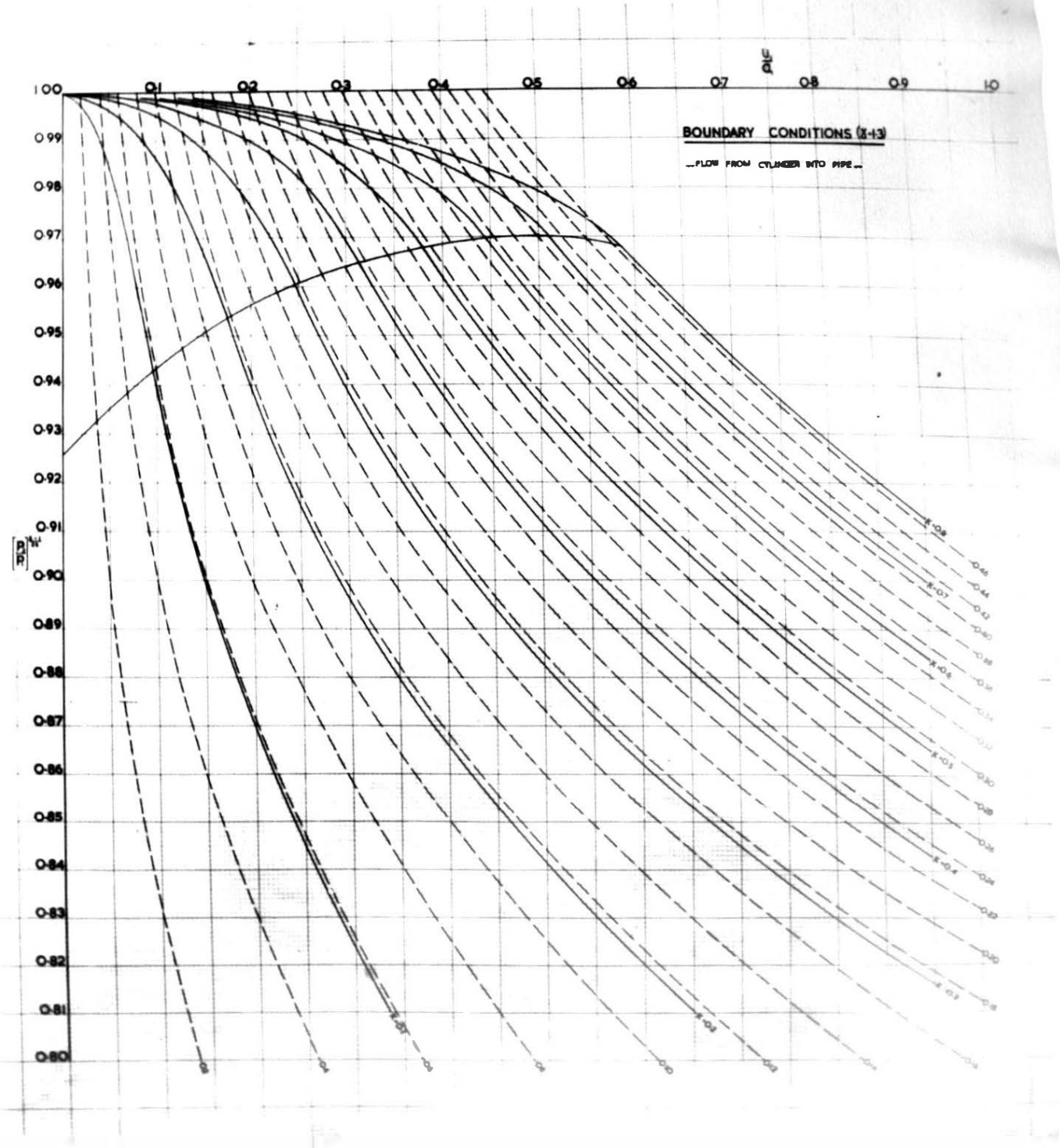
BOUNDARY CONDITIONS (3+3)
--FLOW FROM CYLINDER INTO PIPE--
1.00
0.99
0.98
0.97
0.96
0.95
0.94
0.93
0.92
0.91
0.90
0.89
0.88
0.87
0.86
0.85
0.84
0.83
0.82
0.81
0.80
0.1
0.2
0.3
0.4
0.5
0.6
0.7
0.8
0.9
1.0

Fig. 18.

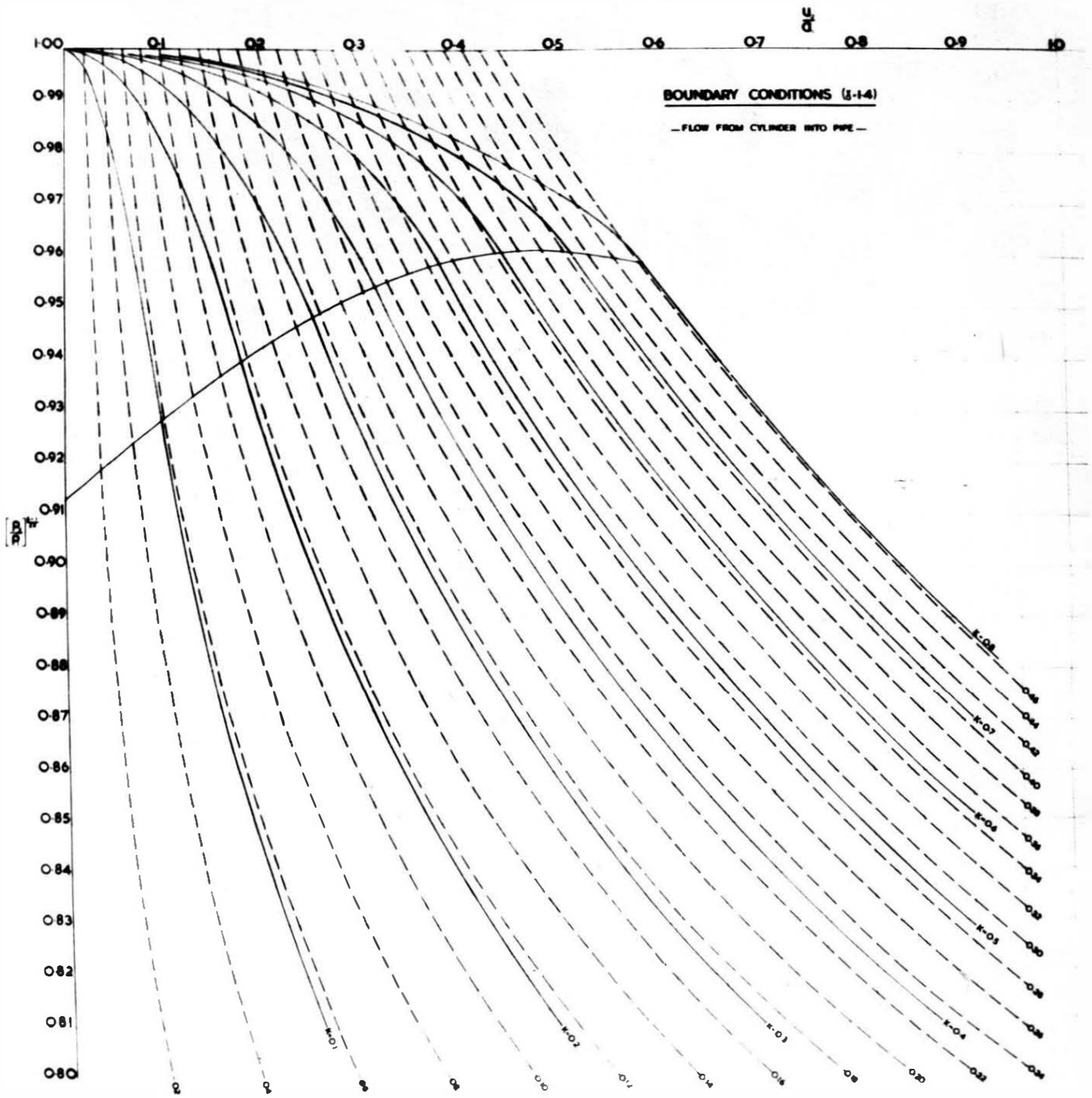
BOUNDARY CONDITIONS (J-1-4)
—FLOW FROM CYLINDER INTO PIPE—
d/L
1·00
0·99
0·98
0·97
0·96
0·95
0·94
0·93
0·92
0·91
0·90
0·89
0·88
0·87
0·86
0·85
0·84
0·83
0·82
0·81
0·80
0·1
0·2
0·3
0·4
0·5
0·6
0·7
0·8
0·9
1·0
K-01
K-02
K-03
K-04
K-05
K-06
K-07
K-08

Fig. 19.

Figs. 18 and 19 show the boundary diagrams for values of $\gamma = 1.3$ and $\gamma = 1.4$ respectively.

Inflow into the cylinder.

Since no pressure recovery is assumed after the vena contracta, the flow equations from the pipe to the vena contracta describe the flow, and are as follows:

Energy equation:

$$u_c^2 - u_2^2 = \frac{2}{\gamma-1}(a_2^2 - a_c^2)$$

Continuity equation:

$$u_2 \rho_2 = k u_c \rho_c$$

Isentropic state equation:

$$\frac{P_2}{P_1} = \frac{P_2}{P_c} = \left(\frac{a_2}{a_c}\right)^{\frac{2\gamma}{\gamma-1}}$$

Solving the above system of equations gives the result:

$$\left(\frac{u_2}{a_1}\right)^2 = \frac{\frac{2}{\gamma-1}\left[\left(\frac{P_2}{P_1}\right)^{\frac{\gamma-1}{\gamma}} - 1\right]}{\frac{1}{k^2}\left[\left(\frac{P_2}{P_1}\right)^{\frac{2}{\gamma}} - 1\right]} \qquad (3.8\text{-}4)$$

The mass flow relationship for inflow is determined by using the mass flow parameter M and the isentropic state relationship.

Substituting $\frac{\rho_2}{\rho_1} = M \frac{a_1}{u_2}$ in $\frac{P_2}{P_1} = \left(\frac{\rho_2}{\rho_1}\right)^{\gamma}$ gives:

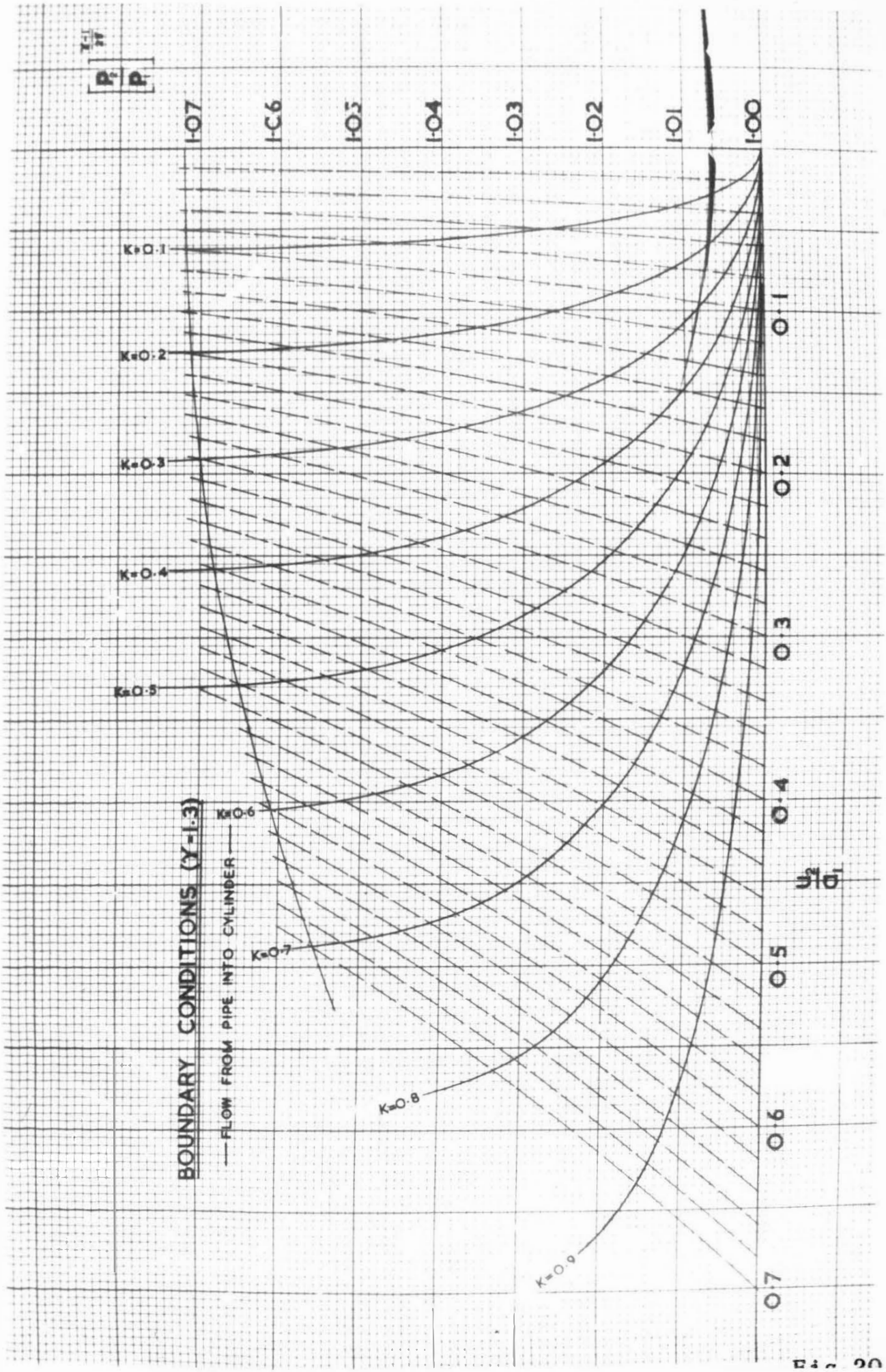
BOUNDARY CONDITIONS (Y=1.3)
—FLOW FROM PIPE INTO CYLINDER—
K=0·1
K=0·2
K=0·3
K=0·4
K=0·5
K=0·6
K=0·7
K=0·8
K=0·9
1·07
1·06
1·05
1·04
1·03
1·02
1·01
1·00
0·1
0·2
0·3
0·4
0·5
0·6
0·7

Fig. 20

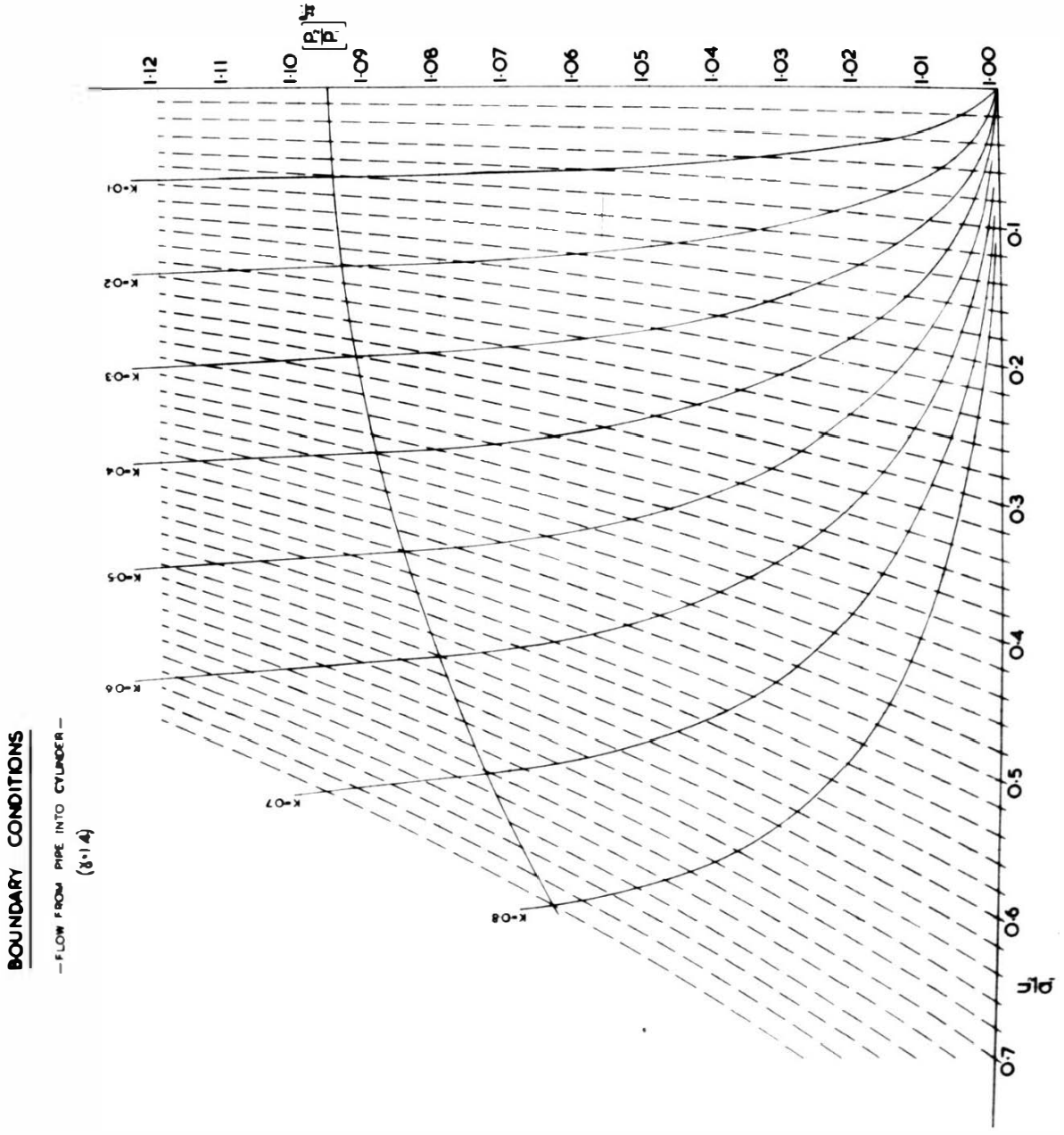
BOUNDARY CONDITIONS
—FLOW FROM PIPE INTO CYLINDER—
(3·1·14)
K=·01
K=·02
K=·03
K=·04
K=·05
K=·06
K=·07
K=·08
1·00
1·01
1·02
1·03
1·04
1·05
1·06
1·07
1·08
1·09
1·10
1·11
1·12
0·1
0·2
0·3
0·4
0·5
0·6
0·7

Fig. 21.

$$\frac{P_2}{P_1} = (M \frac{a_1}{u_2})^{\gamma} \qquad (3.8\text{-}5)$$

Figs. 20 and 21 show the inflow boundary diagrams for values of $\gamma = 1.3$ and $\gamma = 1.4$ respectively, plotted using equation (3.8-4) and (3.8-5).

(b) Variation of pressure in cylinder during blow-down and scavenge periods.

The pressure changes that occur in the cylinder of a reciprocating engine can be ascribed to:

1. Mass addition and rejection through the inlet and exhaust ports.
2. Change in cylinder volume due to the movement of the pistons.
3. Heat exchange with the cylinder boundary.

The assumption of isentropic conditions within the cylinder means that item 3 above is neglected in the following analysis.

Consider an elemental process, of time interval dt, during the scavenge period. Let the net increase in mass of the cylinder contents ($d\,m_1$) be given by:

$$d\,m_1 = d\,m_a - d\,m_e$$

Then the energy equation for the cylinder, neglecting any changes in kinetic and potential energies, is:

$$dQ - dW = d(m\,H)_e - d(m\,H)_a + d(m\,U)_1$$

where dW is the work done on the pistons by the gas, and dQ is the heat transfer into the cylinder.

The process is assumed to be isentropic, hence $dQ = 0$ and $dW = P_l \, dV_l$. Also H and U can be replaced by $C_\rho T$ and $C_v T$ respectively, where C_ρ and C_v are the mean values for the elemental process. Hence the energy equation becomes:

$$- P_l \, dV_l = C_{\rho_e} T_e \, dm_e - C_{\rho_a} T_a \, dm_a + C_{v_e} T_e \, dm_e$$

$$+ C_{v_e} m_e \, dT_e + C_{v_a} T_a \, dm_a + C_{v_a} m_a \, dT_a$$

Dividing throughout by T_e, and putting $C_{v_a} m_a \, dT_a = 0$ since it is assumed that there is no change in internal energy of the entering air, gives the result:

$$- \frac{P_l \, dV_l}{T_e} = C_{\rho_e} \, dm_e - C_{\rho_a} \frac{T_a}{T_e} \, dm_a + C_{v_e} \, dm_e$$

$$+ C_{v_e} m_e \frac{dT_e}{T_e} + C_{v_a} \frac{T_a}{T_e} \, dm_a \qquad (3.8\text{-}6)$$

From the characteristic gas equation applied to the exhaust gas region:

$$T_e = \frac{P_l V_e}{m_e R_e}$$

which on taking logarithms and differentiating gives:

$$\frac{dT_e}{T_e} = \frac{dP_l}{P_l} + \frac{dV_e}{V_e} - \frac{dm_e}{m_e}$$

Substituting in equation (3.8-6) for $\frac{d\ T_e}{T}$, dividing throughout by $m_e\ C_{v_e}$ and rearranging gives:

$$\frac{d\ P_1}{P_1} = \frac{C_{\rho_a}}{C_{v_e}}\ \frac{T_a}{T_e}\ \frac{d\ m_a}{m_e} - \frac{C_{\rho_e}}{C_{v_e}}\ \frac{d\ m_a}{m_e} - \frac{d\ V_e}{V_e} - \frac{P_1\ d\ V_1}{T_e\ C_{v_e}\ m_e}$$

$$- \frac{C_{v_a}}{C_{v_e}}\ \frac{T_a}{T_e}\ \frac{d\ m_a}{m_e} \qquad (3.8\text{-}7)$$

Putting $R_e = (C_{\rho_e} - C_{v_e})$ in the characteristic gas equation for the exhaust gas region gives:

$$\frac{P_1}{m_e\ T_e} = \frac{C_{\rho_e} - C_{v_e}}{V_e}$$

Also $V_e = V_1 - V_a$

hence $d\ V_e = d\ V_1 - d\ V_a$

Substituting for $\frac{P_1}{m_e\ T_e}$ and $d\ V_e$ in equation (3.8-7) replacing $\frac{C_{\rho_e}}{C_{v_e}}$ by γ_e and rearranging gives the result:

$$\frac{d\ P_1}{P_1} = \frac{1}{V_1 - V_a}\left[\frac{C_{\rho_a}\ T_a}{P_1}\ (\gamma_e - 1)\ d\ m_a + d\ V_a - \gamma_e\ d\ V_1\right]$$

$$- \gamma_e\ \frac{d\ m_e}{m_e} \qquad (3.8\text{-}8)$$

or written in finite difference form:

$$\frac{\Delta P_1}{P_1} = \frac{1}{V_1 - V_a}\left[\frac{C_{\rho_a} T_a}{P_1}(\gamma_e - 1)\Delta m_a + \Delta V_a - \gamma_e \Delta V_1\right]$$

$$- \gamma_e \frac{\Delta m_e}{m_e} \qquad (3.8\text{-}9)$$

where the variables are the mean values for the step under consideration.

For the period of blowdown only, i.e. for the period when the exhaust ports only are open, all the terms involving the incoming air are zero and equation (3.8-9) reduces to:

$$\frac{\Delta P_1}{P_1} = -\gamma_e \left(\frac{\Delta V_1}{V_1} + \frac{\Delta m_e}{m_e}\right) \qquad (3.8\text{-}10)$$

The expressions for the associated changes in temperature, density and local acoustic velocity for the exhaust gas region are obtained by logarithmic differentiation of the characteristic gas equation and the isentropic state relationship, i.e. $\frac{P_1}{\rho_e} = R_e T_e$ and $\frac{P_1}{\rho_e^{\gamma}} = \text{constant}$.

Thus:

$$\frac{\Delta T_e}{T_e} = \frac{\gamma_e - 1}{\gamma_e} \frac{\Delta P_1}{P_1} \qquad (3.8\text{-}11)$$

$$\frac{\Delta \rho_e}{\rho_e} = \frac{1}{\gamma_e} \frac{\Delta P_1}{P_1} \qquad (3.8\text{-}12)$$

$$\frac{\Delta a_e}{a_e} = \frac{\gamma_e - 1}{2\gamma_e} \frac{\Delta P_1}{P_1} \qquad (3.8\text{-}13)$$

Equations (3.8-9) to (3.8-13) inclusive, completely define the state parameters for all cylinder changes during the blowdown and scavenge periods.

(c) Open end reflection.

At the open end of the exhaust pipe conditions of outflow and inflow have to be considered.

1. Outflow

Only subsonic outflow can occur in the problem being considered; and if the inertia of the fluid outside the pipe exit is neglected, the state of the gas in the plane of the open end can be assumed to be that of the surroundings. Hence, under all conditions of subsonic outflow the pressure ratio $\frac{P_2}{P_o}$ in the exit plane can be taken as 1.0, and the state at this plane can be represented by a horizontal line through the origin of the state diagram.

2. Inflow

For inflow, the pressure in the plane of the open end is no longer that of the surroundings but must satisfy the theoretical relationship for the Borda mouthpiece configuration.

Assuming isentropic quasi-steady flow from the surroundings to the pipe inlet plane gives the following equations:

Energy equation:

$$\frac{\gamma}{\gamma-1}\frac{P_o}{\rho_o} = \frac{\gamma}{\gamma-1}\frac{P_2}{\rho_2} + \frac{u_2^2}{2}$$

from which $$\frac{\gamma P_2}{\rho_2} = a_o^2\left[1 - \frac{\gamma-1}{2}\left(\frac{u_2}{a_o}\right)^2\right] \qquad (3.8\text{-}14)$$

Momentum equation:

$$P_o - P_2 = \rho_2 u_2^2$$

from which $$\frac{\gamma P_2}{\rho_2} = \frac{\gamma u_2^2}{\frac{P_o}{P_2} - 1} \qquad (3.8\text{-}15)$$

Equating equations (3.8-14) and (3.8-15), and rearranging gives:

$$\frac{P_o}{P_2} = 1 + \frac{\gamma}{\left(\frac{a_o}{u_2}\right)^2 - \frac{(\gamma-1)}{2}} \qquad (3.8\text{-}16)$$

For inflow, all state points in the plane of the pipe open end must lie on the curve defined by equation (3.8-16) and this curve can be plotted on the state diagram. Also, in the derivation of this equation no assumption was made with regard to the flow being sonic or subsonic and hence it is valid for all conditions of flow.

Thus, for both inflow and outflow at the open end of the pipe, the boundary conditions can be directly superimposed upon the state diagram and separate boundary diagrams, as in the case of the cylinder ports, are not required.

(d) Application of the boundary diagrams for the cylinder

To take the variation in specific heats with temperature into account for the products of combustion in the cylinder, strictly requires the use of a boundary diagram drawn for the mean value of γ for the cylinder step under consideration. However, it is considered adequate to use two boundary diagrams for both inflow and outflow drawn for two values of γ. The values of mass flow parameter (M), dimensionless pressure ratio $\left[\bar{X} = \left(\frac{P_2}{P_o}\right)^{\frac{\gamma-1}{2\gamma}}\right]$ and dimensionless particle velocity ($\bar{U} = \frac{u_2}{a_o}$) for the actual value of γ are then determined by a linear interpolation between the results from the two diagrams. Thus, at the cylinder exhaust ports, two imaginary state diagrams, one for each value of γ used for the boundary diagrams, must be inferred and two complete sets of calculations performed to obtain the cylinder and pipe parameter changes.

To illustrate the method of analysis, the two boundary diagram values of γ (and the associated parameters) will be denoted by the index marks ' and "; and in the following explanation of the method of solution, all remarks, although in the singular, apply to both cases where applicable.

Consider the region of state 9.8, commencing 't' seconds after exhaust port opening, see the position diagram Fig.22. The initial values of the parameters for this step are given by the values at the end of the preceeding step

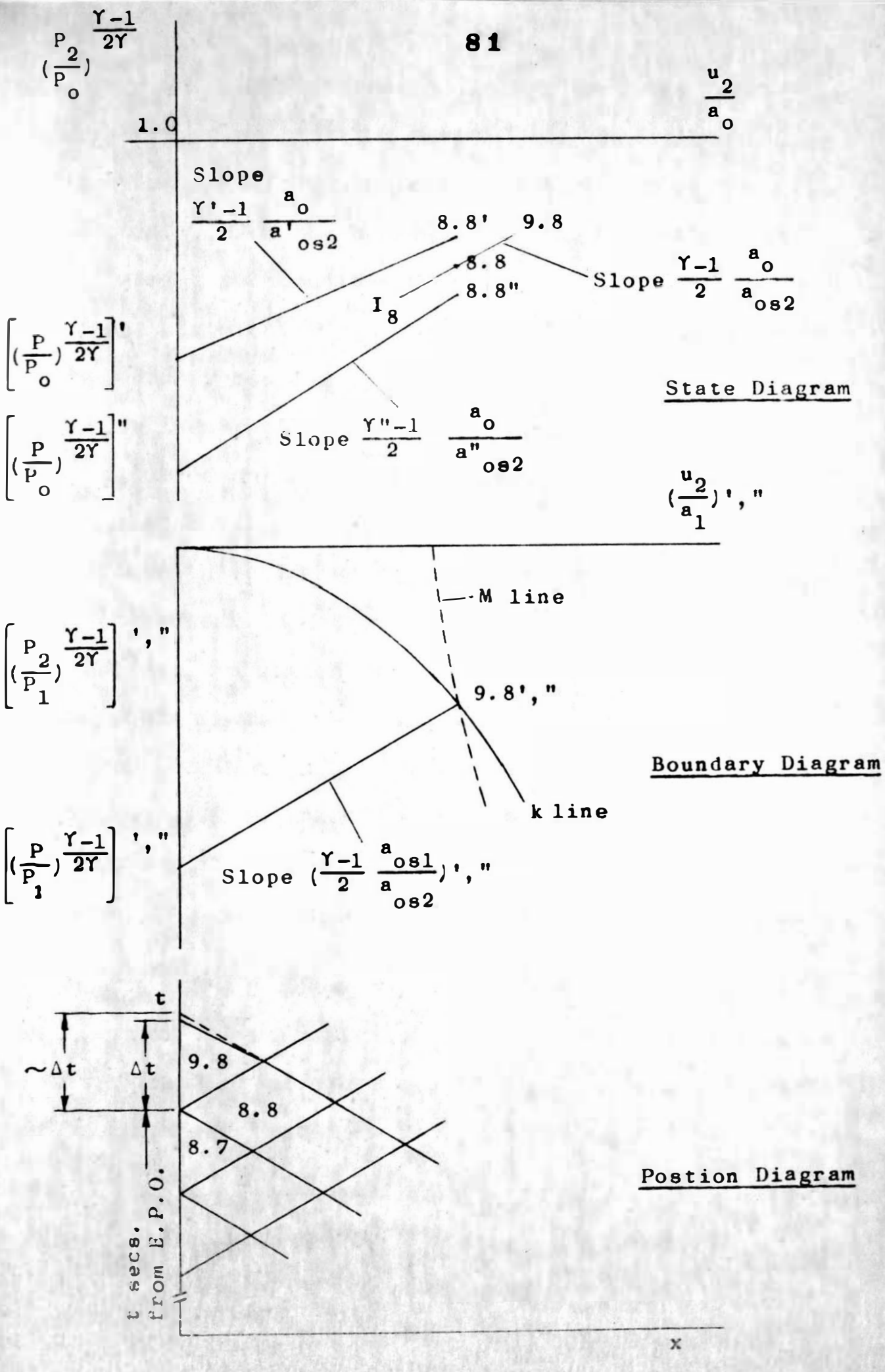
$(\frac{P_2}{P_o})^{\frac{\gamma-1}{2\gamma}}$
1.0
$\frac{u_2}{a_o}$
Slope $\frac{\gamma'-1}{2}$ $\frac{a_o}{a'_{os2}}$
8.8'
9.8
8.8
8.8"
I_8
Slope $\frac{\gamma-1}{2}$ $\frac{a_o}{a_{os2}}$
$\left[(\frac{P}{P_o})^{\frac{\gamma-1}{2\gamma}}\right]'$
$\left[(\frac{P}{P_o})^{\frac{\gamma-1}{2\gamma}}\right]''$
Slope $\frac{\gamma''-1}{2}$ $\frac{a_o}{a''_{os2}}$
State Diagram
$(\frac{u_2}{a_1})',''$
M line
$\left[(\frac{P_2}{P_1})^{\frac{\gamma-1}{2\gamma}}\right]',''$
9.8',"
k line
Boundary Diagram
$\left[(\frac{P}{P_1})^{\frac{\gamma-1}{2\gamma}}\right]',''$
Slope $(\frac{\gamma-1}{2}$ $\frac{a_{osl}}{a_{os2}})',''$
t
$\sim\Delta t$
Δt
9.8
8.8
8.7
t secs. from E.P.O.
x
Postion Diagram

Fig.22

(region 8.7). Using these initial values, the first approximate value of k for step 9.8 can be evaluated, and knowing k it is possible to position the approximate state point 9.8 on the boundary diagram by satisfying the following two conditions.

(i) the state point 9.8 must lie on the k line in the boundary diagram.

(ii) for isentropic flow, state point 9.8 must be situated on the Π_8 characteristic through state point 8.8.

Since the solution requires an iteration procedure, it is convenient to determine the required state point isentropically and then apply the correction for irreversible flow.

For the first approximation to the state 9.8, the known state 8.8 is transferred from the state diagram to the boundary diagram. This entails the transfer of a characteristic between two different sets of co-ordinates, viz: $\left[\left(\frac{P_2}{P_o}\right)^{\frac{\gamma-1}{2\gamma}}\right]'$," and $\left[\frac{u_2}{a_o}\right]'$," to $\left[\left(\frac{P_2}{P_o}\right)^{\frac{\gamma-1}{2\gamma}}\right]'$," and $\left[\left(\frac{u_2}{a_1}\right)\right]'$,". The slope of the characteristic in the state diagram which is to be transferred, is given by equation (3.5-15) in which the friction and heat transfer terms are neglected.

i.e. $(\Delta \bar{U})'_{\Pi}$," $= \left[+\frac{2}{\gamma-1}\ \frac{a_{os}}{a_o}\ (\Delta \bar{X})_{\Pi}\right]'$," (3.8-17)

From equation (3.8-17), the slope of the characteristic relating $\bar{X}$ and $\bar{U}$ in the state diagram is

$$\left(+\frac{\gamma-1}{2}\frac{a_o}{a_{os2}}\right)',''.$$

The cylinder parameters, P_1 and a_1, are taken as constant and equal to the mean values for the region, therefore equation (3.8-17) can be written as:

$$\left[\left(\frac{P_1}{P_o}\right)^{\frac{\gamma-1}{2\gamma}}\Delta\left(\frac{P_2}{P_1}\right)^{\frac{\gamma-1}{2\gamma}}\right]','' = \left[\frac{\gamma-1}{2}\frac{a_o}{a_{os2}}\cdot\frac{a_1}{a_o}\Delta\left(\frac{u_2}{a_1}\right)\right]','' \qquad (3.8\text{-}18)$$

The cylinder process is assumed to be isentropic, hence, $\frac{a_1}{a_{os1}} = \left(\frac{P_1}{P_o}\right)^{\frac{\gamma-1}{2\gamma}}$, and substitution in equation (3.8-18) gives the result:

$$\left[\Delta\left(\frac{P_2}{P_1}\right)^{\frac{\gamma-1}{2\gamma}}\right]','' = \left[\frac{\gamma-1}{2}\frac{a_{os1}}{a_{os2}}\Delta\left(\frac{u_2}{a_1}\right)\right]','' \qquad (3.8\text{-}19)$$

From equation (3.8-19), the slope of the characteristic relating $\left[\left(\frac{P_2}{P_1}\right)^{\frac{\gamma-1}{2\gamma}}\right]',''$ and $\left[\left(\frac{u_2}{a_1}\right)\right]',''$ in the boundary diagram is $\left(+\frac{\gamma-1}{2}\frac{a_{os1}}{a_{os2}}\right)',''$. The intercept of this characteristic with the ordinate axis in the boundary diagram is given by:

$$\left[\left(\frac{P}{P_1}\right)^{\frac{\gamma-1}{2\gamma}}\right]','' = \left[\left(\frac{P}{P_o}\right)^{\frac{\gamma-1}{2\gamma}}\left(\frac{P_o}{P_1}\right)^{\frac{\gamma-1}{2\gamma}}\right]','' \qquad (3.8\text{-}20)$$

where $\left[\left(\frac{P}{P_o}\right)^{\frac{\gamma-1}{2\gamma}}\right]'$," is the intercept with the ordinate axis in the state diagram of the characteristic, slope $\left(\frac{\gamma-1}{2}\frac{a_o}{a_{os2}}\right)'$," , drawn through the inferred state point (8.8)'," . The value used for P_1 in equation (3.8-20) for the first approximation is the initial value for the cylinder step.

Thus the characteristic on which state point 9.8 is situated, to the first approximation, is completely defined in the boundary diagram. Its intersection with the k line locates the state point and gives the pipe to cylinder pressure ratio $\left[\left(\frac{P_2}{P_1}\right)^{\frac{\gamma-1}{2\gamma}}\right]'$,", the exhaust gas mass flow parameter M_e',", and the dimensionless particle velocity $\left(\frac{u_2}{a_1}\right)'$,".

Assuming that region 9.8 comes within the scavenge period, ΔP_1 cannot be evaluated until the air mass flow is determined. Since the entering air is at the ambient condition, γ is constant, and the mass flow parameter can be determined directly from the boundary chart evaluated for $\gamma = 1.4$, the value used for air.

The induction duct, being very short, is assumed to be a neutral system, i.e. one in which wave action can be neglected. Hence, the inflow mass parameter M_a is found by plotting on the inflow boundary diagram, Fig.21, the steady flow isentropic ellipse relationship, viz:

$$\frac{(\frac{u_2}{a_1})^2}{\frac{2}{\gamma-1}(\frac{a_a}{a_1})^2} + \frac{\left[(\frac{P_2}{P_1})^{\frac{\gamma-1}{2\gamma}}\right]^2}{\left[(\frac{P_o}{P_1})^{\frac{\gamma-1}{2\gamma}}\right]^2} = 1 \qquad (3.8\text{-}21)$$

where a_a is the ambient local acoustic velocity. This relationship is derived by assuming that there is no loss of total head pressure between the ambient conditions and the boundary of the inlet ports.

The intersection of the line given by equation (3.8-21) and the appropriate k line for the air ports gives the required mass inflow parameter M_a for the step.

The mass flow of air and exhaust gases is then determined from the mass flow parameter definition, viz:

$$\Delta m_1 = M a_1 \rho_1 A_2 \Delta t$$

where Δt is the approximate time for the cylinder step obtained by extending the field boundary of region 8.8, and the values used for M, a_1, ρ_1, and A_2 are those appropriate to the air and exhaust gas regions respectively.

Use of the Δm_a obtained yields the value of the mean V_a and ΔV_a for the step, and substitution of these, together with the other variables in equation (3.8-8) gives the first approximation to ΔP_1. The mean values of P_1, T_e, ρ_e, a_e and γ_e for the cylinder step can now be evaluated using equations (3.8-11), (3.8-12), and (3.8-13), and the γ_e variation curve Fig. 29 .

Application of the following identities

$$\left[\left(\frac{P_2}{P_o}\right)^{\frac{\gamma-1}{2\gamma}}\right]','' = \left[\left(\frac{P_2}{P_1}\right)^{\frac{\gamma-1}{2\gamma}} \left(\frac{P_1}{P_o}\right)^{\frac{\gamma-1}{2\gamma}}\right]',''$$

and $$\left(\frac{u_2}{a_o}\right)','' = \left[\left(\frac{u_2}{a_1}\right)\left(\frac{a_1}{a_o}\right)\right]',''$$

gives the pressure ratio and particle velocity at the port boundary within the exhaust pipe, and the approximate field boundaries to region 9.8 can be constructed in the position diagram using equation (3.5-5).

Using the nearer approximation to Δt, and the calculated approximate mean values for the cylinder step, the above procedure is repeated until satisfactory convergence of the value of ΔP_1 is obtained.

Having determined the state of region 9.8 for isentropic flow, this now has to be corrected for the effects of friction and heat transfer. The correction is effected by transferring state point (8.8)',' to the boundary diagram and drawing a line of slope $\left[\Delta\left(\frac{u_2}{a_1}\right)/\Delta\left(\frac{P_2}{P_1}\right)^{\frac{\gamma-1}{2\gamma}}\right]',''$ from it to the appropriate k line, see Fig. 23. State point (8.8)',' is transferred to the boundary diagram using the value of P_1 appropriate to region 9.8, and the slope of the characteristic through (8.8)',' is obtained as follows:-

From the characteristic state equation (3.5-15) written in finite difference form:

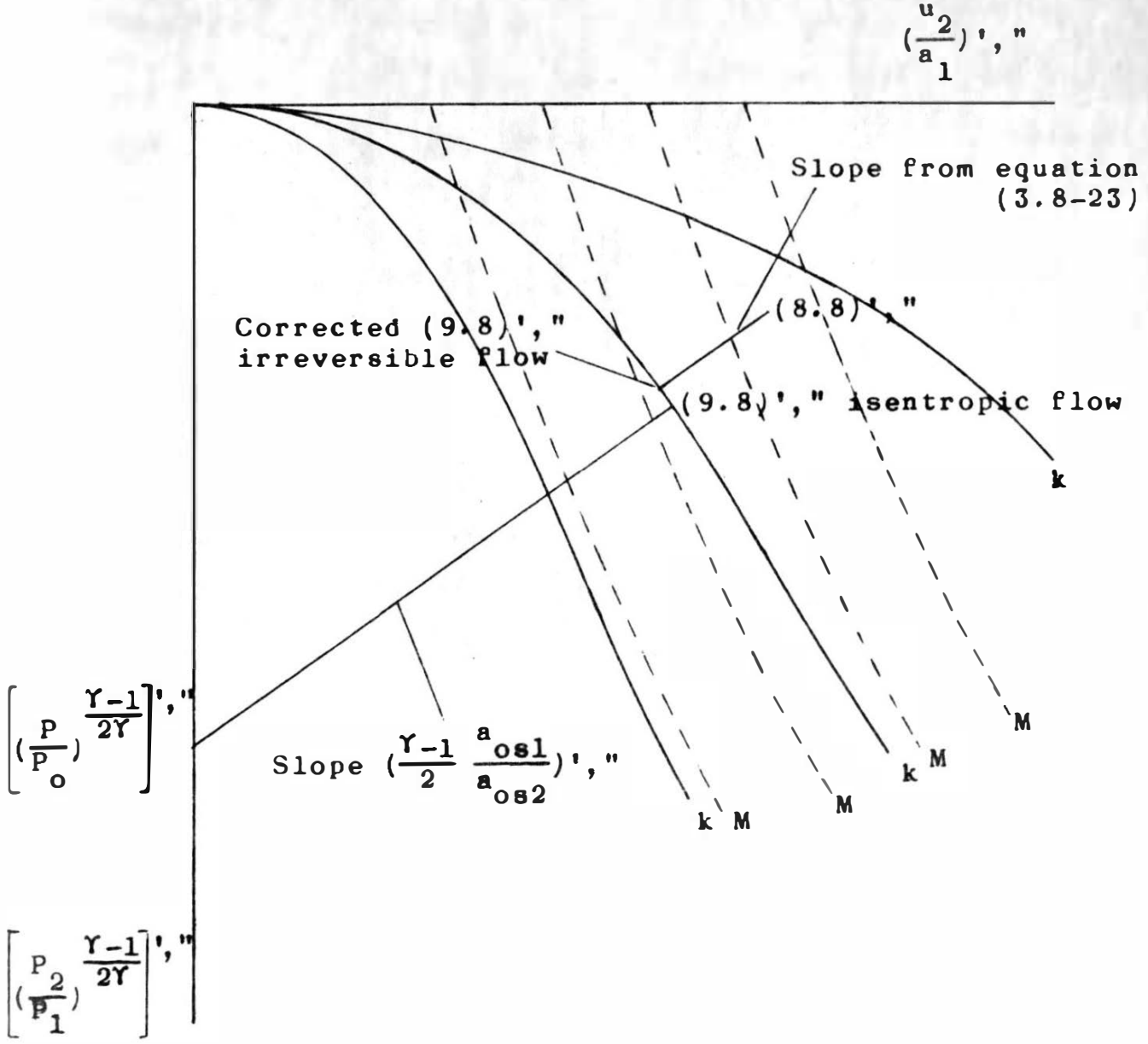

Boundary Diagram

Fig. 23.

$$(\Delta \bar{U})'_{II}{}'' = \left[+\frac{2}{\gamma-1}\frac{a_{os_2}}{a_o}(\Delta \bar{X})_{II}\right]'' + \left[(\Delta \bar{U}_{f+q})_{II}\right]'' \quad (3.8\text{-}22)$$

where $(\Delta \bar{U}_{f+q})_{II}$ represents the combined effect of friction and heat transfer.

This characteristic can be transferred to the boundary diagram by multiplying throughout by $\frac{a_o}{a_{os_1}}(\frac{P_o}{P_1})^{\frac{\gamma-1}{2\gamma}}$, giving:

$$(\Delta \frac{u_2}{a_1})'' = \left[+\frac{2}{\gamma-1}\frac{a_{os2}}{a_{os1}}\Delta(\frac{P_2}{P_1})^{\frac{\gamma-1}{2\gamma}}\right]'' + \left[(\Delta \bar{U}_{f+q})\frac{a_o}{a_{os1}} \times (\frac{P_o}{P_1})^{\frac{\gamma-1}{2\gamma}}\right]''$$

$$\text{i.e.} \left[\frac{\Delta(\frac{u_2}{a_1})}{\Delta(\frac{P_2}{P_1})^{\frac{\gamma-1}{2\gamma}}}\right]'' = \left[\frac{2}{\gamma-1}\frac{a_{os2}}{a_{os1}}\right]'' + \left[\frac{a_o}{a_{os1}}(\Delta \bar{U}_{f+q})\frac{(\frac{P_o}{P_1})^{\frac{\gamma-1}{2\gamma}}}{\Delta(\frac{P_2}{P_1})^{\frac{\gamma-1}{2\gamma}}}\right]'' \quad (3.8\text{-}23)$$

The previously determined provisional value of $\Delta(\frac{P_2}{P_1})^{\frac{\gamma-1}{2\gamma}}$ and the mean values of the variables between regions 8.8 and 9.8 are now used in equation (3.8-23).

The corrected state point (9.8)'' in the boundary diagram gives new values of $(\frac{P_2}{P_1})^{\frac{\gamma-1}{2\gamma}}$, M_e and $(\frac{u_2}{a_1})$ for step 9.8. Using these values, the incremental state

changes in the cylinder are recalculated and a more accurate state point 9.8 plotted, together with the associated correction of the field boundaries in the position diagram.

The procedure is repeated using the last found values until satisfactory convergence of the state changes is obtained.

During the early part of blowdown, choking of the ports occurs, and while this condition persists the mass flow number M_e is unaffected by changes occurring in the exhaust pipe. Hence correction for secondary effects within the pipe will not influence the state changes in the cylinder. Also, for the period of blowdown equation (3.8-10) is used to obtain ΔP_1 instead of equation (3.8-9).

3.9. Summary of all equations.

For convenience and reference, all the equations necessary for the solution of the problem are given below.

Section 3.3.

Mass continuity

$$\rho \frac{\partial u}{\partial x} + u \frac{\partial \rho}{\partial x} + \frac{\partial \rho}{\partial t} = 0 \qquad (3.3\text{-}1)$$

Momentum

$$\frac{\partial u}{\partial t} + u \frac{\partial u}{\partial x} + \frac{1}{\rho} \frac{\partial P}{\partial x} + F = 0 \qquad (3.3\text{-}2)$$

Energy

$$\frac{\partial P}{\partial t} + u \frac{\partial P}{\partial x} - a^2 \left(\frac{\partial \rho}{\partial t} + u \frac{\partial \rho}{\partial x}\right) - (\gamma - 1)(\rho u F + q) = 0 \qquad (3.3\text{-}5)$$

where $F = \frac{f}{2d} \frac{u}{|u|} u^2$

and $a^2 = \frac{\gamma P}{\rho}$

If friction and heat transfer effects are neglected, i.e. $q = F = 0$, then the flow is isentropic, the energy equation becomes redundant and is replaced by the isentropic state relationship, and the resulting equations of flow are:-

Mass continuity:- as equation (3.3-1) above,

Momentum

$$\rho \frac{\partial u}{\partial t} + \rho u \frac{\partial u}{\partial x} + a^2 \frac{\partial \rho}{\partial x} = 0 \qquad (3.3\text{-}7)$$

State equation

$$\frac{P}{\rho^\gamma} = \text{constant}$$

Section 3.4.

The entropy gradient is given by:-

$$\frac{2a_{os}}{1a_{os}} = 1 + \frac{(\gamma-1)}{2} \frac{f}{2d} \frac{u}{|u|} \left(\frac{u}{a_{os}}\right)^2 \frac{\Delta t}{\left(\frac{P}{P_o}\right)^{\frac{\gamma-1}{\gamma}}} + \frac{\gamma-1}{2\gamma} \frac{q}{P} \Delta t \qquad (3.4\text{-}7)$$

where the prefixes 1 and 2 refer to the initial and final conditions respectively.

Section 3.5.

The physical characteristics are:-

$$\left(\frac{dx}{dt}\right)_{I,\,II} = u \pm a \quad \text{(Mach lines)} \qquad (3.5\text{-}5)$$

$$\frac{dx}{dt} = u \quad \text{(Path lines)} \qquad (3.5\text{-}6)$$

The state characteristics are:-

$$(d\,\bar{U})_{I,\,II} = \mp \frac{2}{\gamma-1} \frac{a_{os}}{a_o} (d\,\bar{X})_{I,\,II} - (d\,\bar{U}_f)_{I,\,II} + (d\,\bar{U}_q)_{I,\,II} \qquad (3.5\text{-}15)$$

where

$$(d\,\bar{U}_f)_{I,\,II} = \frac{f}{2d} \frac{u}{|u|} \frac{u^2}{a_o} \left[1 \mp (\gamma-1) \frac{u}{a}\right] (dt)_{I,\,II}$$

and

$$(d\,\bar{U}_q)_{I,\,II} = \pm \frac{\gamma-1}{\gamma} \frac{a\,q}{a_o P} (d\,t)_{I,\,II}$$

and all parameters of state are the mean values between the states under consideration.

Section 3.7.

At a temperature discontinuity:-

$$\frac{a''}{a''_{os}} = \frac{K_3}{1 + K_3 K_4} \qquad (3.7\text{-}13)$$

where

$$K_3 = \left\{ \frac{(\gamma'-1)}{2}(\bar{U}_1 - \bar{U}_2)\frac{a_o}{a'_{os}} + \frac{(\gamma'-1)a_2 + (\gamma''-1)a_1}{(\gamma''-1)a'_{os}} \right.$$

$$\left. - \frac{(\gamma'-1)}{2}\frac{a_o}{a'_{os}}\left[(\Delta \bar{U}'_{f+q})_I + (\Delta \bar{U}''_{f+q})_{II}\right] \right\}^{\frac{\gamma''-1}{\gamma'-1}\frac{\gamma'}{\gamma''}}$$

and

$$K_4 = \frac{2\gamma'}{\gamma''(\gamma'-1)}\frac{a''_{os}}{a_o}\frac{1}{(\bar{U}_1 - \bar{U}_2) + \frac{2}{\gamma''-1}\frac{a_2}{a_o} + \frac{2}{\gamma'-1}\frac{a_1}{a_o} - \left[(\Delta \bar{U}'_{f+q})_I + (\Delta \bar{U}''_{f+q})_{II}\right]}$$

Section 3.8.

(a) Boundary diagrams.

Outflow from the cylinder is defined by equations (3.8-1)(3.8-2) and (3.8-3), and these are shown plotted in Figs. 18 and 19 for values of $\gamma = 1.3$ and $\gamma = 1.4$ respectively.

Inflow into the cylinder is defined by equations (3.8-4) and (3.8-5), and these are shown plotted in Figs. 20 and 21 for values of $\gamma = 1.3$ and $\gamma = 1.4$ respectively.

The steady flow isentropic ellipse for inflow with zero pipe length is:-

$$\frac{(\frac{u_2}{a_1})^2}{\frac{2}{\gamma-1}(\frac{a_a}{a_1})^2} + \frac{\left[(\frac{P_2}{P_1})^{\frac{\gamma-1}{2\gamma}}\right]^2}{\left[(\frac{P_o}{P_1})^{\frac{\gamma-1}{2\gamma}}\right]^2} = 1 \qquad (3.8\text{-}21)$$

The slope of the transferred characteristic to the boundary diagram, which gives the correction for irreversibility in the pipe is given by:-

$$\frac{\Delta(\frac{u_2}{a_1})}{\Delta(\frac{P_2}{P_1})^{\frac{\gamma-1}{2\gamma}}} = \frac{2}{\gamma-1}\frac{a_{os2}}{a_{os1}} + \frac{a_o}{a_{os1}}(\Delta \bar{U}_{f+q})\frac{(\frac{P_o}{P_1})^{\frac{\gamma-1}{2\gamma}}}{\Delta(\frac{P_2}{P_1})^{\frac{\gamma-1}{2\gamma}}} \qquad (3.8\text{-}23)$$

4. Procedure.

4.1. Determination of the system parameters.

Included in this Section is the preliminary experimental work to obtain the fuel injection system characteristics, and the determination, either by calculation or measurement, of all the parameters required to perform the evaluation of the theoretical analyses.

Fuel pump calibration

The calibration of the fuel pump was necessary to enable the pump rack position to be determined accurately and quickly knowing the air mass flow at any given engine speed.

To calibrate the fuel pump the injection nozzle was removed from the engine cylinder and allowed to discharge into a collector vessel. At selected motored engine speeds, and pump rack micrometer settings which varied from 0.75 to 3.00, the fuel flow was measured by means of the pipettes in the fuel line for incremental rack settings of 0.15. The engine speed was accurately monitored, with the aid of a stop watch and the revolution counter, for the speed range 600 to 1500 rpm. by increments of 100 rpm. Corrections, where necessary, for engine speed variation from the selected datum was made to all fuel flow measurements.

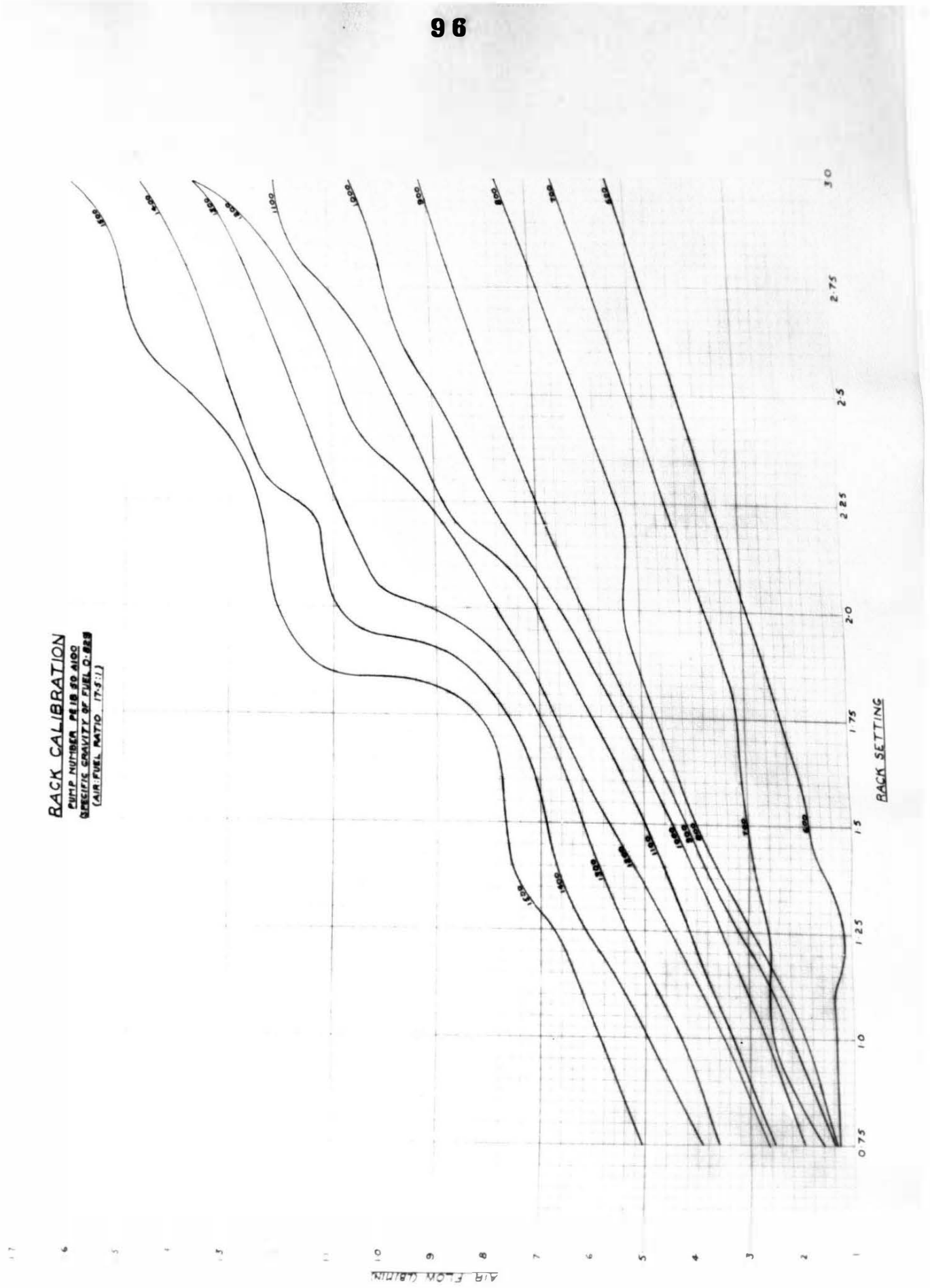
BACK CALIBRATION
PUMP NUMBER PLIB 80 A100
SPECIFIC GRAVITY OF FUEL 0·838
(AIR:FUEL RATIO 17·5:1)
AIR FLOW (lb/min)
BACK SETTING
0·75
1·0
1·25
1·5
1·75
2·0
2·25
2·5
2·75
3·0

Fig.24

The fuel flow rates were then converted to air flow rates for an air-fuel ratio of 17.5 to 1, which gives an excess air for combustion of 25% when using Shell Gas Oil.

The resulting family of curves are shown in Fig.24.

Cylinder parameters.

The evaluation of the cylinder gas parameter changes occurring during the blowdown and scavenge period requires a knowledge of the variation with crank angle of the cylinder volume, the ratio of port area to pipe area and the hydraulic radius of both the air and exhaust ports. The changes occurring in these physical parameters were calculated from the geometry of the engine system, and are shown plotted in Figs. 25, 26 and 27 respectively.

A further parameter required is the coefficient of discharge (C_d) for the engine ports. Owing to the experimental difficulties, no data is available concerning the variation of the C_d term for a port system at the high temperatures encountered in a firing engine. Using the cylinder liner and air as the fluid medium, previous research[4] has, however, been carried out to determine the coefficient of discharge at temperatures up to 160°F, and Fig.28 shows the variation in C_d with modified Reynolds number (R_m) , for a variation in pressure ratio across

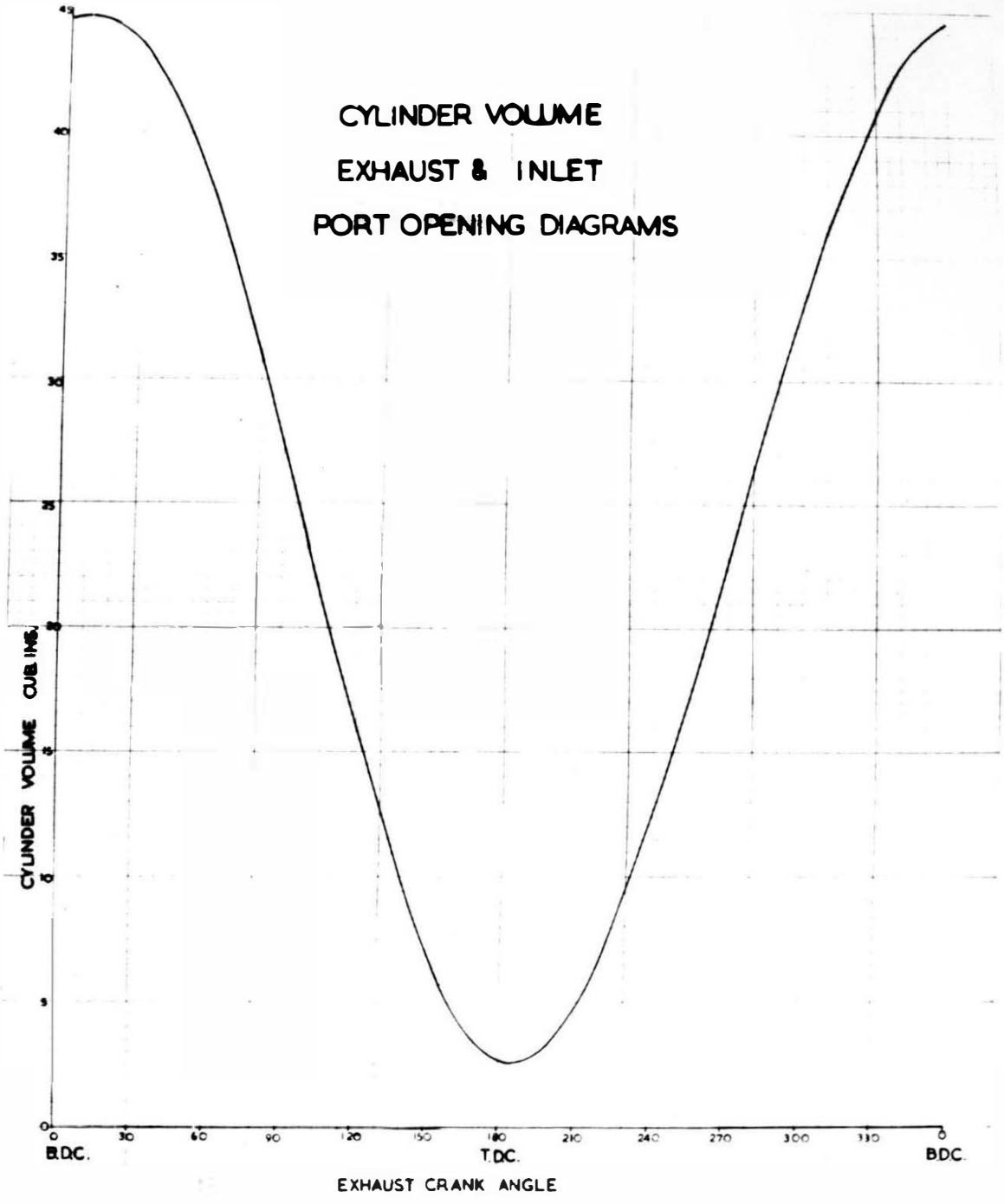
CYLINDER VOLUME
EXHAUST & INLET
PORT OPENING DIAGRAMS
CYLINDER VOLUME CUB. INS.
0
5
35
B.D.C.
30
60
90
120
150
180
T.D.C.
210
240
270
300
330
B.D.C.
EXHAUST CRANK ANGLE

Fig.25

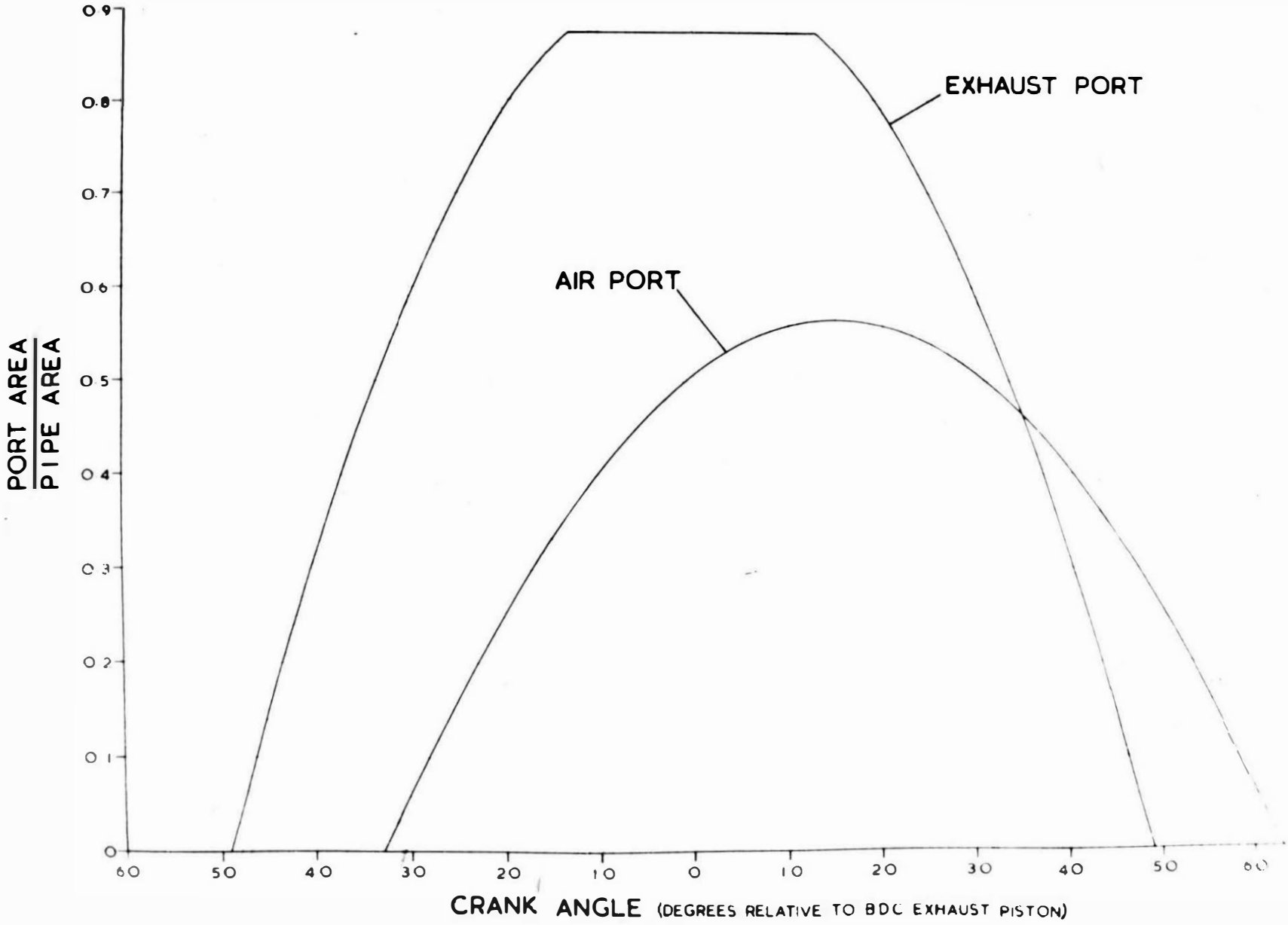
EXHAUST PORT
AIR PORT
PORT AREA / PIPE AREA
0.9
0.8
0.7
0.6
0.5
0.4
0.3
0.2
0.1
0
60
50
40
30
20
10
0
10
20
30
40
50
60
CRANK ANGLE (DEGREES RELATIVE TO BDC EXHAUST PISTON)

Fig. 26

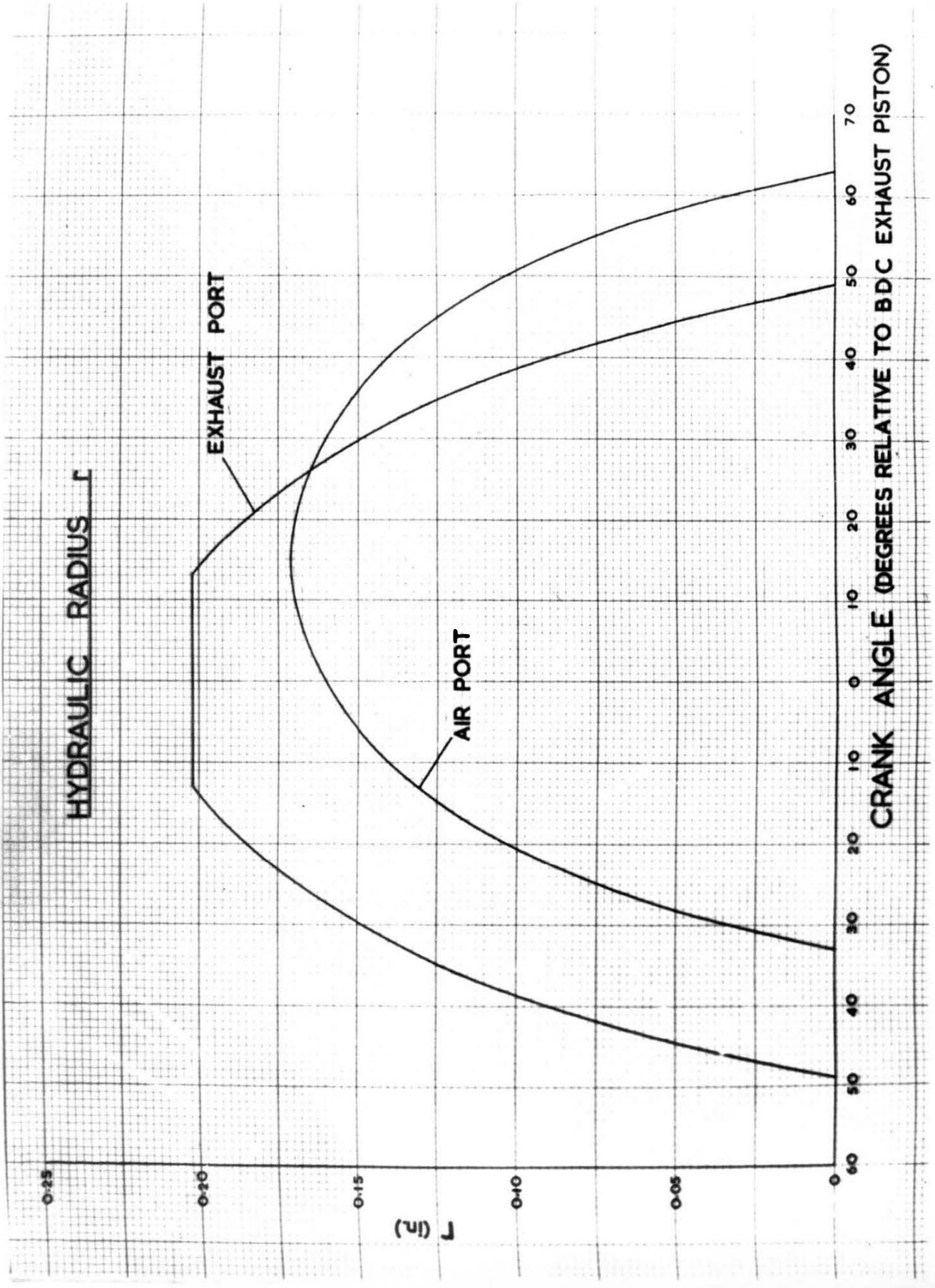
HYDRAULIC RADIUS r
EXHAUST PORT
AIR PORT
r (in)
0·25
0·20
0·15
0·10
0·05
0
60
50
40
30
20
10
0
10
20
30
40
50
60
70
CRANK ANGLE (DEGREES RELATIVE TO BDC EXHAUST PISTON)

Fig. 27

the cylinder ports.

Modified Reynolds number (R_m) is defined as:

$$R_m = \frac{a_1 r}{\nu} \qquad (4.1\text{-}1)$$

where a_1 is the instantaneous local acoustic velocity of the cylinder contents,

r is the hydraulic radius of the ports,

ν is the instantaneous kinematic viscosity of the cylinder contents.

Although no direct evidence is available to confirm that Fig.28 is applicable at high gas temperatures, the relationships shown therein have been accepted.

Exhaust gas analysis

To facilitate the evaluation of the characteristic gas constant (R) for the exhaust gases of this engine, and the variation of the ratio of the specific heats (γ) and viscosity (μ) with temperature of these exhaust gases, Orsat analyses were taken at various engine loads and engine speeds using the constant air-fuel ratio of 17.5 to 1. No significant variation in gas composition was found, and the mean composition by weight for a number of samples is given below:-

Carbon dioxide	13.93%
Carbon monoxide	1.01%
Oxygen	4.57%
Nitrogen	73.11%
Water vapour	7.38%

RELATION BETWEEN C_d, R_m & $\frac{P}{P_o}$

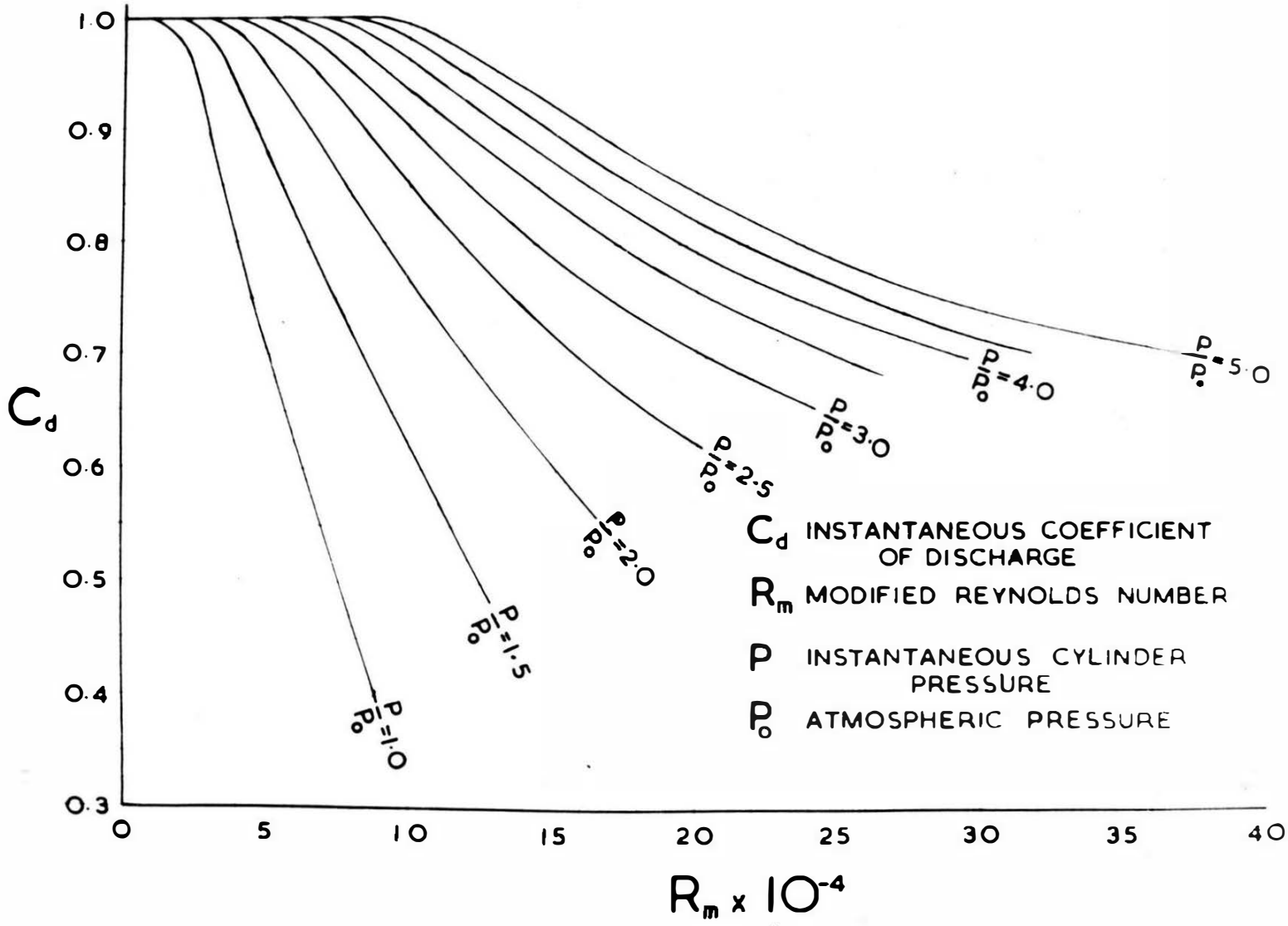

Fig. 28

The water vapour content was determined from a knowledge of the fuel used and the assumption that all the hydrogen content burned to water vapour.

The characteristic gas constant for the exhaust gas, using the mass mean of the values for the individual constituents is:

$R = 97.80$ ft.lb./lb.°C.

Variation of the ratio of the specific heats (γ) for the exhaust gases with temperature.

The values of the specific heats at constant pressure and constant volume of the constituents for the exhaust gases were obtained from gas tables[7] for a temperature range of 500°K to 1180°K. The mass mean values for the specific heats were then calculated using the mean exhaust gas analysis and their ratio (γ) is shown plotted in Fig.29.

Viscosity of exhaust gases.

The nomogram[8], Fig.30, gives the relationship between the absolute viscosity and temperature of the individual gas constituents.

The mass mean value for viscosity was evaluated from the values for the exhaust gas constituents for a range of temperatures and superimposed upon the nomogram. These lines were found to intersect within a very small region, the centre of which is shown on Fig.30 as the mass mean. This mass mean point was used to determine the absolute viscosity of the exhaust gases.

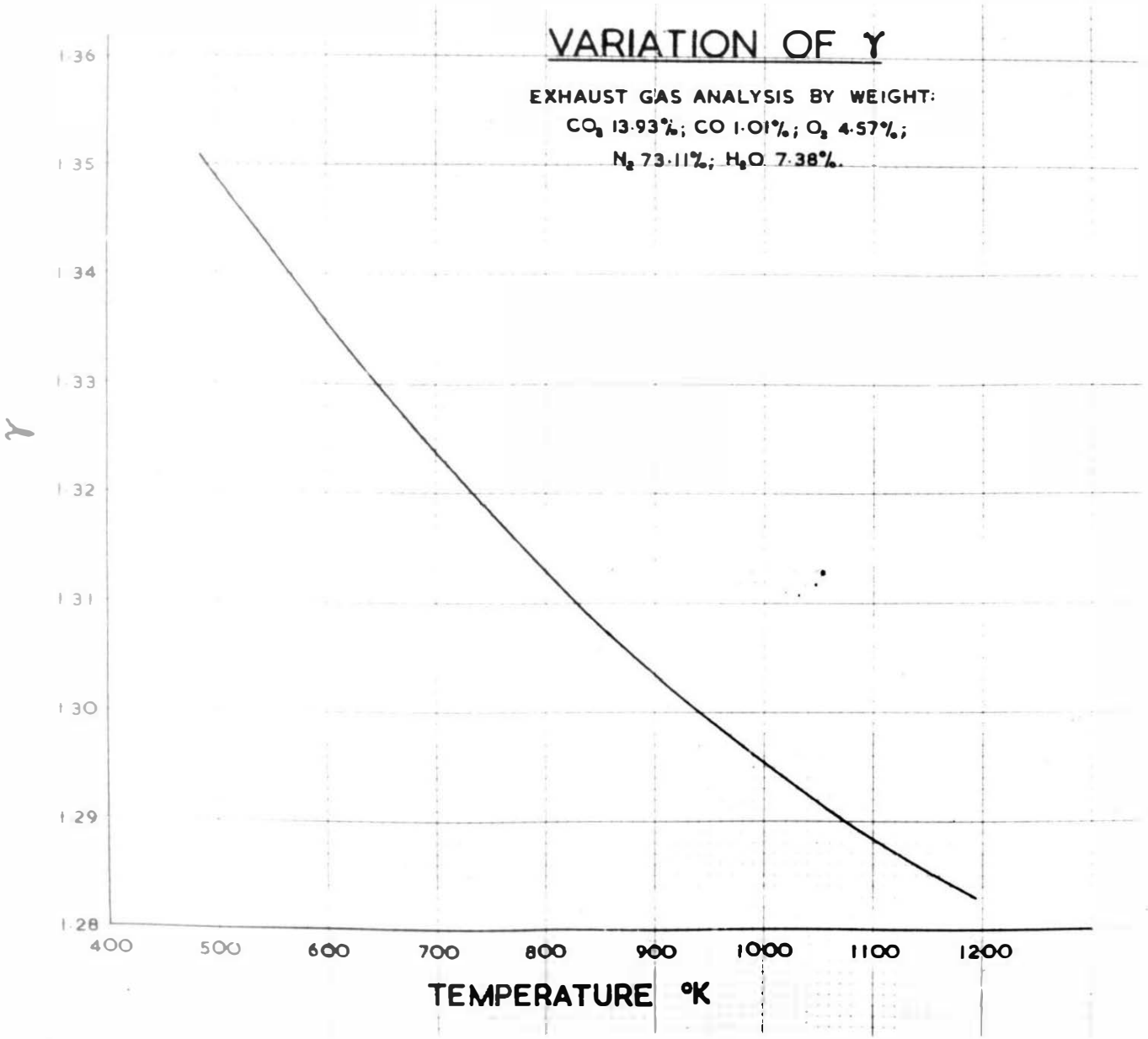
VARIATION OF γ
EXHAUST GAS ANALYSIS BY WEIGHT:
CO_2 13·93%; CO 1·01%; O_2 4·57%;
N_2 73·11%; H_2O 7·38%.
γ
1·36
1·35
1·34
1·33
1·32
1·31
1·30
1·29
1·28
400
500
600
700
800
900
1000
1100
1200
TEMPERATURE °K

Fig. 29

VISCOSITY OF EXHAUST GASES

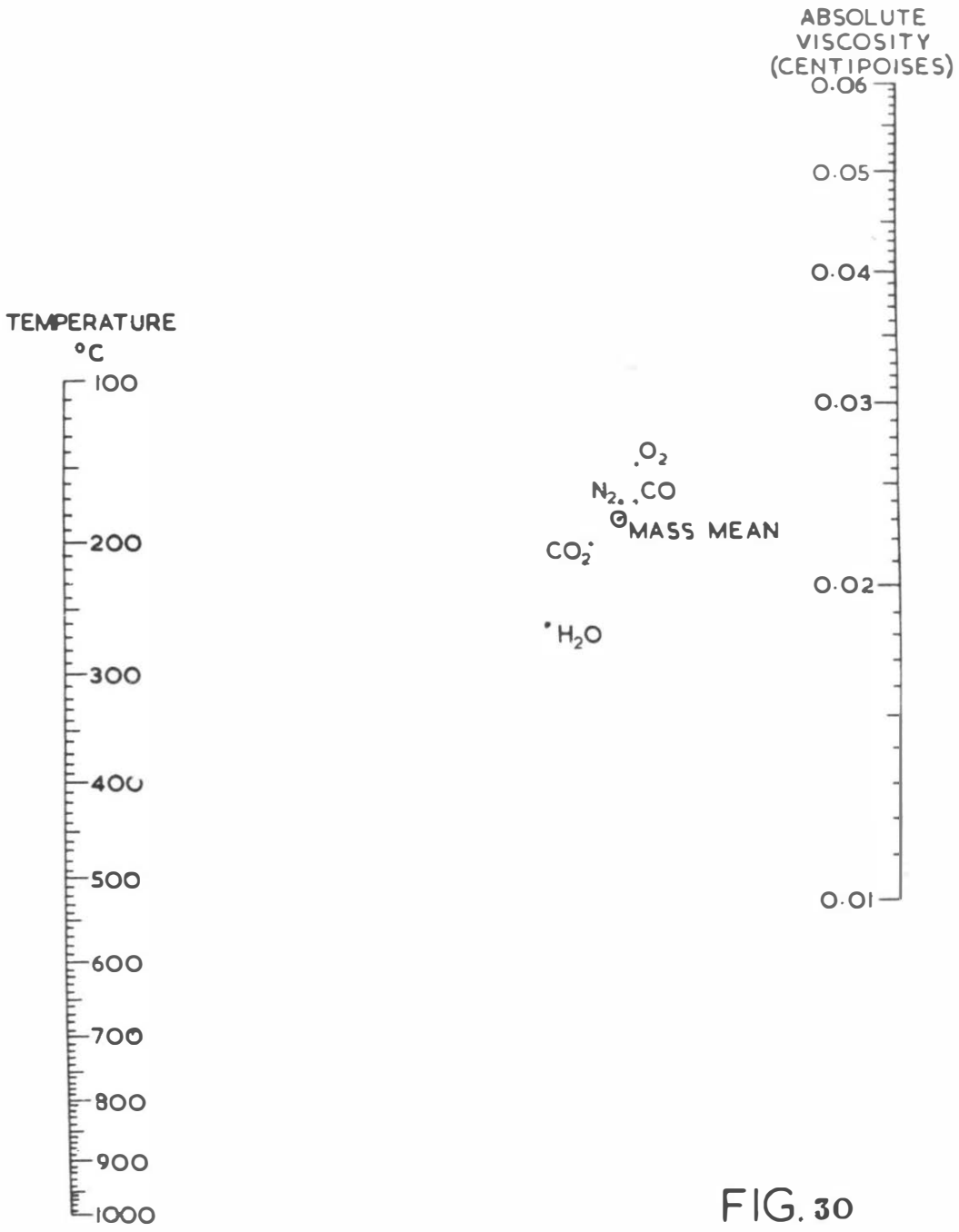

FIG. 30

The assumption of mass mean values for viscosity is not strictly correct, but in view of the probable smallness of the error, a full analysis of the problem is not justified.

Heat transfer coefficient for the exhaust pipe.

Assuming that the temperature gradient across the bulk of the fluid is negligible or small in comparison to the mean bulk temperature, then the pipe temperature can be assumed to be the same as the exhaust gases. This neglects the effect of heat conduction along the pipe and also the thermal inertia of the pipe material, but since the pipe is thin walled, then the error introduced is probably small.

Thus the heat transfer coefficient (q) for the exhaust gas can be obtained by evaluating the rate of heat transfer from the pipe to the surroundings by natural convection and radiation.

The heat transfer by natural convection[9] (h_c) is given by:-

$$h_c = C K \left(\frac{a\ \theta}{L}\right)^{.25} \text{ Btu/hr.ft.}^2\ ^\circ\text{F} \qquad (4.1\text{-}2)$$

where the value of 'a' in equation (4.1-2), for air, is listed in reference 9 and

C is a constant depending upon the shape and position of the hot surface,

K is the coefficient of thermal conductivity for air in Btu/ft.hr.°F.

Θ is the temperature difference between the pipe and the surroundings in fahrenheit degrees,

L is the diameter of the pipe in feet.

Hence, using C = 0.45 for horizontal cylinders, and changing the units from Btu, hr., ft., F°, to ft., lb., sec., C°, units gives the result:

$$h_c = 9.873\ K\Theta\ (a\ \Theta)^{.25}\ \text{ft.lb./ft.}^3\ \text{sec.}^\circ\text{C} \qquad (4.1\text{-}3)$$

where Θ = the temperature difference between the pipe and the surroundings in centigrade degrees,

and 'a' and K are the values listed for air in reference 9 in Btu., ft., hr., °F units.

The heat transfer by radiation (h_r)[9] is given by:

$$h_r = \epsilon\ \sigma (T_2^4 - T_a^4) \qquad (4.1\text{-}4)$$

where ϵ is the emissivity of the pipe surface

σ is the Stefan-Boltzmann constant

T_2 is the pipe absolute temperature

T_a is the absolute temperature of the surroundings.

For steel oxidized at 1100°F, the emissivity ϵ is 0.79[8], and its substitution with the Stefan-Boltzmann constant in equation (4.1-4) gives the result:

$$h_r = 9.158 \times 10^{-8}\ (T_2^4 - T_a^4)\ \text{ft.lb./ft}^3\text{.sec.} \qquad (4.1\text{-}5)$$

Combining equations (4.1-3) and (4.1-5) gives:

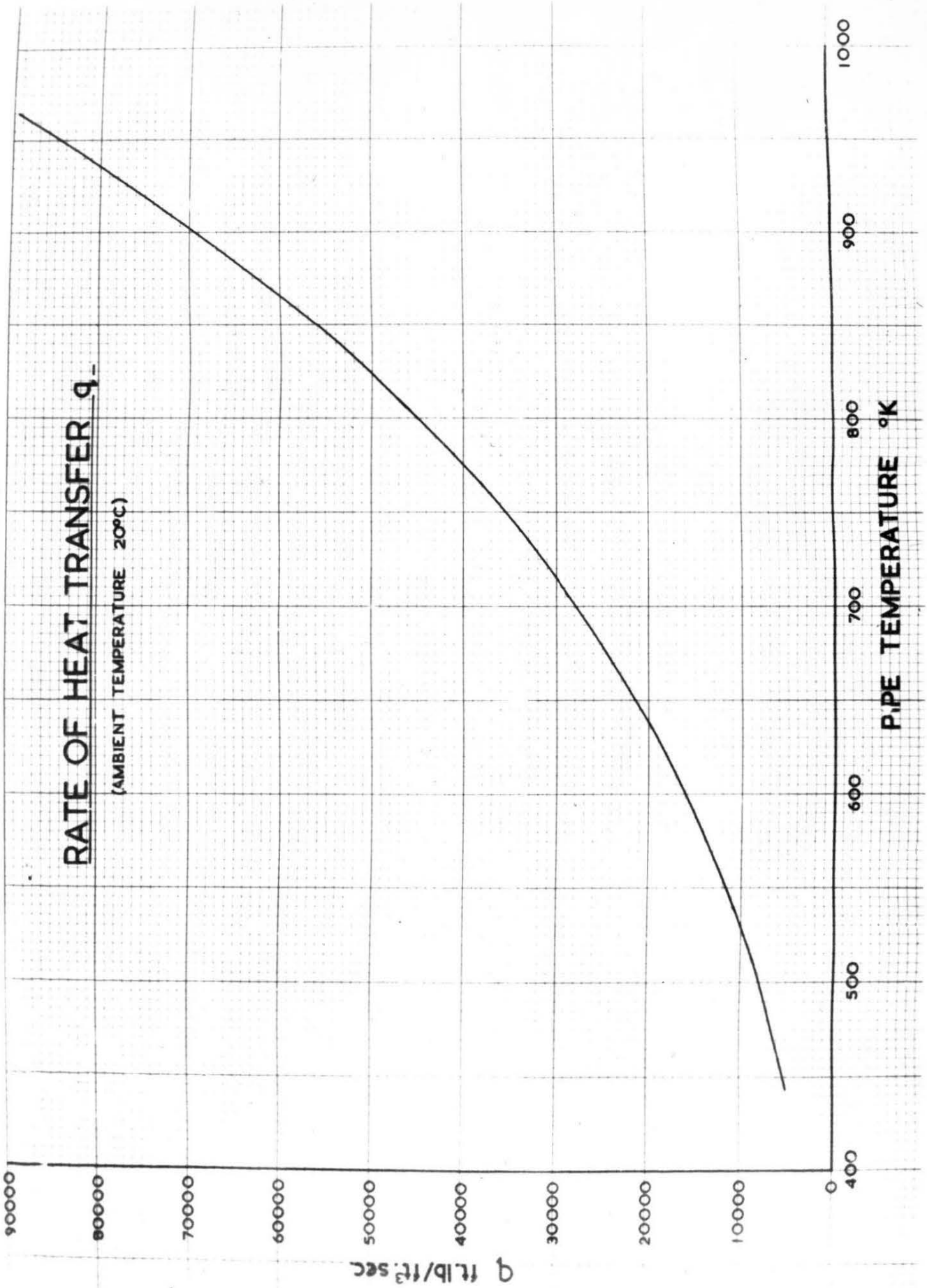
RATE OF HEAT TRANSFER q
(AMBIENT TEMPERATURE 20°C)
q ft.lb/ft³sec
90000
80000
70000
60000
50000
40000
30000
20000
10000
0
400
500
600
700
800
900
1000
PIPE TEMPERATURE °K

Fig.31

$$q = h_c + h_r = 9.873\ K\theta\ (a\ \theta)^{.25} + 9.158 \times 10^{-8}(T_2^4 - T_a^4)$$

ft.lb./ft.^{3} sec. (4.1-6)

Equation (4.1-6) evaluated for an ambient temperature of 20°C and for the temperature range 450 to 960°C absolute is shown plotted in Fig.31.

Friction coefficient for the exhaust pipe.

Determination of the friction coefficient (f) for the inside surface of the exhaust pipes required the measurement of the roughness of the soot deposit on the pipe inner surface.

For this measurement, a Taylor Hobson Model 3 Talysurf was used. Difficulty, however, was experienced in obtaining a true reading, the pressure of the Talysurf stylus was sufficient to remove carbon from the soft soot surface, resulting in a false measurement.

Preliminary experiments were carried out using soot surface samples obtained by inserting flat plates longitudinally in an exhaust pipe. To harden the soot surface, a shellac-alcohol solution was lightly sprayed onto the surface using a very fine atomizer. The strength of the shellac solution was increased, on successive samples, until the surface as seen under a microscope was not 'cut up' by the measuring stylus. Plate 2(d) shows a sample with two stylus tracks and the resulting disturbance of the soot on an inadequately treated surface.

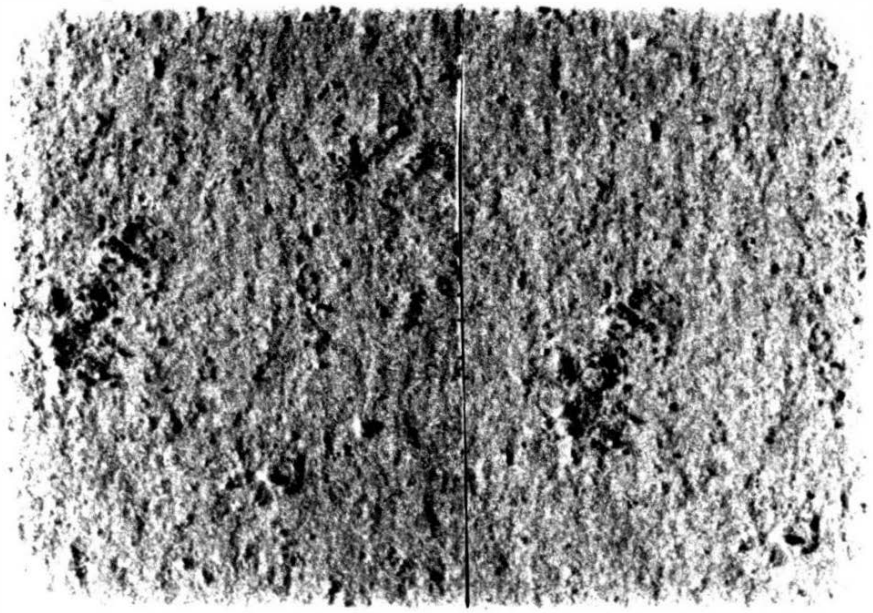

(a) (b)

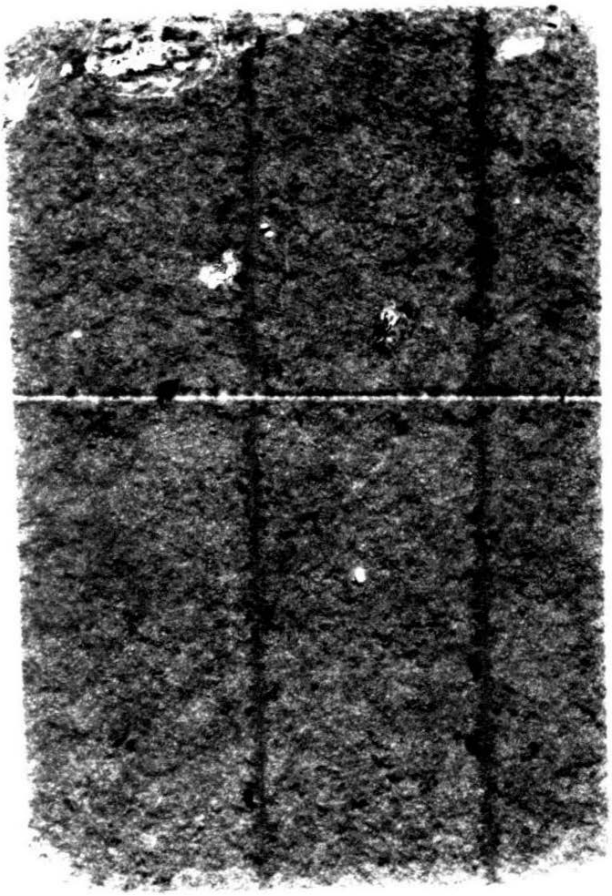

(c)

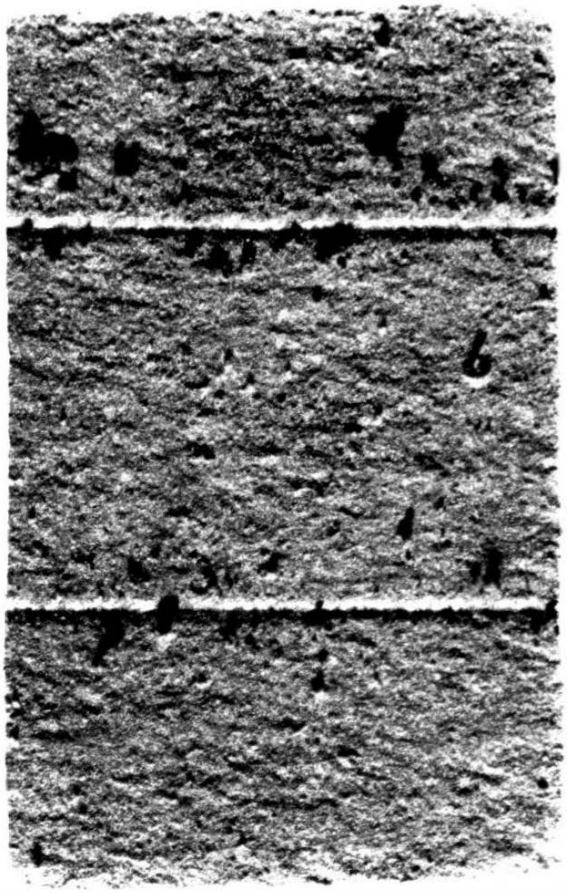

(d)

Plate 2.

Using a Vickers microscope at a magnification of 40X, and oblique lighting at an angle of approximately 15° to the plate surface, photographs of a sample before and after treatment with the correct strength shellac solution, is shown in Plates 2(a) and 2(b) respectively. These photographs show that the soot surface was unaffected by the treatment.

Two surface roughness measurements were taken, and to show conclusively that after shellac treatment, tracking by the Talysurf stylus produced no apparent damage to the surface, the sample plate was turned through 90° and the stylus taken across the two existing tracks; see Plate 2(c). Examination of this latter recording showed no trace of the previous trackings.

To determine the roughness of an actual soot surface within an exhaust pipe, one section of pipe was removed from the engine and the inner surface of the pipe end treated with shellac solution. To measure its roughness, however, the skid and stylus shield had to be removed from the Talysurf since it was too large to insert in the pipe.

Since the straight line motion of the Talysurf carriage head now had to be relied upon to provide the datum, the test pipe and the Talysurf had to be placed on a specially mounted table having a natural frequency of 2 c.p.s. This eliminated the possibility of any external vibration affecting the equipment. After setting up, the equipment was left for a period of time before taking each

reading.

Several recordings were taken with vertical and horizontal magnification of 1000 and 20 respectively, and the average mean height of the surface projections determined. The surface roughness ϵ, defined as the dimensionless ratio of the mean height of the surface projections to the diameter of the pipe, was found to be 0.000202.

Using the Colebrooke-White function[10], and the suggested modification by Moody[11], yields the following close approximation for the variation in the friction coefficient (f) with Reynolds number (R_e):

$$\sqrt{\frac{1}{f}} = -2 \log_{10} \left[\frac{33.85}{R_e \sqrt{1 + (20{,}000\, t + \frac{10^6}{R_e})^{\frac{1}{3}}}} + 0.2703\, \epsilon \right] \qquad (4.1\text{-}7)$$

where ϵ is the surface roughness.

Equation (4.1-7) is shown graphically in Fig.32 using the determined value for ϵ.

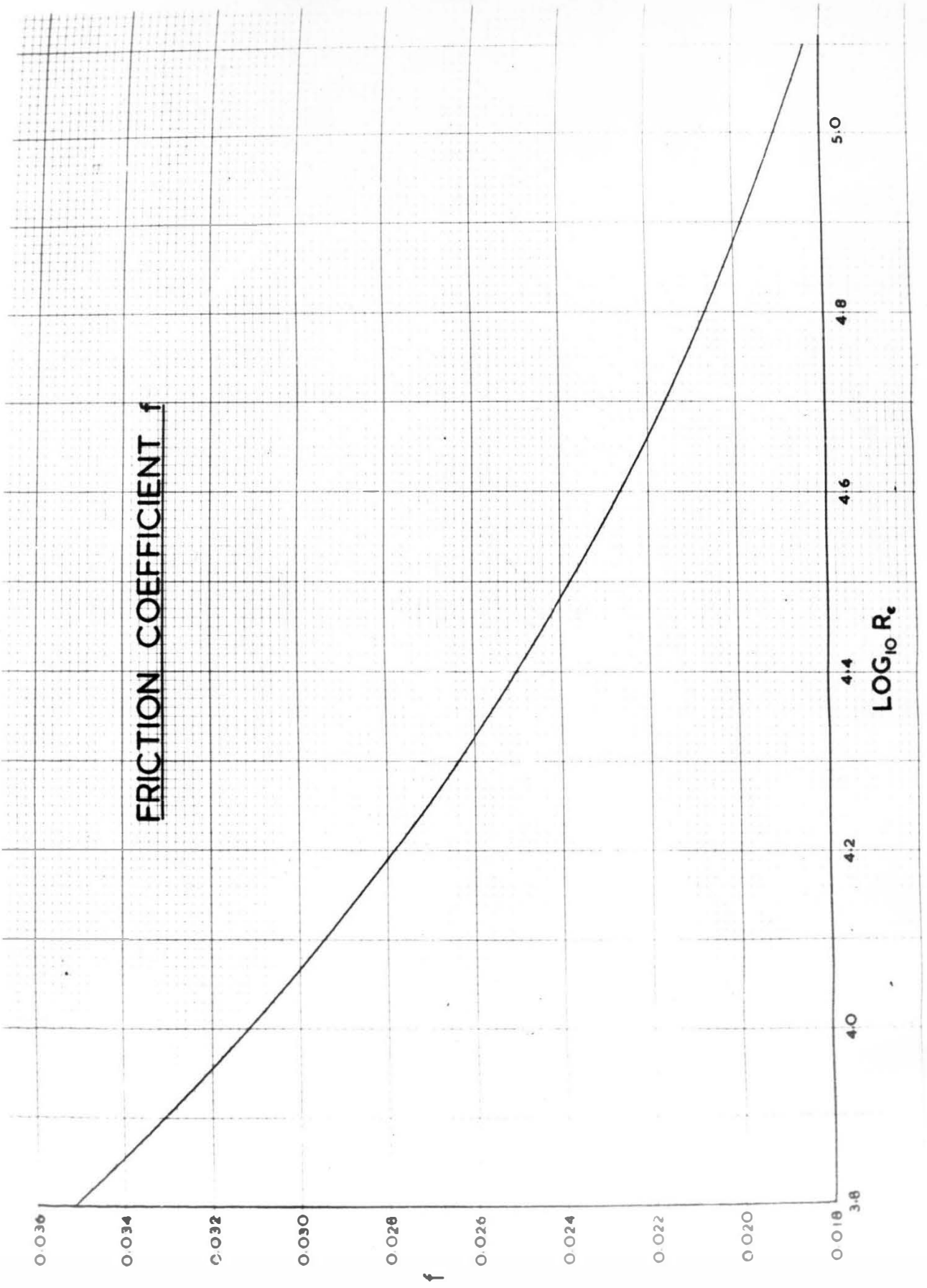
FRICTION COEFFICIENT f
f
0.036
0.034
0.032
0.030
0.028
0.026
0.024
0.022
0.020
0.018
3.8
4.0
4.2
4.4
4.6
4.8
5.0
LOG10 Re

Fig.32

4.2. Air consumption trials.

The engine was operated with a constant air-fuel ratio of 17.5 to 1, a constant cooling jacket water outlet temperature of 165°F, and with varying exhaust pipe lengths.

The exhaust pipe length was varied by increments of 6 inches from the minimum length of 2 feet 2 inches to the maximum length of 10 feet 2 inches, these pipe lengths representing the limiting values beyond which it was not possible to run the engine without the supply of scavenge air.

For each pipe length used, the engine was operated over the speed range of 500 to 1600 rpm., and results were recorded at approximately 25 rpm. intervals within this range wherever the engine performance was sufficiently stable for accurate readings to be taken.

At each selected test speed, the fuel pump rack was progressively adjusted until the air mass flow and rack setting were consistent with the appropriate interpolated speed calibration curve of Fig.24.

During the course of each test, the number of engine revolutions made during the time taken to use a pipette of fuel (either 22 cc or 66 cc depending upon the consumption rate) was noted, together with the time taken. Also, readings were taken of engine torque, micromanometer head, the differential pressures in the air expansion chamber and

the exhaust collector, exhaust gas temperatures, and the ambient pressure and temperature.

4.3. Indicating trial.

An exhaust pipe length of 6 feet 8 inches was chosen as a typical example for the theoretical analysis. With this pipe length the engine exhibited a stable performance when operating within the speed range in which the scavenging was achieved with the primary rarefaction wave only.

The most stable speed within this range was found to be just in excess of 1100 rpm. With the engine running at this speed, the fuel pump rack was positioned to give an air-fuel ratio of 17.5 to 1, as described in Section 4.2, and the coolant jacket water flow was adjusted to give an outlet temperature of 165°F.

When steady state condition had been achieved, the trial was conducted in two parts, viz: (a) recording of all the performance data, and (b) recording of the indicator diagrams for the cylinder and at three positions along the exhaust pipe.

(a) Performance data.

The following readings were noted and checked for consistency at intervals of time throughout the trial:- engine speed and torque, fuel consumption, micromanometer head, exhaust gas temperature at six intervals along the exhaust pipe, jacket coolant outlet temperature, differential pressure of the air expansion chamber and exhaust collector, ambient pressure and temperature.

(b) Indicator diagrams.

Preliminary recording trials had shown that calibration using the two-way cock introduced serious errors. In the case of the cylinder record, the sensitivity of the G 204 capacitance transducer to large changes in temperature resulted in a marked drift of the oscilloscope trace when the relatively cold calibrating air was applied to the transducer diaphragm. Calibration of the exhaust pipe diagrams, however, was not subject to this phenomenon, but the recorded traces exhibited spurious oscillations when compared with records taken with the transducer inserted directly into the pipe socket. These spurious oscillations were attributed to wave action in the connecting passage between the pipe and the transducer diaphragm, their marked effect being due to the steepness of the pressure pulses.

As a result of the above observations, the methods of obtaining the cylinder and pipe records were as follows.

The light spring diagram for the cylinder was recorded using the G 204 transducer and the Southern Instrument Engine Indicator. The transducer was then replaced by the balanced disc calibration pick-up, and using the Sunbury Engine Indicator, the crank angles at which the cylinder pressure balanced a range of applied pressures were noted. The exact cylinder

pressure at the point of exhaust port opening was also found and noted. These latter readings were then used to calibrate the light spring diagram previously recorded.

At each of the indicating positions in the exhaust pipe, two recordings were made using the G 204 transducers. The first was obtained using the two-way cock and calibration lines were superimposed on the recording. The second recording was made with the transducer inserted directly into the pipe socket and the first recording was used for its calibration.

The procedure for taking the indicator diagram film records was as follows:-

1. The drum camera was motored at a speed just less than that of the engine. This was done to obtain a diagram which contained a little more than one cycle.
2. The pressure and crank angle marker traces were adjusted for amplitude and brilliance.
3. The time sweep was switched off and the tube beams suppressed.
4. The camera trip button was then operated which switched on the tube beams for one revolution of the camera, thus exposing the film.
5. The marker trace was switched off and the two-way cock was turned to expose the transducer to the

calibrating air. The air potentiometer was used to apply known values of both positive and negative gauge pressures, and operation 4 above was performed for each calibration line. An atmospheric line was recorded by opening the blow-off valve of the air potentiometer unit.

5. Results

5.1. Air consumption trials.

AIR CONSUMPTION
DIMENSIONLESS AIR FLOW
100
90
80
70
60
50
40
30
20
0
1
2
3
4
5
6
nL/a
LEGEND
PIPE LENGTH
1-1 2' 2"
2-2 3' 2"
3-3 4' 2"
4-4 5' 2"
5-5 6' 2"
6-6 8' 2"
7-7 9' 2"
8-8 10' 2"

Fig. 33

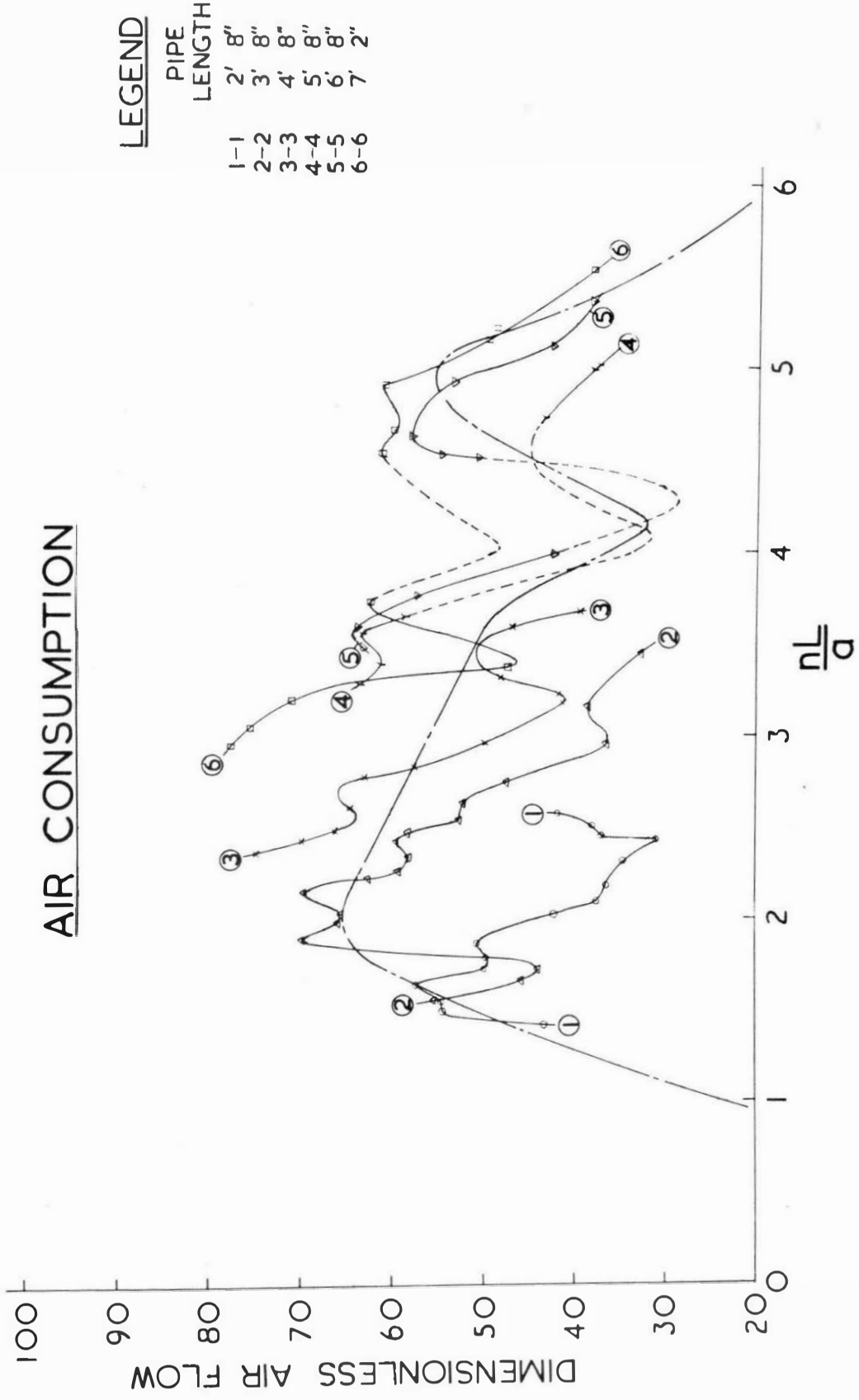
AIR CONSUMPTION
LEGEND
PIPE LENGTH
1-1 2' 8"
2-2 3' 8"
3-3 4' 8"
4-4 5' 8"
5-5 6' 8"
6-6 7' 2"
DIMENSIONLESS AIR FLOW
100
90
80
70
60
50
40
30
20
0
1
2
3
4
5
6
nL/d

Fig.34

5.2. Indicated trial and theoretical results.

Performance data and deduced results for the indicated trials are as follows:

Exhaust pipe length	6ft. 8ins.
Ambient pressure	14.322 psia.
Ambient temperature	19.67°C
Engine speed	1110.5 rpm.
Time for one degree of crank movement	15.008×10^{-5} secs.
Engine torque	19.4 lb.ft.
Brake horse power	4.1
Fuel consumption	0.05068 lb./min.
Air consumption	0.93804 lb./min.
Air-fuel ratio	18.5 to 1
Volumetric efficiency	53.4%
Cylinder pressure at exhaust port opening	26.0 psig.

Exhaust gas temperatures

Distance from ports	11"	23"	35"	53"	65"	77"
Temperature °K	677	588	541	501	474	397

Mean exhaust gas temperature 547°K

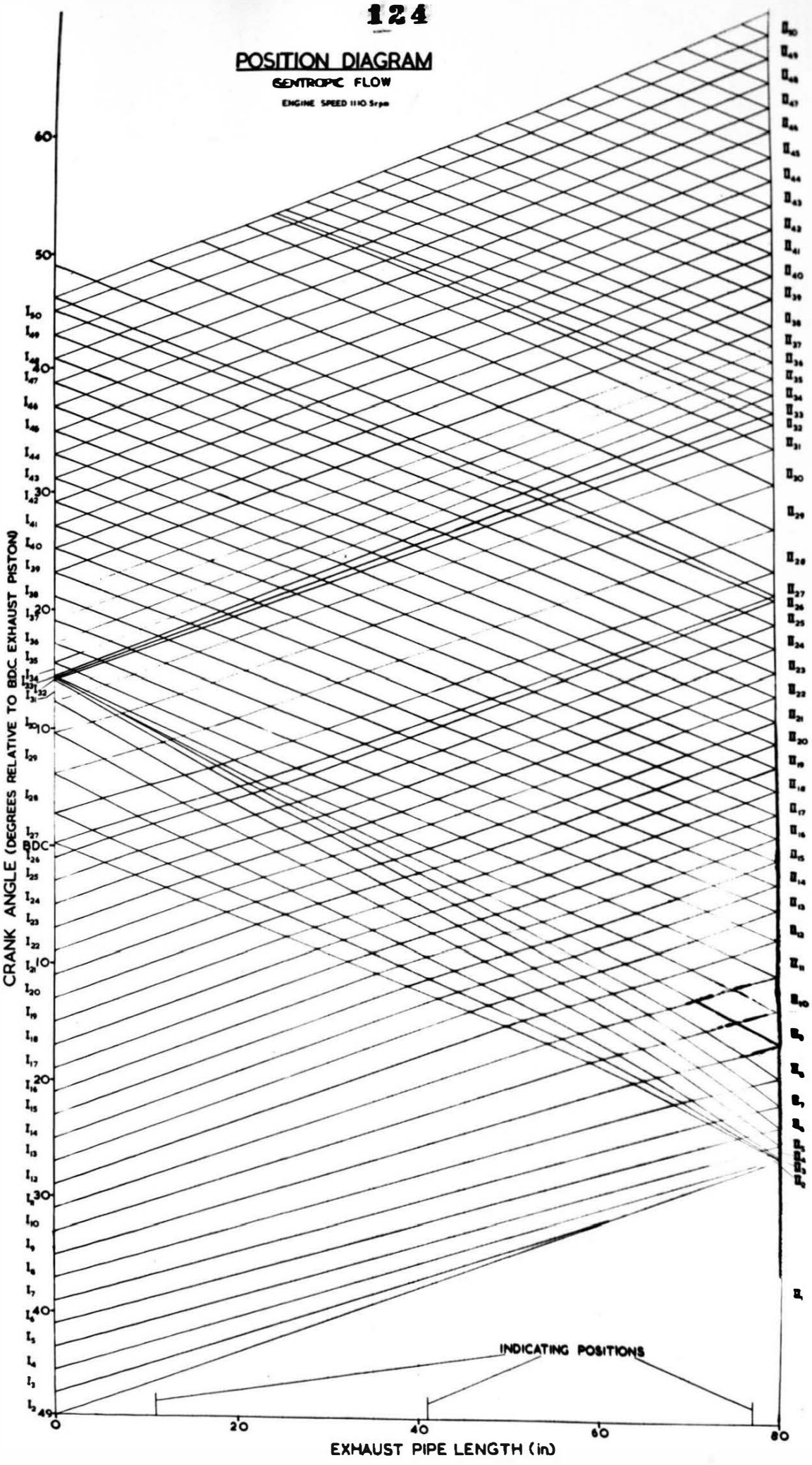
POSITION DIAGRAM
CENTROPIC FLOW
ENGINE SPEED 1110 Srpm
CRANK ANGLE (DEGREES RELATIVE TO BDC EXHAUST PISTON)
BDC
INDICATING POSITIONS
EXHAUST PIPE LENGTH (in)
0
20
40
60
80

Fig.35

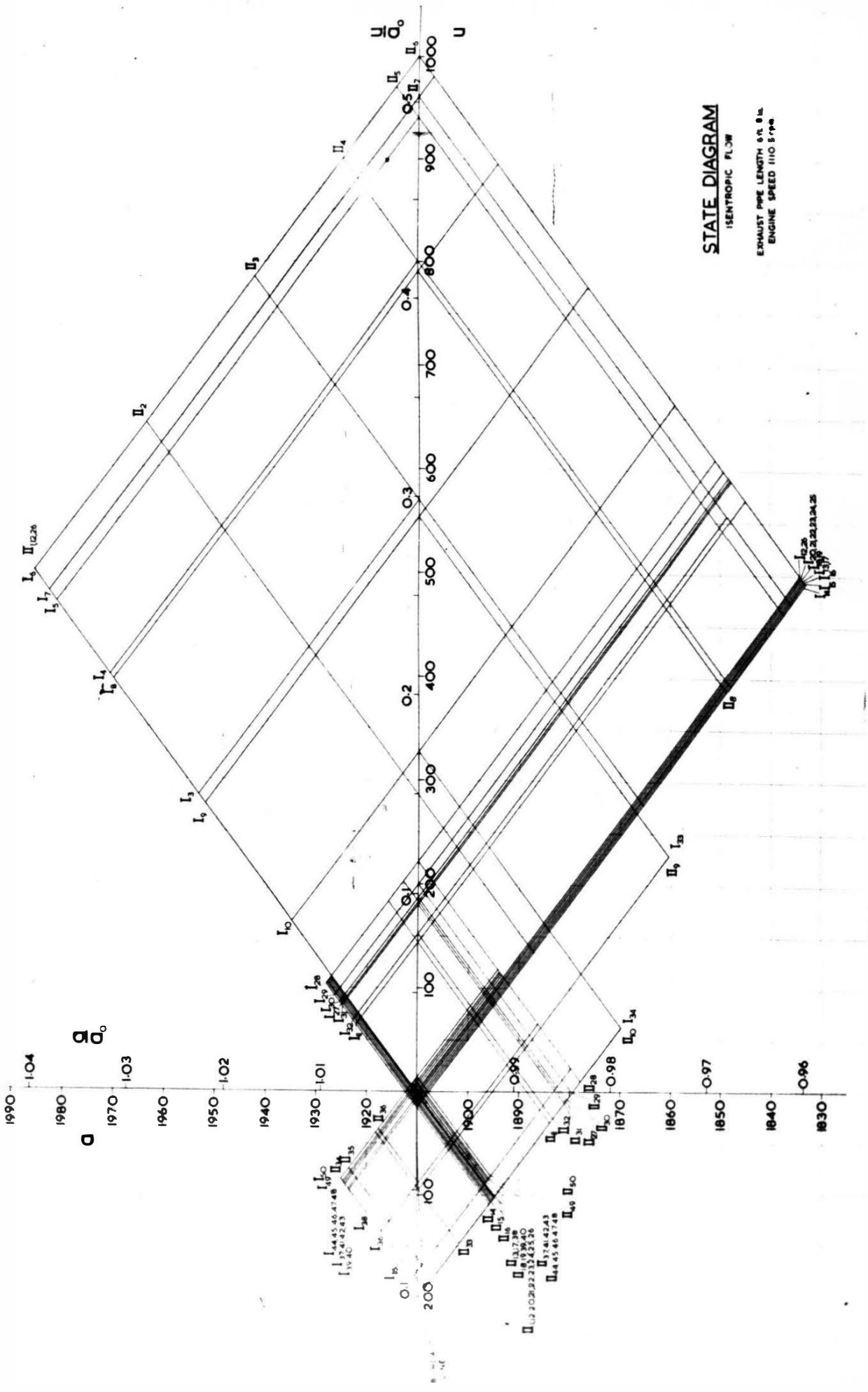
STATE DIAGRAM
ISENTROPIC FLOW
EXHAUST PIPE LENGTH 6 ft 8 in.
ENGINE SPEED 1110 R.P.M.
u/a₀
u
a/a₀
a

Fig.36

EXHAUST GAS TEMPERATURE
MEASURED PROFILE
ASSUMED PROFILE FOR THEORETICAL ANALYSIS
TEMPERATURE °K
800
700
600
500
400
300
0
20
40
60
80
EXHAUST PIPE LENGTH (in.)

Fig. 37

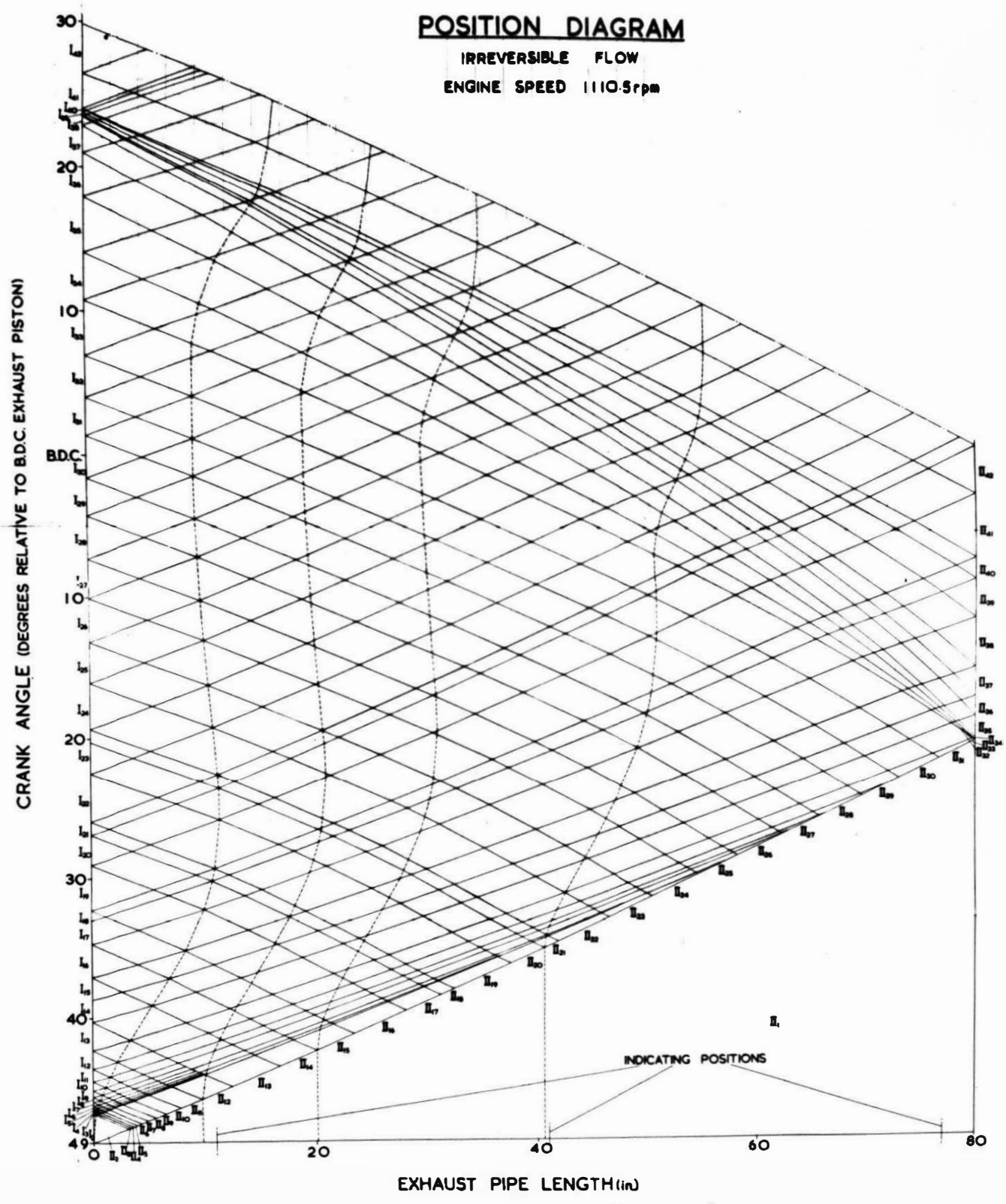
POSITION DIAGRAM
IRREVERSIBLE FLOW
ENGINE SPEED 1110·5rpm
CRANK ANGLE (DEGREES RELATIVE TO B.D.C. EXHAUST PISTON)
B.D.C.
INDICATING POSITIONS
EXHAUST PIPE LENGTH (in)
0
20
40
60
80

Fig.38

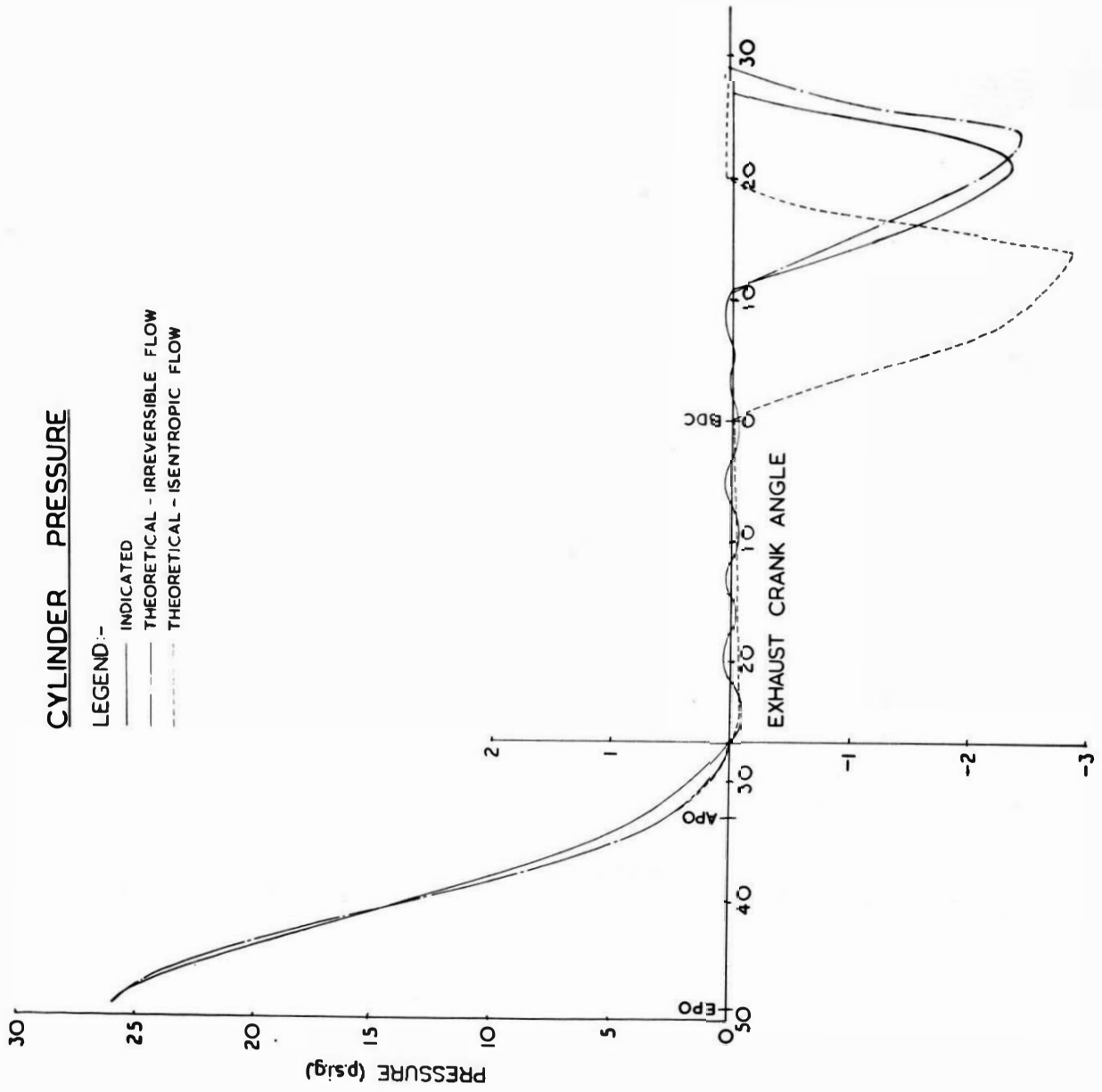
CYLINDER PRESSURE
LEGEND:-
INDICATED
THEORETICAL - IRREVERSIBLE FLOW
THEORETICAL - ISENTROPIC FLOW
PRESSURE (p.s.i.g)
EXHAUST CRANK ANGLE
EPO
APO
BDC

Fig.39

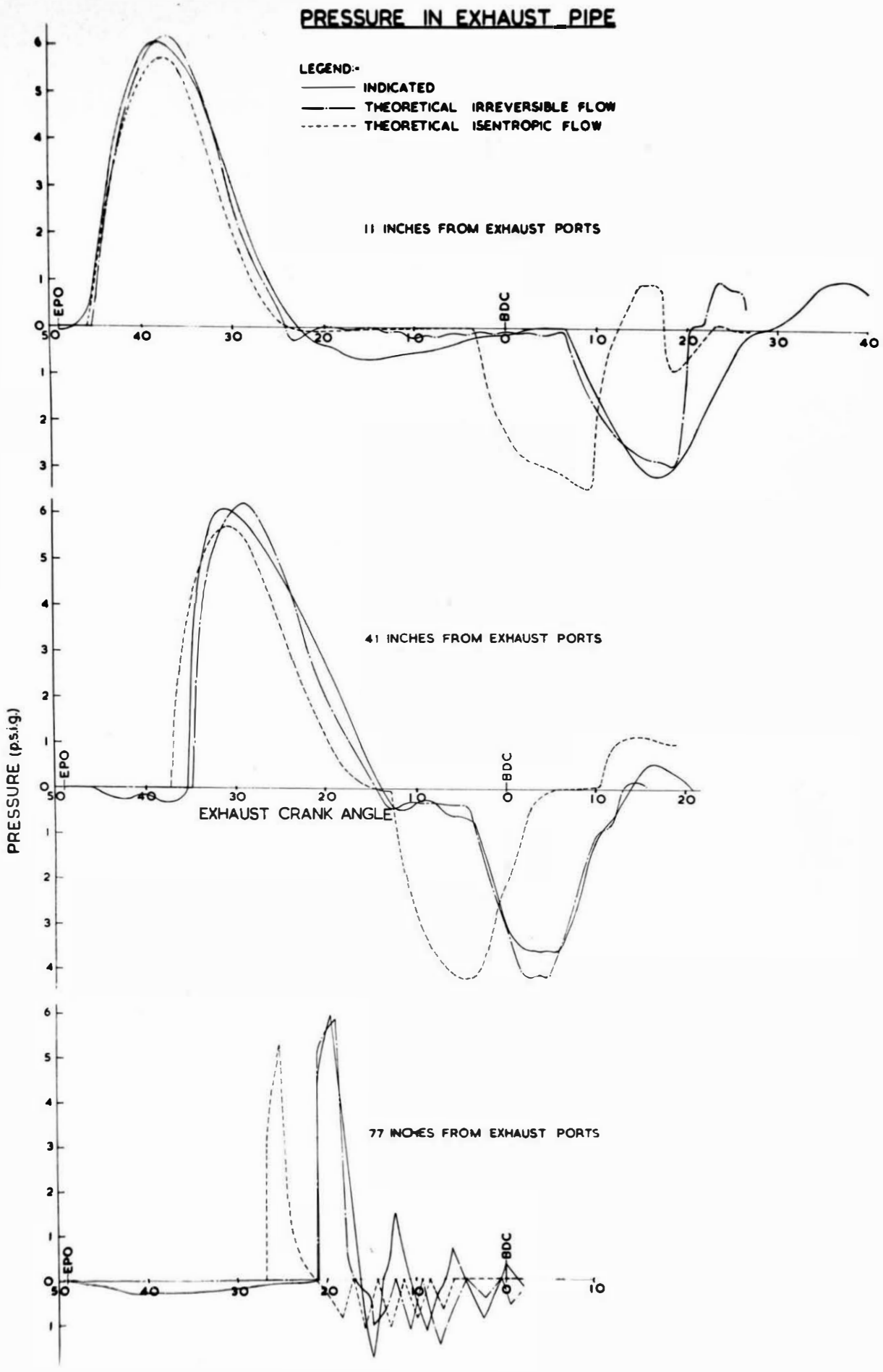
PRESSURE IN EXHAUST PIPE
LEGEND:-
INDICATED
THEORETICAL IRREVERSIBLE FLOW
THEORETICAL ISENTROPIC FLOW
11 INCHES FROM EXHAUST PORTS
41 INCHES FROM EXHAUST PORTS
77 INCHES FROM EXHAUST PORTS
EPO
BDC
PRESSURE (p.s.i.g.)
EXHAUST CRANK ANGLE

Fig.40

THEORETICAL RESULTS

STATE I - II,	PRESSURE p.s.i.a.	PARTICLE VELOCITY ft./sec.	ACOUSTIC VELOCITY ft./sec.	GAS TEMPERATURE °K	$\gamma = \frac{C_p}{C_v}$
1.1	14.322	0.0	1725.4	724.6	1.3211
1.1	14.322	0.0	1637.8	640.0	1.3309
1.1	14.322	0.0	1550.7	570.0	1.3397
1.1	14.322	0.0	1457.3	500.0	1.3487
2.1	15.388	104.1	1926.3	903.2	1.3046
2.2	15.428	97.8	1741.1	737.8	1.3211
2.3	15.427	97.4	1741.0	737.8	1.3211
2.4	15.427	97.4	1740.9	737.7	1.3211
2.5	15.427	97.4	1740.9	737.7	1.3211
2.6	15.427	97.4	1740.9	737.6	1.3211
2.7	15.427	97.3	1740.8	737.6	1.3211
2.8	15.424	97.2	1740.7	737.5	1.3211
2.9	15.423	97.0	1740.5	737.3	1.3211
2.10	15.420	96.8	1740.3	737.2	1.3211
2.11	15.416	96.7	1740.0	737.1	1.3211
2.12	15.445	92.3	1740.5	737.5	1.3211
2.12'			1653.0	652.0	1.3309
2.13	15.427	91.9	1652.8	651.8	1.3309
2.14	15.421	91.3	1652.5	651.5	1.3309
2.15	15.449	87.3	1652.8	652.0	1.3309
2.15'			1565.4	580.9	1.3397
2.16	15.438	86.9	1565.3	580.0	1.3397
2.17	15.432	86.7	1565.1	579.8	1.3397
2.18	15.429	86.5	1564.9	579.7	1.3397
2.19	15.425	86.3	1564.8	579.6	1.3397
2.20	15.421	86.0	1564.7	579.5	1.3397
2.21	15.462	81.9	1565.3	580.0	1.3397
2.21'			1471.6	509.9	1.3487
2.22	15.448	81.9	1471.5	509.8	1.3487
2.23	15.442	81.6	1471.4	509.8	1.3487
2.24	15.436	81.4	1471.4	509.7	1.3487
2.25	15.434	81.0	1471.3	509.7	1.3487
3.2	16.418	199.0	1940.9	916.9	1.3046
3.3	16.520	184.9	1942.9	918.9	1.3046
3.3'			1755.0	749.7	1.3211
3.4	16.474	184.7	1755.0	749.6	1.3211
3.5	16.472	184.7	1754.9	749.6	1.3211
3.6	16.472	184.5	1754.9	749.5	1.3211
3.7	16.470	184.3	1754.8	749.5	1.3211
3.8	16.469	184.1	1754.8	749.5	1.3211
3.9	16.466	184.0	1754.7	749.4	1.3211
3.10	16.462	183.8	1754.6	749.4	1.3211
3.11	16.458	182.4	1754.6	749.3	1.3211
3.12	16.501	179.0	1755.1	749.7	1.3211

STATE I - II	P	U	a	T	γ
4.3	16.487	208.2	1941.7	917.8	1.3046
4.4	16.614	192.0	1944.0	919.9	1.3046
4.4'			1756.1	750.6	1.3211
4.5	16.561	192.0	1756.0	750.5	1.3211
4.6	16.560	191.8	1756.0	750.5	1.3211
4.7	16.560	191.6	1756.0	750.5	1.3211
4.8	16.558	191.4	1755.9	750.4	1.3211
4.9	16.556	191.2	1755.8	750.4	1.3211
4.10	16.552	191.0	1755.8	750.3	1.3211
4.11	16.548	190.0	1755.7	750.2	1.3211
4.12	16.589	186.1	1756.2	750.7	1.3211
5.4	16.709	229.0	1944.9	920.8	1.3046
5.5	16.855	211.1	1947.3	923.0	1.3046
5.5'			1759.1	753.1	1.3211
5.6	16.798	210.9	1759.0	753.1	1.3211
5.7	16.798	210.7	1759.0	753.1	1.3211
5.8	16.797	210.5	1758.9	753.0	1.3211
5.9	16.795	210.3	1758.8	752.9	1.3211
5.10	16.790	210.1	1758.8	752.8	1.3211
5.11	16.786	209.7	1758.7	752.8	1.3211
5.12	16.829	205.2	1759.2	753.2	1.3211
5.13	16.650	185.1	1756.6	751.2	1.3211
5.13'			1668.3	664.1	1.3309
5.14	16.615	184.5	1668.2	664.0	1.3309
5.15	16.655	180.3	1668.7	664.4	1.3309
5.16	16.654	175.9	1580.5	592.1	1.3309
5.17	16.645	175.5	1580.4	592.0	1.3309
5.18	16.640	175.4	1580.3	592.0	1.3309
5.19	16.633	175.0	1580.2	591.9	1.3309
6.5	16.880	244.3	1947.6	923.3	1.3046
6.6	17.163	226.4	1949.9	925.5	1.3046
6.6'			1761.5	755.2	1.3211
6.7	17.100	226.2	1761.4	755.1	1.3211
6.8	16.993	226.0	1761.4	755.1	1.3211
6.9	16.990	225.8	1761.3	755.0	1.3211
6.10	16.986	225.6	1761.1	754.9	1.3211
6.11	16.981	225.2	1761.0	754.8	1.3211
6.12	17.025	220.6	1761.5	755.2	1.3211
7.6	17.195	269.1	1951.4	926.9	1.3046
7.7	17.354	249.1	1953.8	929.2	1.3046
7.7'			1765.1	758.3	1.3211

STATE I - II	P	U	a	T	γ
-8	17.286	248.9	1765.0	758.2	1.3211
-9	17.280	248.5	1764.9	758.1	1.3211
-10	17.276	248.3	1764.7	758.0	1.3211
-11	17.272	247.9	1764.6	757.9	1.3211
-12	17.315	243.4	1765.1	758.3	1.3211
-13	17.209	226.7	1763.7	757.1	1.3211
-14	17.151	224.3	1674.6	669.1	1.3309
-15	17.190	220.1	1675.0	669.4	1.3309
-16	17.199	213.9	1587.0	597.0	1.3397
-17	17.187	213.4	1586.8	596.9	1.3397
-18	17.181	213.2	1586.7	568.0	1.3397
-19	17.172	212.6	1586.6	596.7	1.3397
-20	17.163	211.8	1586.4	596.6	1.3397
-21	17.215	207.6	1587.1	597.1	1.3397
7-22	17.219	201.7	1492.8	525.5	1.3487
8-7	17.453	290.9	1954.8	930.2	1.3046
-8	17.625	269.3	1957.2	932.4	1.3046
-8'			1768.3	761.0	1.3211
-9	17.549	269.1	1768.1	760.9	1.3211
-10	17.543	269.0	1768.0	760.8	1.3211
-11	17.536	268.4	1767.8	760.6	1.3211
-12	17.581	263.8	1768.3	761.0	1.3211
9-8	17.796	319.4	1959.3	934.4	1.3046
-9	17.985	295.9	1961.6	936.6	1.3046
-9'			1772.4	764.6	1.3211
-10	17.894	295.3	1772.2	764.4	1.3211
-11	17.887	294.9	1772.0	764.2	1.3211
-12	17.930	290.2	1772.4	764.6	1.3211
-13	17.797	271.6	1770.6	763.1	1.3211
-14	17.746	267.2	1681.5	674.6	1.3309
-15	17.785	262.8	1681.8	674.9	1.3309
-16	17.805	255.0	1598.7	602.2	1.3397
-17	17.792	254.4	1593.7	602.1	1.3397
-18	17.784	254.1	1593.5	601.9	1.3397
-19	17.775	253.5	1593.4	601.8	1.3397
-20	17.764	252.5	1593.2	601.7	1.3397
-21	17.817	247.9	1593.7	602.1	1.3397
-22	18.000	240.5	1499.4	530.1	1.3487
-23	17.824	239.7	1499.2	529.9	1.3487
-24	17.812	239.0	1499.1	529.8	1.3487
-25	17.801	238.2	1498.9	529.7	1.3487
9-26	17.789	237.6	1498.8	529.6	1.3487

STATE I - II	P	U	a	T	γ
10-9	18.203	351.5	1964.4	939.3	1.3046
-10	18.404	326.3	1966.6	941.4	1.3046
-10'			1777.1	768.6	1.3211
-11	18.304	325.7	1776.8	768.4	1.3211
-12	18.346	320.9	1777.2	768.7	1.3211
-13	18.387	315.4	1777.5	769.0	1.3211
-14	18.346	309.1	1688.3	680.1	1.3309
-15	18.383	304.5	1688.7	680.4	1.3309
-16	18.452	294.4	1690.0	681.4	1.3309
-16'			1600.6	607.3	1.3397
-17	18.389	293.6	1600.4	607.1	1.3397
-18	18.380	293.2	1600.3	607.0	1.3397
-19	18.368	292.5	1600.1	606.9	1.3397
-20	18.356	291.5	1599.9	606.7	1.3397
-21	18.411	286.9	1600.5	607.2	1.3397
-22	18.442	277.7	1506.0	534.7	1.3487
-23	18.428	276.8	1505.8	534.6	1.3487
-24	18.414	276.0	1505.6	534.5	1.3487
-25	18.402	275.3	1505.5	534.4	1.3487
-26	18.389	274.5	1505.4	534.4	1.3487
10-27	18.377	273.7	1505.2	534.2	1.3487
11-10	18.711	392.9	1970.8	945.4	1.3046
-11	18.943	364.1	1972.8	947.3	1.3046
-11'			1783.0	773.7	1.3211
-12	18.879	359.3	1783.3	774.0	1.3211
-13	18.919	353.6	1783.5	774.2	1.3211
-14	18.885	345.6	1694.3	684.9	1.3309
-15	18.922	341.0	1694.6	685.1	1.3309
-16	19.038	330.7	1695.7	686.1	1.3309
-17	18.937	328.7	1606.3	611.6	1.3397
-18	18.927	328.2	1606.1	611.5	1.3397
-19	18.914	327.2	1605.9	611.3	1.3397
-20	18.898	326.1	1605.7	611.2	1.3397
-21	18.952	321.5	1606.2	611.6	1.3397
-22	19.050	310.6	1607.9	612.8	1.3397
-22'			1511.7	538.8	1.3487
-23	18.978	309.6	1511.5	538.7	1.3487
-24	18.958	308.7	1511.3	538.5	1.3487
-25	18.944	307.7	1511.1	538.4	1.3487
-26	18.931	306.8	1511.0	538.2	1.3487
-27	18.916	306.0	1510.8	538.1	1.3487
11-28	18.901	305.2	1510.6	538.0	1.3487

STATE I - II	P	U	a	T	γ
12-11	19.289	440.5	1977.8	952.1	1.3046
-12	19.621	402.1	1980.3	954.5	1.3046
-12'			1790.1	780.3	1.3211
-13	19.534	396.6	1790.2	780.3	1.3211
-14	19.570	386.1	1791.3	781.0	1.3211
-14'			1701.0	690.4	1.3309
-15	19.538	381.3	1701.2	690.5	1.3309
-16	19.656	370.8	1702.3	691.6	1.3309
-17	19.616	368.8	1702.5	691.6	1.3309
-17'			1612.7	616.6	1.3397
-18	19.544	366.0	1612.5	616.5	1.3397
-19	19.528	365.0	1612.2	616.3	1.3397
-20	19.507	363.9	1611.9	616.0	1.3397
-21	19.565	359.1	1612.5	616.5	1.3397
-22	19.706	348.6	1613.9	617.5	1.3397
-23	19.597	345.4	1517.8	543.1	1.3487
-24	19.574	344.4	1517.5	542.9	1.3487
-25	19.557	343.1	1517.3	542.8	1.3487
-26	19.538	341.9	1517.1	542.6	1.3487
-27	19.522	341.4	1516.9	542.5	1.3487
-28	19.505	340.2	1516.7	542.3	1.3487
-29	19.485	339.3	1516.4	542.2	1.3487
-30	19.459	338.1	1516.2	542.0	1.3487
-31	19.448	337.2	1516.0	541.9	1.3487
13-12	19.793	482.7	1983.7	957.9	1.3046
-13	20.237	433.8	1986.3	960.4	1.3046
-13'			1796.3	785.6	1.3211
-14	20.200	423.3	1797.0	786.2	1.3211
-15	20.179	416.4	1797.7	786.5	1.3211
-15'			1707.2	695.4	1.3309
-16	20.218	405.7	1708.2	696.2	1.3309
-17	20.236	401.5	1708.2	696.2	1.3309
-18	20.178	399.2	1708.5	696.4	1.3309
-18'			1618.4	621.0	1.3397
-19	20.055	398.3	1618.1	620.7	1.3397
-20	20.069	396.9	1617.7	620.5	1.3397
-21	20.122	392.2	1618.3	620.9	1.3397
-22	20.251	382.4	1619.4	621.8	1.3397
-23	20.231	376.7	1619.8	622.1	1.3397
-23'			1523.3	547.1	1.3487
-24	20.137	375.5	1523.0	546.9	1.3487
-25	20.118	373.8	1522.7	546.7	1.3487
-26	20.095	372.5	1522.5	546.5	1.3487
-27	20.065	371.5	1522.2	546.3	1.3487

STATE I - II	P	U	a	T	γ
-28	20.049	370.2	1521.9	546.1	1.3487
-29	20.026	369.1	1521.6	545.9	1.3487
-30	20.002	367.9	1521.3	545.7	1.3487
-31	19.985	367.1	1521.1	545.6	1.3487
-32	18.071	479.8	1501.5	531.5	1.3487
-33	16.327	592.2	1481.9	517.8	1.3487
-34	14.727	704.5	1462.3	504.2	1.3487
-35	14.322	734.7	1457.0	500.5	1.3487
14-13	20.021	499.1	1986.4	960.5	1.3046
-14	20.604	438.8	1989.6	963.6	1.3046
-14'			1799.7	788.6	1.3211
-15	20.510	432.1	1800.0	788.8	1.3211
-16	20.552	420.1	1801.3	789.7	1.3211
-16'			1710.8	698.4	1.3309
-17	20.486	415.9	1710.8	698.4	1.3309
-18	20.492	413.6	1710.8	698.3	1.3309
-19	20.411	411.6	1710.7	698.3	1.3309
-19'			1620.6	617.2	1.3397
-20	20.317	410.3	1620.3	622.5	1.3397
-21	20.370	405.5	1620.8	622.8	1.3397
-22	20.498	395.8	1622.0	623.8	1.3397
-23	20.548	390.1	1622.4	624.0	1.3397
-24	20.460	388.2	1622.2	623.9	1.3397
-24'			1525.4	548.6	1.3487
-25	20.372	386.4	1525.2	548.5	1.3487
-26	20.346	385.1	1525.0	548.3	1.3487
-27	20.324	384.3	1524.7	548.1	1.3487
-28	20.307	383.0	1524.5	548.0	1.3487
-29	20.281	382.0	1524.2	547.8	1.3487
-30	20.258	380.9	1524.0	547.6	1.3487
-31	20.236	380.1	1523.7	547.4	1.3487
-32	18.293	493.4	1503.9	533.3	1.3487
-33	16.529	605.7	1484.3	519.5	1.3487
-34	14.912	718.0	1464.7	505.9	1.3487
-35	14.505	748.2	1459.5	502.2	1.3487
-36	14.322	761.8	1457.1	500.6	1.3487
15-13	19.663	471.4	1982.2	956.4	1.3046
-14	20.390	411.3	1989.7	963.6	1.3046
-15	20.275	405.7	1984.8	959.9	1.3046
-15'			1795.9	785.6	1.3211
-16	20.259	393.7	1796.9	786.5	1.3211
-17	20.181	390.4	1796.9	785.9	1.3211
-17'			1706.8	695.1	1.3309

STATE I - II	P	U	a	T	γ
15-18	20.110	388.2	1706.8	695.1	1.3309
-19	20.103	386.4	1706.5	694.8	1.3309
-20	20.000	385.6	1706.2	694.6	1.3309
-20'			1616.4	619.4	1.3397
-21	19.989	381.1	1616.9	619.8	1.3397
-22	20.114	371.5	1618.1	620.7	1.3397
-23	20.163	365.8	1618.4	621.0	1.3397
-24	20.148	363.7	1618.1	620.8	1.3397
-25	20.049	362.9	1617.7	620.5	1.3397
-25'			1521.4	545.7	1.3487
-26	19.958	361.4	1521.0	545.5	1.3487
-27	19.930	360.5	1520.7	545.3	1.3487
-28	19.912	359.1	1520.5	545.1	1.3487
-29	19.886	358.0	1520.0	544.8	1.3487
-30	19.862	356.8	1519.9	544.7	1.3487
-31	19.839	356.3	1519.6	544.4	1.3487
-32	17.927	468.4	1499.8	530.4	1.3487
-33	16.205	579.9	1480.4	516.7	1.3487
-34	14.633	691.1	1460.8	503.1	1.3487
-35	14.223	721.9	1455.6	499.5	1.3487
-36	14.038	734.1	1453.1	497.8	1.3487
-37	14.322	710.0	1457.0	500.5	1.3487
16-14	18.572	385.7	1969.0	943.8	1.3046
-15	19.319	322.1	1977.1	951.5	1.3046
-16	19.242	315.0	1971.1	946.7	1.3046
-16'			1784.2	775.4	1.3211
-17	19.132	312.1	1783.8	775.1	1.3211
-18	19.037	312.9	1783.9	774.6	1.3211
-18'			1694.5	685.1	1.3309
-19	18.972	311.4	1694.1	684.7	1.3309
-20	18.941	311.0	1693.5	660.9	1.3309
-21	18.903	308.9	1694.0	684.7	1.3309
-21'			1604.9	610.7	1.3397
-22	18.972	299.3	1606.0	611.5	1.3397
-23	19.025	294.0	1606.4	611.8	1.3397
-24	19.020	292.1	1606.1	611.6	1.3397
-25	18.990	291.7	1605.6	611.2	1.3397
-26	18.873	293.6	1604.8	610.6	1.3397
-26'			1509.5	537.2	1.3487
-27	18.806	292.8	1509.2	537.0	1.3487
-28	18.790	291.7	1509.0	536.9	1.3487
-29	18.765	290.9	1508.5	536.6	1.3487
-30	18.753	289.8	1508.4	536.4	1.3487
-31	18.729	289.6	1508.1	536.2	1.3487

STATE I - II	P	U	a	T	γ
16-32	16.924	401.1	1488.4	522.4	1.3487
-33	15.303	511.6	1469.2	508.9	1.3487
-34	13.823	621.6	1450.0	495.7	1.3487
-35	13.435	652.1	1444.8	492.1	1.3487
-36	13.259	664.6	1442.4	490.5	1.3487
-37	13.546	639.9	1446.5	493.3	1.3487
-38	14.322	577.3	1457.0	500.52	1.3487
17-15	17.136	259.2	1950.6	926.2	1.3046
-16	17.853	194.5	1959.0	934.1	1.3046
-17	17.675	200.0	1950.3	926.8	1.3046
-17'			1765.8	759.5	1.3211
-18	17.573	201.0	1765.3	759.0	1.3211
-19	17.422	204.0	1764.7	758.0	1.3211
-19'			1676.5	670.6	1.3309
-20	17.412	204.0	1675.9	670.2	1.3309
-21	17.397	201.9	1676.1	670.3	1.3309
-22	17.266	196.4	1676.6	670.7	1.3309
-22'			1588.6	598.3	1.3397
-23	17.476	191.4	1589.0	598.6	1.3397
-24	17.477	189.9	1588.8	598.5	1.3397
-25	17.457	189.9	1588.3	598.1	1.3397
-26	17.403	192.4	1587.4	597.7	1.3397
-27	17.295	196.4	1586.4	596.9	1.3397
-27'			1492.5	525.2	1.3487
-28	17.258	195.6	1492.4	525.1	1.3487
-29	17.244	195.4	1492.1	524.9	1.3487
-30	17.242	194.5	1491.9	524.8	1.3487
-31	17.225	194.6	1491.6	524.6	1.3487
-32	15.557	306.0	1472.1	510.9	1.3487
-33	14.060	415.9	1452.9	497.7	1.3487
-34	12.705	524.3	1434.0	484.9	1.3487
-35	12.342	554.0	1428.7	481.3	1.3487
-36	12.181	566.6	1426.3	479.7	1.3487
-37	12.449	542.3	1430.4	482.4	1.3487
-38	13.169	480.4	1440.9	489.5	1.3487
-39	14.322	388.0	1456.7	500.3	1.3487
18-15	16.368	191.8	1940.0	916.2	1.3046
-16	17.061	127.4	1948.5	924.5	1.3046
-17	16.963	133.3	1947.1	922.9	1.3046
-18	16.822	138.9	1938.5	915.6	1.3046
-18'			1755.3	750.6	1.3211
-19	16.713	142.3	1754.3	749.7	1.3211

STATE I - II	P	U	a	T	γ
18-20	16.633	144.6	1753.9	748.7	1.3211
-20'			1666.2	662.4	1.3309
-21	16.625	142.5	1666.3	662.5	1.3309
-22	16.682	137.2	1666.9	663.0	1.3309
-23	16.674	134.1	1667.0	663.1	1.3309
-23'			1579.2	591.2	1.3397
-24	16.648	132.6	1579.1	591.2	1.3397
-25	16.631	132.6	1578.7	590.9	1.3397
-26	16.579	135.1	1578.0	590.5	1.3397
-27	16.509	138.9	1577.1	589.8	1.3397
-28	16.445	140.6	1576.6	589.4	1.3397
-28'			1482.7	518.3	1.3487
-29	16.406	140.4	1482.5	518.2	1.3487
-30	16.405	139.4	1482.4	518.1	1.3487
-31	16.390	139.6	1482.1	517.9	1.3487
-32	14.797	250.6	1462.6	504.4	1.3487
-33	13.374	359.5	1443.6	491.4	1.3487
-34	12.081	467.6	1424.8	478.6	1.3487
-35	11.735	497.2	1419.5	475.1	1.3487
-36	11.581	509.8	1417.1	473.5	1.3487
-37	11.838	485.8	1421.2	476.2	1.3487
-38	12.527	424.1	1431.7	483.2	1.3487
-39	13.631	331.8	1447.5	494.0	1.3487
-40	14.322	277.4	1456.8	500.3	1.3487
19-16	15.419	100.9	1925.9	902.9	1.3046
-17	15.970	45.8	1932.7	909.3	1.3046
-18	15.891	51.6	1931.1	907.8	1.3046
-19	15.736	60.9	1921.4	899.5	1.3046
-19'			1740.6	738.0	1.3211
-20	15.660	63.4	1739.5	737.0	1.3211
-21	15.644	64.4	1740.5	737.3	1.3211
-21'			1653.5	652.4	1.3309
-22	15.678	60.0	1653.7	652.5	1.3309
-23	15.701	57.1	1653.6	652.7	1.3309
-24	15.654	58.8	1634.5	652.2	1.3309
-24'			1566.3	581.7	1.3397
-25	15.621	58.8	1565.8	581.3	1.3397
-26	15.576	61.5	1565.0	580.9	1.3397
-27	15.514	65.7	1564.0	580.1	1.3397
-28	15.476	67.6	1563.2	579.6	1.3397
-29	15.412	71.1	1562.4	579.0	1.3397
-29'			1470.2	509.7	1.3487
-30	15.406	70.3	1470.1	509.6	1.3487
-31	15.386	70.7	1469.9	509.4	1.3487

STATE I - II	P	U	a	T	γ
19-32	13.890	181.7	1450.4	496.0	1.3487
-33	12.552	289.8	1431.6	483.2	1.3487
-34	11.333	396.9	1421.8	470.6	1.3487
-35	11.009	426.4	1407.5	467.1	1.3487
-36	10.867	439.2	1405.1	465.5	1.3487
-37	11.110	415.1	1409.3	468.2	1.3487
-38	11.761	354.0	1419.7	475.2	1.3487
-39	12.805	262.5	1435.4	485.8	1.3487
-40	13.454	209.0	1444.6	492.0	1.3487
-41	14.322	140.8	1456.4	500.1	1.3487
20-17	14.466	6.5	1911.9	889.8	1.3046
-18	14.910	-39.5	1918.1	895.6	1.3046
-19	14.790	-30.0	1915.2	892.8	1.3046
-20	14.670	-21.6	1904.3	883.6	1.3046
-20'			1725.6	725.3	1.3211
-21	14.656	-21.4	1725.3	725.0	1.3211
-22	14.667	-22.9	1724.8	724.8	1.3211
-22'			1639.5	641.4	1.3309
-23	14.673	-25.8	1639.4	641.3	1.3309
-24	14.683	-24.5	1634.1	640.7	1.3309
-25	14.594	-21.0	1637.7	639.9	1.3309
-25'			1552.5	571.2	1.3397
-26	14.535	-17.4	1551.5	570.4	1.3397
-27	14.484	-13.6	1550.2	569.9	1.3397
-28	14.458	-12.0	1549.4	569.5	1.3397
-29	14.401	-8.0	1548.6	568.8	1.3397
-30	14.364	-5.5	1548.0	568.3	1.3397
-30'			1456.7	500.3	1.3487
-31	14.352	-5.0	1456.5	500.2	1.3487
-32	12.944	105.6	1437.1	486.9	1.3487
-33	11.692	213.0	1418.3	474.3	1.3487
-34	10.546	320.1	1399.5	461.8	1.3487
-35	10.250	349.0	1394.3	458.4	1.3487
-36	10.120	361.4	1392.0	456.9	1.3487
-37	10.346	337.9	1396.0	459.5	1.3487
-38	10.955	277.4	1406.3	466.3	1.3487
-39	11.936	186.6	1421.9	476.7	1.3487
-40	12.536	133.3	1430.9	482.8	1.3487
-41	13.887	65.1	1442.6	490.7	1.3487
-42	14.322	-10.7	1455.6	499.6	1.3487
21-18	14.353	-95.5	1909.4	887.4	1.3046
-19	14.133	-75.3	1904.6	883.4	1.3046
-20	14.117	-76.6	1895.2	875.1	1.3046

STATE I - II	P	U	a	T	γ
21-21			1894.4	874.4	1.3046
-21'	14.072	-73.2	1716.8	718.0	1.3046
-22	14.084	-74.5	1716.7	717.8	1.3211
-23			1716.5	717.7	1.3211
-23'	14.082	-75.6	1630.9	634.7	1.3309
-24	14.093	-77.6	1630.4	634.3	1.3309
-25	14.010	-70.9	1629.2	633.3	1.3309
-26			1628.05	632.5	1.3309
-26'	13.941	-64.9	1543.3	564.4	1.3397
-27	13.894	-61.1	1542.0	563.9	1.3397
-28	13.871	-59.6	1541.3	563.5	1.3397
-29	13.816	-55.4	1540.4	562.8	1.3397
-30	13.781	-52.9	1539.8	562.3	1.3397
-31			1539.2	561.9	1.3397
-31'	13.752	-50.4	1448.5	494.7	1.3487
-32	12.401	60.2	1429.1	481.5	1.3487
-33	11.199	167.1	1410.3	469.0	1.3487
-34	10.098	274.1	1391.7	456.6	1.3487
-35	9.815	302.8	1386.4	453.2	1.3487
-36	9.833	315.2	1384.1	451.7	1.3487
-37	9.908	291.9	1388.1	454.3	1.3487
-38	10.494	231.7	1398.4	461.1	1.3487
-39	11.435	141.2	1414.0	471.4	1.3487
-40	12.018	88.4	1423.1	477.5	1.3487
-41	12.807	20.4	1434.8	485.4	1.3487
-42	13.741	-55.0	1447.9	494.2	1.3487
22-19	14.340	-48.9	1906.9	885.6	1.3046
-20	14.338	-51.8	1897.5	877.2	1.3046
-21	14.271	-48.1	1897.1	876.9	1.3046
-22			1896.3	876.2	1.3046
-22'	14.302	-53.5	1719.3	720.1	1.3211
-23	14.297	-54.6	1718.5	719.4	1.3211
-24			1718.4	718.9	1.3211
-24'	14.317	-54.6	1633.1	636.4	1.3309
-25	14.229	-51.0	1631.9	635.5	1.3309
-26	14.156	-45.1	1630.8	634.6	1.3309
-27			1630.0	633.9	1.3309
-27'	14.117	-42.2	1544.9	567.0	1.3397
-28	14.100	-40.7	1544.2	565.5	1.3397
-29	14.032	-36.5	1543.3	564.9	1.3397
-30	14.002	-34.0	1542.6	564.4	1.3397
-31	13.969	-31.5	1542.1	564.0	1.3397
-32			1522.6	549.9	1.3397
-32'	12.652	82.9	1433.0	484.1	1.3487

STATE I - II	P	U	a	T	γ
22-33	11.446	189.5	1414.2	471.5	1.3487
-34	10.328	296.1	1395.5	459.1	1.3487
-35	10.038	324.7	1390.3	455.7	1.3487
-36	9.911	337.2	1388.0	454.2	1.3487
-37	10.314	313.8	1392.0	456.8	1.3487
-38	10.727	253.9	1402.3	463.6	1.3487
-39	11.685	163.5	1417.8	473.9	1.3487
-40	12.277	110.8	1426.9	480.0	1.3487
-41	13.078	43.0	1438.5	487.9	1.3487
-42	14.027	-32.7	1450.5	496.7	1.3487
23-20	14.333	-52.8	1897.5	877.2	1.3046
-21	14.332	-51.2	1897.7	877.4	1.3046
-22	14.300	-50.2	1894.8	874.8	1.3046
-23	14.294	-53.1	1894.7	874.7	1.3046
-23'			1718.5	719.4	1.3211
-24	14.317	-53.1	1717.2	718.3	1.3211
-25	14.282	-49.7	1716.7	717.9	1.3211
-25'			1631.6	635.2	1.3309
-26	14.157	-43.9	1630.4	634.3	1.3309
-27	14.116	-41.1	1629.2	633.7	1.3309
-28	14.095	-39.7	1620.0	633.2	1.3309
-28'			1543.9	565.4	1.3397
-29	14.040	35.5	1543.0	564.7	1.3397
-30	14.004	-33.0	1542.3	564.2	1.3397
-31	13.971	-30.8	1541.7	563.7	1.3397
-32	12.638	83.5	1522.2	549.5	1.3397
-33	11.480	191.4	1503.7	536.3	1.3397
-33'			1415.2	472.2	1.3487
-34	10.386	300.3	1396.5	459.8	1.3487
-35	10.096	328.7	1391.4	456.5	1.3487
-36	9.972	341.0	1389.1	454.9	1.3487
-37	10.372	317.9	1393.0	457.5	1.3487
-38	10.784	258.3	1403.2	464.3	1.3487
-39	11.744	168.3	1418.7	474.6	1.3487
-40	12.337	115.8	1427.8	480.7	1.3487
-41	13.139	47.8	1439.4	488.5	1.3487
-42	14.089	-27.7	1452.4	497.3	1.3487
24-22	14.335	-44.5	1894.6	874.6	1.3046
-23	14.323	-46.6	1894.0	873.7	1.3046
-24	14.347	-48.7	1893.4	873.5	1.3046
-24'			1718.1	719.0	1.3211
-25	14.223	-48.9	1715.9	717.2	1.3211

STATE I - II	P	U	a	T	γ
24-26			1714.3	715.9	1.3211
-26'	14.151	-43.4	1629.9	633.9	1.3309
-27	14.112	-40.5	1629.2	633.3	1.3309
-28	14.088	-39.2	1628.5	632.8	1.3309
-29			1627.4	631.9	1.3309
-29'	14.035	-34.8	1542.8	564.5	1.3397
-30	14.003	-32.5	1542.1	564.0	1.3397
-31	13.970	-30.2	1541.4	563.5	1.3397
-32	12.638	83.9	1521.8	549.3	1.3397
-33	11.458	194.1	1502.9	535.8	1.3397
-34	10.375	304.1	1484.0	522.4	1.3397
-35	10.094	333.5	1478.7	518.8	1.3397
-36	9.972	346.3	1476.4	517.1	1.3397
-37			1480.3	519.9	1.3397
-37'	10.219	322.6	1394.1	458.2	1.3487
-38	10.847	263.2	1404.3	464.9	1.3487
-39	11.808	173.6	1419.7	475.3	1.3487
-40	12.403	121.3	1428.8	481.3	1.3487
-41	13.209	53.7	1440.3	489.1	1.3487
-42	14.163	-21.6	1453.1	497.9	1.3487
25-23	14.335	-44.7	1893.6	873.2	1.3046
-24	14.315	-45.7	1892.0	872.2	1.3046
-25			1891.2	871.5	1.3046
-25'	14.264	-43.6	1716.7	717.9	1.3211
-26	14.191	-38.0	1714.3	715.9	1.3211
-27			1713.3	715.1	1.3211
-27'	14.154	-35.7	1629.4	633.5	1.3309
-28	14.132	-34.4	1628.7	633.0	1.3309
-29	14.074	-30.2	1627.6	632.1	1.3309
-30			1626.9	635.1	1.3309
-30'	14.045	-28.3	1542.4	564.2	1.3397
-31	14.015	-26.0	1541.8	563.8	1.3397
-32	12.680	88.1	1522.3	549.6	1.3397
-33	11.500	197.9	1503.4	536.0	1.3397
-34	10.418	307.4	1484.6	522.7	1.3397
-35	10.136	336.6	1479.3	519.0	1.3397
-36	10.013	349.2	1477.0	517.4	1.3397
-37	10.225	325.5	1480.9	520.1	1.3397
-38	10.804	263.6	1491.2	527.4	1.3397
-39	11.754	170.4	1506.7	538.4	1.3397
-40			1515.9	544.9	1.3397
-40'	12.326	115.9	1427.9	480.7	1.3487
-41	13.145	48.5	1439.2	488.4	1.3487
-42	14.093	-26.7	1452.1	497.1	1.3487

STATE I - II	P	U	a	T	γ
26-24	14.335	-43.6	1891.7	871.9	1.3046
-25	14.259	-43.6	1890.5	870.8	1.3046
-26	14.157	-39.4	1888.0	868.5	1.3046
-26'			1714.4	716.0	1.3211
-27	14.128	-37.1	1712.4	714.3	1.3211
-28	14.104	-35.7	1711.5	713.6	1.3211
-28'			1627.9	632.3	1.3309
-29	14.048	-31.5	1626.8	631.5	1.3309
-30	14.020	-29.6	1626.1	630.9	1.3309
-31	13.987	-27.3	1625.3	630.3	1.3309
-31'			1541.4	563.4	1.3397
-32	12.658	86.5	1521.9	549.2	1.3397
-33	11.484	196.0	1503.0	535.7	1.3397
-34	10.408	305.1	1484.2	522.4	1.3397
-35	10.129	334.1	1479.1	518.8	1.3397
-36	10.006	346.7	1476.8	517.2	1.3397
-37	10.217	323.2	1480.6	519.9	1.3397
-38	10.792	261.7	1490.9	527.1	1.3397
-39	11.698	168.9	1506.5	538.2	1.3397
-40	12.292	114.6	1515.6	544.8	1.3397
-41	13.080	44.3	1527.1	553.1	1.3397
-41'			1438.1	487.8	1.3487
-42	14.033	-30.8	1451.2	496.5	1.3487
27-25	14.333	-33.4	1892.2	872.3	1.3046
-26	14.241	-27.3	1888.6	869.2	1.3046
-27	14.216	-27.3	1887.6	868.2	1.3046
-27'			1714.7	716.2	1.3211
-28	14.191	-26.0	1712.2	714.2	1.3211
-29	14.140	-22.3	1711.1	713.2	1.3211
-29'			1627.8	632.2	1.3309
-30	14.112	-20.4	1627.1	631.7	1.3309
-31	14.077	-18.1	1626.3	631.1	1.3309
-32	12.785	99.5	1606.4	615.8	1.3309
-32'			1523.9	550.7	1.3397
-33	11.617	208.6	1505.1	537.2	1.3397
-34	10.533	317.1	1486.4	523.9	1.3397
-35	10.252	345.9	1481.2	520.3	1.3397
-36	10.129	358.4	1478.9	518.7	1.3397
-37	10.339	335.0	1482.8	521.4	1.3397
-38	10.917	273.7	1493.0	528.6	1.3397
-39	11.849	181.3	1508.5	539.7	1.3397
-40	12.427	127.0	1517.6	546.2	1.3397
-41	13.208	56.9	1529.1	554.5	1.3397
-42	14.144	-22.2	1542.2	567.0	1.3397
-42'			1452.5	497.4	1.3487

STATE I - II	P	U	a	T	γ
28-26	14.323	-18.5	1889.6	870.0	1.3046
-27	14.283	-17.4	1887.4	868.0	1.3046
-28	14.261	-18.1	1886.9	867.5	1.3046
-28'			1714.6	716.2	1.3211
-29	14.208	-14.5	1711.5	713.6	1.3211
-30	14.182	-13.4	1710.6	712.8	1.3211
-30'			1627.7	632.2	1.3309
-31	14.149	-11.1	1626.9	631.6	1.3309
-32	12.838	106.4	1607.0	616.3	1.3309
-33	11.704	218.9	1588.0	601.7	1.3309
-33'			1506.7	538.3	1.3397
-34	10.619	326.8	1488.1	525.1	1.3397
-35	10.356	355.5	1482.9	521.5	1.3397
-36	10.229	367.5	1480.5	519.8	1.3397
-37	10.440	344.2	1484.3	522.5	1.3397
-38	11.020	283.3	1494.4	529.6	1.3397
-39	11.956	191.2	1509.9	540.6	1.3397
-40	12.538	137.0	1518.9	547.1	1.3397
-41	13.323	67.2	1530.4	555.4	1.3397
-42	14.265	-11.8	1543.4	564.9	1.3397
29-27	14.323	-12.3	1887.3	867.9	1.3046
-28	14.293	-11.8	1886.1	866.8	1.3046
-29	14.244	-9.7	1885.4	866.1	1.3046
-29'			1713.8	715.5	1.3211
-30	14.218	-8.6	1710.6	712.8	1.3211
-31	14.188	-6.9	1707.4	710.1	1.3211
-31'			1627.2	631.8	1.3309
-32	12.876	110.4	1607.4	616.5	1.3309
-33	11.718	222.5	1588.3	602.2	1.3309
-34	10.687	333.9	1569.5	588.0	1.3309
-34'			1489.2	525.9	1.3397
-35	10.436	362.2	1484.1	522.3	1.3397
-36	10.311	374.6	1481.8	520.7	1.3397
-37	10.522	351.3	1485,6	523.4	1.3397
-38	11.103	290.7	1495.7	530.5	1.3397
-39	12.041	199.0	1511.1	541.5	1.3397
-40	12.627	144.8	1520.2	548.0	1.3397
-41	13.413	75.3	1531.7	556.3	1.3397
-42	14.358	-3.8	1544.6	565.7	1.3397
30-28	14.323	-8.0	1886.0	866.7	1.3046
-29	14.261	-4.8	1884.4	865.2	1.3046

STATE I - II	P	U	a	T	γ
30-30			1883.9	864.7	1.3046
-30'	14.238	-5.3	1713.1	714.9	1.3211
-31	14.208	-3.4	1710.3	712.5	1.3211
-32			1687.8	694.0	1.3211
-32'	12.932	117.7	1608.4	617.3	1.3309
-33	11.788	229.4	1589.4	602.8	1.3309
-34	10.723	340.4	1570.7	588.7	1.3309
-35	10.452	369.1	1565.5	584.9	1.3309
-36	10.330	381.8	1563.2	583.1	1.3309
-37	10.539	358.2	1567.0	586.0	1.3309
-38			1577.2	593.6	1.3309
-38'	11.133	295.5	1496.6	531.1	1.3397
-39	12.099	204.2	1511.9	542.1	1.3397
-40	12.687	150.1	1521.0	548.6	1.3397
-41	13.473	80.4	1532.4	556.8	1.3397
-42	14.419	1.5	1545.4	566.3	1.3397
31-29	14.322	0.0	1884.7	865.5	1.3046
-30	14.276	+1.7	1883.2	864.1	1.3046
-31			1883.0	863.9	1.3046
-31'	14.252	+1.9	1712.7	714.6	1.3211
-32	12.960	123.0	1692.1	697.5	1.3211
-33			1672.7	682.1	1.3211
-33'	11.851	238.0	1590.6	603.7	1.3309
-34	10.807	348.2	1571.9	589.6	1.3309
-35	10.597	377.5	1566.8	585.8	1.3309
-36	10.410	390.1	1564.4	584.0	1.3309
-37	10.620	365.8	1568.3	586.9	1.3309
-38	11.188	303.7	1578.4	594.0	1.3309
-39	12.110	208.6	1593.9	606.3	1.3309
-40	12.686	152.4	1603.1	613.3	1.3309
-41			1614.6	622.1	1.3309
-41'	13.462	80.4	1532.1	556.7	1.3397
-42	14.416	1.7	1545.2	566.2	1.3397
32-30	14.320	4.6	1883.2	864.1	1.3046
-31	14.270	6.7	1882.2	863.2	1.3046
-32			1862.1	844.9	1.3046
-32'	13.049	135.1	1693.2	698.5	1.3211
-33	11.933	249.5	1674.0	682.6	1.3211
-34			1655.0	667.3	1.3211
-34'	10.922	362.6	1574.4	591.5	1.3309
-35	10.666	390.8	1569.1	587.5	1.3309
-36	10.544	403.4	1566.7	585.8	1.3309

STATE I - II	P	U	a	T	γ
32-37	10.755	379.2	1570.6	588.6	1.3309
-38	11.325	317.5	1580.7	596.2	1.3309
-39	12.254	222.7	1596.2	607.9	1.3309
-40	12.836	166.8	1605.4	615.0	1.3309
-41	13.609	94.9	1616.4	623.5	1.3309
-42	14.546	12.4	1629.2	633.4	1.3309
-42'			1546.7	567.3	1.3397
33-31	14.322	11.5	1882.5	863.4	1.3046
-32	13.054	141.4	1861.7	844.4	1.3046
-33	12.006	261.7	1841.6	826.3	1.3046
-33'			1675.3	683.8	1.3211
-34	10.998	374.2	1656.5	668.5	1.3211
-35	10.728	403.1	1651.3	664.3	1.3211
-36	10.607	415.9	1649.0	662.4	1.3211
-37	10.813	391.2	1652.8	665.5	1.3211
-38	11.369	327.4	1662.8	673.6	1.3211
-39	12.280	229.0	1678.3	686.2	1.3211
-40	12.866	171.2	1687.5	693.8	1.3211
-40'			1606.0	615.5	1.3309
-41	13.652	99.8	1617.3	624.2	1.3309
-42	14.596	17.4	1630.5	634.4	1.3309
34-32	13.856	201.5	1901.4	880.0	1.3046
-33	12.595	336.2	1878.8	859.1	1.3046
-34	11.650	450.0	1859.4	841.2	1.3046
-34'			1668.7	677.9	1.3211
-35	11.414	478.3	1663.5	674.1	1.3211
-36	11.281	490.0	1661.1	672.1	1.3211
-37	11.491	465.5	1664.8	675.1	1.3211
-38	12.073	402.1	1674.7	683.1	1.3211
-39	13.031	304.5	1690.2	696.0	1.3211
-40	13.631	246.0	1699.5	703.4	1.3211
-41	14.456	168.9	1710.0	713.0	1.3211
-42	15.412	82.7	1724.0	723.1	1.3211
-42'			1641.0	642.4	1.3309
35-33	12.794	358.0	1883.8	863.7	1.3046
-34	11.788	472.6	1864.6	845.9	1.3046
-35	11.499	499.5	1858.7	841.0	1.3046
-36	11.379	512.5	1855.8	838.4	1.3046
-37	11.578	486.7	1859.4	841.5	1.3046
-38	12.135	419.5	1869.0	850.3	1.3046
-39	13.035	314.4	1884.2	864.0	1.3046
-40	14.036	251.6	1893.4	872.6	1.3046

STATE I - II	P	U	a	T	γ
35-41			1904.4	882.8	1.3046
-41'	14.382	168.5	1710.3	712.3	1.3211
-42	15.336	82.9	1722.9	722.3	1.3211
36-34	11.788	472.4	1865.9	847.4	1.3046
-35	11.541	498.8	1860.7	842.8	1.3046
-36	11.421	511.6	1858.3	840.5	1.3046
-37	11.622	486.1	1862.0	843.9	1.3046
-38	12.174	420.2	1871.7	852.7	1.3046
-39	13.080	315.8	1887.0	866.7	1.3046
-40	13.653	253.1	1896.2	875.2	1.3046
-41	14.430	170.6	1907.1	885.3	1.3046
-42			1919.4	896.8	1.3046
-42'	15.340	75.8	1721.0	721.4	1.3211
37-35	11.405	478.9	1859.1	841.3	1.3046
-36	11.284	492.3	1856.6	839.6	1.3046
-37	11.481	466.9	1860.3	843.0	1.3046
-38	12.025	401.1	1870.2	852.0	1.3046
-39	12.925	298.0	1886.0	866.3	1.3046
-40	13.500	235.5	1895.2	875.0	1.3046
-41	14.266	153.2	1906.5	885.4	1.3046
-42	15.168	59.2	1920.0	897.6	1.3046
38-36	11.300	487.1	1858.1	840.4	1.3046
-37	11.473	465.3	1861.7	843.6	1.3046
-38	12.014	401.1	1871.7	852.8	1.3046
-39	12.907	296.7	1887.4	867.1	1.3046
-40	13.474	234.6	1897.0	875.8	1.3046
-41	14.242	152.8	1909.0	887.0	1.3046
-42	15.143	57.9	1910.6	888.6	1.3046
39-39	11.492	396.9	1861.7	843.1	1.3046
-40	12.880	232.5	1887.7	866.5	1.3046
-41	13.909	119.6	1903.5	882.0	1.3046
-42	14.802	25.6	1917.3	893.9	1.3046
40-40	11.932	116.7	1869.9	851.1	1.3046
-41	12.867	6.9	1886.4	866.2	1.3046
-42	13.703	-86.9	1900.2	878.9	1.3046

STATE I - II	P	U	a	T	γ
41-41	12.790	-2.3	1883.7	863.7	1.3046
-42	13.613	-95.1	1896.2	875.3	1.3046
42-42	14.018	-46.2	1903.2	881.7	1.3046

6. Specimen Calculations

6.1. Calculation of the cylinder gas release temperature

Cylinder release pressure P_r = 40.322 psia.

Cylinder release volume V_r = 0.02121 cu.ft.

Cylinder trapped volume V_t = 0.02109 cu.ft.

From the indicator record, the cylinder pressure at air port closure = 14.37 psia.

The measured air mass flow = 0.93804 lb/min.

Hence, assuming that no air is short circuited, then:

Weight of air in cylinder = $\frac{0.93804}{1110.5}$

= 8.4470×10^{-4} lb.

From the characteristic gas equation:-

Volume of air in cylinder at air port closure

= $\frac{8.447 \times 10^{-4} \times 96 \times 292.7}{144 \times 14.37}$

= 0.01147 cu.ft.

Thus the volume occupied by the residual exhaust gas

= trapped volume - volume of air

= 0.02109 - 0.01147

= 0.00962 cu.ft.

The release temperature is obtained by an iteration process to obtain a mass balance, and the last step of this process is given below.

Assume the temperature of the residual exhaust gas at air port closure to be 888 °K.

From Section 4.1, R for the exhaust gas = 97.80 ft.lb/lb.°C.

Hence, from the characteristic gas equation,

weight of residual gas in the cylinder

$$= \frac{144 \times 14.37 \times 0.00962}{97.80 \times 888}$$

$$= 2.2921 \times 10^{-4} \text{ lb.}$$

The measured fuel consumption = 0.05068 lb/min.,

thus the weight of fuel injected per cycle $= \frac{0.05068}{1110.5}$

$$= 0.4564 \times 10^{-4} \text{ lb.}$$

Hence, the total weight of the cylinder contents at exhaust port opening

$$= (8.4470 + 2.2921 + 0.4564) \times 10^{-4} \text{ lb.}$$

$$= 11.196 \times 10^{-4} \text{ lb.}$$

Now T release = T residuals $\left(\frac{\text{P release}}{\text{P residuals}}\right)^{\frac{\gamma-1}{\gamma}}$

Based on the previous step, the mean $\gamma = 1.2954$,

thus T release $= 888 \left(\frac{40.322}{14.37}\right)^{\frac{.2954}{1.2954}}$

$$= 1125 \text{ °K.}$$

Using this temperature, and the characteristic gas equation gives:

weight of cylinder contents at release

$$= \frac{144 \times 40.322 \times 0.2121}{97.80 \times 1125}$$

$$= 11.193 \times 10^{-4} \text{ lb.}$$

This value compares with that obtained above and therefore the release temperature is 1125 °K.

6.2. Temperature in the exhaust pipe adjacent to the ports at the beginning of blowdown.

The temperature existing in the exhaust pipe at the commencement of blowdown is the downstream temperature at the major temperature discontinuity. This temperature is determined by considering the heat loss from the gases during the period in which the exhaust ports are closed.

Assuming that the gases existing adjacent to the ports at the instant of port closure have just been ejected from the cylinder, and that the pressure there is P_o = 14.322 psia., then their temperature, and the datum value a_o, are obtained by considering an isentropic expansion of the cylinder contents from the release conditions to the datum pressure P_o. The initial evaluation of these values requires the use of an iteration process using a mean value of γ for the expansion. If, however, an isentropic step by step analysis of the cylinder expansion is performed, then the accurate values for the temperature and a_o are obtained.

From the isentropic step by step analysis, the temperature of the cylinder gases at the end of blowdown is 888.2 °K. (and a_o = 1910.2 ft/sec).

The exhaust ports are closed for 262° of crank angle. Hence the time for which the ports are closed

$$= 262 \times 15.008 \times 10^{-5}$$

$$= 3.932 \times 10^{-2} \text{ secs.}$$

Assuming the mean temperature of the gas in the pipe during this time is 805 °K, then from Fig. 31, the rate of heat transfer is 46,014 ft.lb/ft^3.sec.

Thus the loss of energy by the gases in this period

$$= 46{,}014 \times 3.932 \times 10^{-2}$$

$$= 1809 \text{ ft.lb./ft.}^3$$

and this can be equated to $\rho C_p \Delta T$.

The density of the exhaust gas $\rho = \frac{P}{RT}$

$$= \frac{144 \times 14.322}{97.80 \times 805}$$

$$= 0.02620 \text{ lb/ft.}^3$$

The value for C_p, at the temperature of 805 °K, is evaluated from gas tables and the exhaust gas analysis, and its value is 0.3015.

Hence, $\Delta T = \frac{1809}{1400} \times \frac{0.0262}{0.3015}$

$$= 163.6 \text{ °C}$$

This gives a mean temperature of 806 °K. which compares with the assumed value of 805 °K.

Thus the temperature in the pipe at the instant of exhaust port opening = 888.2 - 163.6

$$= 724.6 \text{ °K.}$$

6.3. Cylinder step calculation.

Consider the boundary region $I_{15}\,II_{13}$, which occurs within the blowdown period.

The initial cylinder parameters for this step are:-

Pressure (P_1)	=	24.778 psia.
Volume (V_e)	=	38.883 cu.in.
Temperature (T_e)	=	1008.1 °K
Density (ρ_e)	=	0.036194 lb/ft^3
Local acoustic velocity (a_e)	=	2018.4 ft/sec.
Mass (m_e)	=	8.14409×10^{-4} lb.
Ratio of specific heats (γ_e)	=	1.2948

From experience, it is possible to reduce the number of iteration steps by 'guessing' the slope of the reflected wave which completes the field boundary of region $I_{15}\,II_{13}$, and the first approximation to ΔP_1.

Using a 'guessed' slope in the position diagram gives the following:

initial crank angle for step	=	38.70°	before B.D.C.E.P
final " " " "	=	37.09°	" "
mean " " " " (α_m)	=	37.895°	" "
change of " " " " ($\Delta\alpha$)	=	1.61°	" "

Using the above values of crank angle for the step:- from Fig.25:

final cylinder volume	=	39.244 cu.in.
mean " " " (Ve_m)	=	39.063 cu.in.
change of " " (ΔV_e)	=	0.361 cu.in.

from Figs. 26 and 27:

mean $\frac{\text{port area}}{\text{pipe area}}$ for the exhaust ports = 0.374.

mean hydraulic radius (r) for exhaust ports = 0.1061 in.

Taking ΔP_1 for the step as -2.910 psi. gives the mean P_1 = 23.323 psia, and from equations (3.8-11), (3.8-12) and (3.8-13), the values of ΔT_e, $\Delta \rho_e$, Δa_e are found, thus giving:

mean T_e for the step = 993.8 °K

mean ρ_e for the step = 0.034450 lb/ft^3

mean a_e for the step = 2004.1 ft/sec.

At the mean temperature of the exhaust gases (993.8°K), from Figs.29 and 30:-

γ_e = 1.2958

and μ = 0.0413 centipoises

Modified Reynolds number $(R_m) = \frac{a\, r\, \rho}{\mu}$ which on substitution of the above mean values gives:

R_m for step = 2.199×10^4

An approximate value for the pressure ratio across the ports $\frac{P_1}{P_2}$ is obtained by using the pipe pressure for the previous cylinder step,

i.e. $\frac{P_1}{P_2} = \frac{23.323}{20.021} = 1.165$

Using the above value for R_m, and this value of $\frac{P_1}{P_2}$ for the ratio $\frac{P}{P_o}$ in Fig.28, determines the coefficient

of discharge as:-

$$C_d = 0.999$$

Hence, k for the step = $\frac{\text{port area}}{\text{pipe area}} \times C_d$

$$= 0.374 \times .999$$

$$\doteq 0.374$$

Transfer of state point from state diagram to boundary diagram.

The previous state point lying on the Π_{13} characteristic is $I_{14}\,\Pi_{13}$ (or 14.13).

Now in this pipe region, $\gamma = 1.3046$ and for region 14.13, $\bar{X} = 1.03988$.

Hence using the index marks ' and " for $\gamma = 1.3$ and $\gamma = 1.4$ respectively, then the values of $\bar{X}$ for the inferred states 14.13' and 14.13" in the state diagram are:-

$$\bar{X}' = 1.03941$$

$$\bar{X}'' = 1.04902$$

The values of $(a_{os2})'$," for the pipe region 14.13'," are calculated using equation (3.4-7) and the appropriate initial values of $(a_{os2})'$,". The initial values of $(a_{os2})'$," are identical with the $(a_{os1})'$," values obtained by expanding the cylinder gases to the datum pressure P_o according to the appropriate indices for $\gamma = 1.3$ and $\gamma = 1.4$.

a'_{os1} = initial a'_{os2} = 1894.6 ft/sec.

a''_{os1} = initial a''_{os2} = 1841.7 ft/sec.

Hence using equation (3.4-7), for region 14.13

a'_{os2} = 1893.8 ft/sec.

a''_{os2} = 1840.7 ft/sec.

The slopes of the characteristics in the state diagram through the state points 14.13','' are given by equation (3.8-17), viz:

$$\left(\frac{\Delta \bar{X}}{\Delta \bar{U}}\right)','' = \left(\frac{\gamma-1}{2}\ \frac{a_o}{a_{os2}}\right)',''$$

Substitution of the appropriate values for γ and a_{os2}, and the value of a_o = 1910.2 ft/sec., gives:

$$\left(\frac{\Delta \bar{X}}{\Delta \bar{U}}\right)' = 0.1513$$

and $$\left(\frac{\Delta \bar{X}}{\Delta \bar{U}}\right)'' = 0.2076$$

The intercepts on the ordinate axis of these characteristics drawn in the state diagram are:-

$$\left(\frac{P}{P_o}\right)^{\frac{\gamma-1}{2\gamma}}{}' = 1.00077$$

$$\left(\frac{P}{P_o}\right)^{\frac{\gamma-1}{2\gamma}}{}'' = 0.98800$$

The intercept of these characteristics with the ordinate axis in the appropriate boundary diagrams are given by equation (3.8-20).

Now

$$\left[\left(\frac{P_o}{P_1}\right)^{\frac{\gamma-1}{2\gamma}}\right]' = \left(\frac{14.322}{23.323}\right)^{\frac{.2}{2.6}} = 0.94529$$

and

$$\left[\left(\frac{P_o}{P_1}\right)^{\frac{\gamma-1}{2\gamma}}\right]'' = \left(\frac{14.322}{23.323}\right)^{\frac{1}{7}} = 0.93271$$

Hence, in the boundary diagrams, the intercepts are:-

$$\left[\left(\frac{P}{P_1}\right)^{\frac{\gamma-1}{2\gamma}}\right]' = 1.00077 \times 0.94529 = 0.94602$$

$$\left[\left(\frac{P}{P_1}\right)^{\frac{\gamma-1}{2\gamma}}\right]'' = 0.98800 \times 0.93271 = 0.92152$$

The slopes of these characteristics in the boundary diagrams are given by equation (3.8-19), i.e.

$$\left[\frac{\Delta\left(\frac{P_2}{P_1}\right)^{\frac{\gamma-1}{2\gamma}}}{\Delta\left(\frac{u_2}{a_1}\right)}\right]' = \frac{0.3}{2} \times \frac{1894.6}{1893.8} = 0.1501$$

$$\left[\frac{\Delta\left(\frac{P_2}{P_1}\right)^{\frac{\gamma-1}{2\gamma}}}{\Delta\left(\frac{u_2}{a_1}\right)}\right]'' = \frac{0.4}{2} \times \frac{1841.7}{1840.7} = 0.2001$$

The interception of these characteristics, plotted in the appropriate boundary diagrams, with the k = 0.374 line gives:-

$$M' = 0.2020; \left[\left(\frac{P_2}{P_1}\right)^{\frac{\gamma-1}{2\gamma}}\right]' = 0.98110; \quad \left(\frac{u_2}{a_1}\right)' = 0.2360$$

$$M'' = 0.2027; \left[\left(\frac{P_2}{P_1}\right)^{\frac{\gamma-1}{2\gamma}}\right]'' = 0.97062; \quad \left(\frac{u_2}{a_1}\right)'' = 0.2463$$

Hence the extrapolated value of M for γ=1.2958 is 0.2027

Mass flow out of cylinder (Δm_e) = $M a_1 \rho_1 A_2 \Delta t$

$$= 3.0953\ a_1\ \rho_1\ M_1\ \Delta a \times 10^{-6}$$

$$= 3.0953 \times 2004.1 \times 0.03445 \times 0.2027 \times 1.61 \times 10^{-6}$$

$$= 0.69501 \times 10^{-4} \text{ lb.}$$

Thus the mean mass in the cylinder $= \left(8.14409 - \frac{.69501}{2}\right) \times 10^{-4}$ lb.

$$= 7.79659 \times 10^{-4} \text{ lb.}$$

Hence, from equation (3.8-10):

$$\frac{\Delta P_1}{P_1} = -1.2958 \left(\frac{0.361}{39.063} + \frac{0.69501}{7.79659}\right)$$

$$= -1.2958 \times 0.09838$$

therefore, $\Delta P_1 = -23.323 \times 1.2958 \times 0.09838$

$$= -2.973 \text{ psi.}$$

Hence the new approximate mean values for the step are:

P_1 = 23.291 psia.

T_e = 993.6 °K

ρ_e = 0.034497 lb/ft^3

a_e = 2003.8 ft/sec.

Approximate state of region 15.13.

$$\left[\left(\frac{P_2}{P_o}\right)^{\frac{\gamma-1}{2\gamma}}\right]','' = \left[\left(\frac{P_2}{P_1}\right)^{\frac{\gamma-1}{2\gamma}}\left(\frac{P_1}{P_o}\right)^{\frac{\gamma-1}{2\gamma}}\right]',''$$

and

$$\left(\frac{u_2}{a_o}\right)','' = \left[\left(\frac{u_2}{a_1}\right)\left(\frac{a_1}{a_o}\right)\right]',''$$

Substituting in the above expressions gives:

$\bar{X}'$ = 0.98110 x 1.05788 = 1.03789

$\bar{X}''$ = 0.97062 x 1.07215 = 1.04065

$\bar{U}'$ = $0.2360 \times \frac{1894.6}{1910.2} \times 1.05788 = 0.2476$

$\bar{U}''$ = $0.2463 \times \frac{1841.7}{1910.2} \times 1.07215 = 0.2546$

Interpolating for the value of γ = 1.3046 for the pipe, gives the state of the region 15.13 as:-

$\bar{X}$ = 1.03802

$\bar{U}$ = 0.2479

Using these state parameters, the field boundaries to region 15.13 can be redrawn, using equation (3.5-5), if the 'guessed' boundary lines are found to be incorrect.

The approximate state point (15.13) is also plotted on the state diagram and the states (15.13)'," inferred, from which new ordinate intercepts are found.

The new mean crank angle for the step (if different from that already selected), is used with the new mean state parameters for the cylinder, and the calculation repeated until satisfactory convergence for the value ΔP_1 is obtained.

The correction of region 15.13 for the irreversibility occurring in the pipe flow is next applied. To apply this correction, the regions (14.13)'," are transferred to the boundary diagrams in a similar manner to that already described, and lines are drawn of slopes given by equation (3.8-23) to intersect the appropriate k line. These intersections give the new values for all the parameters.

The new values obtained from the boundary diagrams are now used to repeat the whole iteration procedure.

6.4. Solution of a region containing a temperature discontinuity.

Consider region I_{13} II_{13} (or 13.13), through which the major temperature discontinuity passes.

The adjacent regions on the temperature discontinuity and the rightward and leftward moving waves are 12.12',", 13. 12 and 12.13 respectively and the state parameters for these regions are known from previous calculations.

The state of region 13.13 is first determined assuming isentropic conditions to apply.

For the rightward moving wave I_{13},

a_{os} (for region 13.12) = 1909.90 ft./sec.

and the slope of the I_{13} characteristic $= \frac{2}{\gamma-1} \frac{a_{os}}{a_o}$

$$= \frac{2}{1.3046-1} \frac{1909.9}{1910.2}$$

$$= 6.5659$$

For the leftward moving wave II_{13},

a_{os} (for region 12.13) = 1723.98 ft./sec.

and the slope of the II_{13} characteristic $= \frac{2}{1.3211-1} \frac{1723.98}{1910.2}$

$$= 5.6214$$

Substituting these slopes, together with the appropriate state parameters for regions 13.12 and 12.13 in equation (3.5-16) gives:

$\bar{U} - 0.2527 = -6.5659\ (\bar{X} - 1.03849)$

$\bar{U} - 0.2076 = +5.6214\ (\bar{X} - 1.03844)$

Solving these equations for region 13.13 gives:

$\bar{U} = 0.2286$

$\bar{X} = 1.04217$

Hence, $u = 436.7$ ft./sec.

$P = 20.260$ psia.

$a' = 1990.8$ ft./sec.; $a'' = 1796.7$ ft./sec.

$T' = 964.7\ ^\circ K.$; $T'' = 786.0\ ^\circ K$

These results are used to draw in the approximate particle path, and the approximate field boundaries which complete the region 13.13, using equations (3.5-6) and (3.5-5) respectively.

The value of a_{os} and the state parameters $\bar{U}$ and $\bar{X}$ for region 13.13 are also determined using the above results to obtain the appropriate mean values for substitution in equations (3.4-7) and (3.5-15).

Determination of a'_{os}," for region 13.13',"

The particle on either side of the temperature discontinuity and arriving in region 13.13',", have come from region 12.12',". Hence, the initial values for a_{os} and T_{os} for the path line are those of region 12.12',".

For the particle path from 12.12' to 13.13', the initial $a_{os} = 1907.40$ ft./sec., the initial $T_{os} = 885.59\ ^\circ K$,

and the mean state parameters are:

$u = 419.4$ ft./sec.

$T = 959.6$ °K

$P = 19.940$ psia.

Also $\left(\frac{P_2}{P_o}\right)^{\frac{\gamma-1}{\gamma}} = 1.08199.$

Now $R_m = 124 \frac{a r \rho}{\mu} = 251.06 \frac{u P}{T \mu}$ and from Fig.30,

$\mu = 0.0402$ centipoises which on substitution gives

$R_m = 54{,}430$

and $\log_{10} R_m = 4.7358$

Hence, from Figs. 31 and 32 respectively,

$q = 87510$ ft.lb./ft.^{3}sec.

$f = 0.02128$

The Δt path, measured in the position diagram, is 1.89101×10^{-4} secs., and its substitution, together with the other variables in equation (3.4-7) gives:

$$\frac{2^a os}{1^a os} = 1 + \frac{1.3046}{2} (1.7402 - 23.6309)\, 1.89101 \times 10^{-4}$$

$$= 0.999377$$

Also, $\frac{2^T os}{1^T os} = 2 \frac{2^a os}{1^a os} - 1 = 0.998755$

Therefore, $2^a os = 1906.22$ ft./sec.

and $2^T os = 884.49$ °K.

Proceeding in a similar manner for the particle path from 12.12" to 13.13" gives:

$$2^{a}_{os} = 1723.81 \text{ ft./sec.}$$

$$2^{T}_{os} = 723.5 \text{ °K.}$$

Determination of $\bar{U}$ and $\bar{X}$ for region 13.13.

For the I_{13} wave, the mean a_{os} between regions 13.12 and 13.13' is 1908.21 ft./sec.

Thus the slope of the characteristic $= \frac{2}{\gamma-1} \frac{a_{os\ mean}}{a_o}$

$$= 6.5590$$

The mean state parameters are:-

$u = 459.7$ ft./sec.

$P = 20.027$ psia.

$a = 1987.3$ ft./sec.

$T = 961.3$ °K.

Hence, $\mu = 0.0402$

$R_m = 59{,}810$

$\log_{10} R_m = 4.7768$

giving $f = 0.0209$

$q = 88{,}660$ ft.lb./ft.^{3} sec.

The wave time Δt, measured in the position diagram is 1.54282×10^{-4} secs.

Substituting the above values in equation (3.5-15) gives:-

$$(\Delta \bar{U})_I = -6.5590\ (\Delta \bar{X})_I - (15.282 + 14.125) \frac{1.5428 \times 10^{-4}}{1910.2}$$

$$= -6.5590\ (\Delta \bar{X})_I - 23.75 \times 10^{-4}$$

Similarly, for the Π_{13} wave,

$$\frac{2}{\gamma-1}\ \frac{a_{\text{os mean}}}{a_o} = 5.6211$$

and $(\Delta \bar{U})_{\Pi} = + 5.6211\ (\Delta \bar{X})_{\Pi} - 6.16 \times 10^{-4}$

Substitution of the appropriate values for $\bar{U}$ and $\bar{X}$ for regions 13.12 and 12.13 in the above gives

$$\bar{U} - 0.2527 = -6.5590\ (\bar{X} - 1.03849) - 23.75 \times 10^{-4}$$

$$\bar{U} - 0.2076 = +5.6211\ (\bar{X} - 1.03844) - 6.16 \times 10^{-4}$$

Hence, solving for $\bar{X}$ and $\bar{U}$ gives:-

$$\bar{X} = 1.04203$$

$$\bar{U} = 0.2271$$

from which the following state parameters are obtained:-

P' = 20.378 psia.; P" = 20.097 psia.

P = 20.237 psia.

u = 433.8 ft./sec.

a' = 1986.3 ft./sec.; a" = 1796.3 ft./sec.

T' = 960.4 °K.; T" = 785.6 °K.

These results completely define the state of region 13.13',".

6.5. Inflow at the open end.

When inflow occurs at the open end of the exhaust pipe, the equations to be satisfied are:-

$$(\Delta \bar{U})_I = -\frac{2}{\gamma-1} \frac{a_{os2}}{a_o} (\Delta \bar{X})_I - (\Delta \bar{U}_{f+q})_I \qquad (3.5\text{-}15)$$

and

$$\frac{P_o}{P_2} = 1 + \frac{\gamma}{(\frac{a_o}{u_2})^2 - \frac{(\gamma-1)}{2}} \qquad (3.8\text{-}16)$$

Consider region 20.42 at the pipe open end.

From previous calculation, the state of 20.41, which is the preceeding region on the rightward moving wave I_{20}, is known. The change in a_{os2}, together with the correction term $(\Delta \bar{U}_{f+q})_I$, between regions 20.41 and 20.42 can be obtained in a similar manner to that outlined in Section 6.4.

Whence, the change of state between regions 20.41 and 20.42 is defined by:-

$$(\Delta \bar{U})_I = -\frac{2}{1.3487-1} \cdot \frac{1455.63}{1910.2} (\Delta \bar{X})_I - 0.00034$$

$$\text{i.e. } (\Delta \bar{U})_I = -4.3707 (\Delta \bar{X})_I - 0.00034$$

For a first approximation to the solution of this equation, the unknown pressure in the region of the open end (20.42) is assumed to be atmospheric. Hence, substituting $\bar{X}_{20.42} = 1$, and inserting the appropriate values for region 20.41, this equation becomes:-

$$\bar{U} - 0.0341 = -4.3707\,(1.000 - 0.9910) - 0.00034$$

i.e. $\bar{U} = -0.00558$

Inserting this value of $\bar{U}(= \frac{u_2}{a_o})$ in equation (3.8-16) gives:

$$\left(\frac{P_o}{P_2}\right)^{\frac{\gamma-1}{2\gamma}} = 1 + \frac{1.3487}{\left(\frac{1}{0.00558}\right)^2 - \frac{1.3487-1}{2}}^{\frac{0.3487}{2.6974}}$$

$$= 1.0000$$

In this case, no further calculation is necessary, and the final value of pressure and particle velocity for region 20.42 at the open end of the pipe is:

$P_2 = 14.322$ psia.

$u_2 = -10.66$ ft/sec.

When the value of $\left(\frac{P_o}{P_2}\right)^{\frac{\gamma-1}{2\gamma}}$ differs from the initial value assumed (i.e. atmospheric), then the final solution is obtained by an iteration process.

7. Discussion of Results

7.1. Air consumption trials.

The results of the air consumption trials carried out with varying lengths of exhaust pipe, are shown plotted in dimensionless form in Figs. 33 and 34.

The scavenging in a naturally aspirated engine is effected by utilization of the wave effects in the exhaust pipe, and thus the criterion for dynamical similarity, termed 'the natural pipe length', is $\frac{n\ L}{a}$, where n, L and a denote the engine speed, exhaust pipe length, and mean local acoustic velocity in the exhaust pipe, respectively. The scale for the abscissae in Figs.33 and 34 is actually $60(\frac{n\ L}{a})$ since rpm. was substituted for n when evaluating this group.

The ordinate axis represents the dimensionless group of $\frac{V\ air}{V\ cyl.}$, where V air is the volume of air aspirated per cycle at ambient conditions, and V cyl. is the effective cylinder volume at air port closure, i.e. 'trapped' volume.

Operating the engine at a constant air-fuel ratio implies that the temperature of the exhaust gases leaving the cylinder will be sensibly constant. Thus, for any given running condition, the volumetric efficiency will primarily be a function of engine speed. Hence, for stable breathing, i.e. speed stability, the curve relating dimensionless air flow and $\frac{n\ L}{a}$ requires to be

of negative slope. Ideally, therefore, the characteristic curve required to successfully operate a naturally aspirated two-stroke cycle engine, is one which has a constant negative slope for its operating speed range.

The plotted results of the air trials do, in general, lie on negative slope curves, although for some pipe lengths, running was achieved on the unstable portion of the curves. This can only be ascribed to small inflexions in the curves at these isolated running conditions.

The $\frac{n\ L}{a}$ group does not fully account for the effect of gas particle velocity on the time taken for a wave to travel from the engine ports to the pipe open end, and back again. The engine speed, n, is directly proportional to the mean propagation time for a wave, but the mean exhaust gas acoustic velocity is not.

The lower particle velocities associated with a smaller air mass flow causes an earlier return of the scavenging pulse, and to maintain a constant scavenging efficiency, i.e. the presentation of the same port configuration to the rarefaction pulse, requires a reduction in engine speed. Hence, for example, the peaks for the differing values of dimensionless air flow obtained with different pipe lengths should lie on a line of positive slope, and not in a vertical line. This slope of the peak values can be seen in Figs.33 and 34, the maxima around $\frac{n\ L}{a} = 5$ exhibiting this behaviour clearly.

The chain dotted line superimposed on Figs. 33 and 34 is the curve obtained from the previous simulated work. Above a value of $\frac{n\ L}{a} = 3.5$, which is the region of operation in which the scavenging is performed by the primary rarefaction pulse, the trend compares with the firing engine results, although the amplitudes of the latter vary considerably. The unique simulated result curve was, however, obtained by using a constant cylinder release pressure, a condition which is not constant in the operation of the firing engine.

The amplitude of the scavenge pulse is affected by the irreversibilities and the temperature discontinuities, and their combined effect will vary with different pipe lengths. For the same values of $\frac{n\ L}{a}$, therefore, the air mass flow, and thus the cylinder release pressure will vary and a unique line will not be obtainable.

For the curves in the region below a value of $\frac{n\ L}{a} = 3.5$, no marked general trend can be seen. This region of operation is that in which, during the time the exhaust ports are open, the pressure waves traverse the exhaust pipe several times, the scavenging being the result of the cumulative effect of the various wave trains. Thus no marked general trend can be expected with a firing engine when such a complex wave action is involved.

Induction pipes of the correct length to provide a ramming pulse just before the air ports close would

improve the air mass flow , and preliminary experimentation was carried out using a limited range of induction pipe lengths. Although dimensionless air flows greater than 100 were obtained, the air flow curves exhibited pronounced peaks similar to those for the engine without induction pipes. Hence, investigation of induction pipe ramming was suspended until work with the more stable exhaust pipe-diffuser configuration had been carried out.

7.2. Indicated trial.

The measured exhaust gas temperature in the exhaust pipe is shown plotted in Fig.37. A calculation based on the mass discharge per cycle and the mean temperatures for the appropriate sections of the exhaust pipe, indicates that two successive temperature discontinuities should exist at approximately 20 inches and 37 inches from the engine ports. The inflexion of the plotted curve at approximately 20 inches from the ports indicates that this discontinuity still exists, although very much attenuated by mixing and diffusion. The next, and successive discontinuities, however, are not at all apparent. This indicates that a temperature discontinuity has decayed considerably by the time one engine cycle is completed, and that after this time, no measurable temperature interface exists.

In the theoretical analysis,therefore, all reflections at the temperature discontinuity formed at the commencement of blowdown are fully considered for the first 55° of crank angle from exhaust port opening. After this time, the approximate procedure, as outlined later, is used.

Solution of the exhaust gas flow equations allowing for the measured temperature gradient, would involve assuming a small temperature interface to exist in each region used in the construction of the characteristic net along the first wave I_2, Fig.38. The resulting increase

in computation time would be prohibitive, see comments later regarding time for calculation. Hence to facilitate the pipe flow analysis, a coarse stepped temperature profile is assumed, the second and third steps approximately coinciding with the position of the decayed temperature discontinuities created by the two previous engine cycles. The first step, however, is inserted to divide the large temperature drop in this region into two smaller ones. Consideration of these temperature steps in the theoretical analysis can be regarded as summations of the changes occurring in the regions between them, and the result of this is to alter the timing of the effect of the temperature gradient on the diffusion waves promoted by friction and heat transfer effects back towards the ports.

The predominant effect of the main temperature discontinuity results in an increase of 0.538 psi. in the calculated value of the initial pressure pulse amplitude as compared with the isentropic analysis, whereas the subsequent temperature steps along the pipe only produce a pressure rise of approximately 0.09 psi. in the peak value. Thus the effects of mistiming are very small.

The temperature in the exhaust pipe in the region of the cylinder ports would be very severely effected, and the theoretical evaluation of the flow process very much complicated, if air was short circuited. This would

establish a 'plug' of cold air in the pipe just outside the ports and the effect of the large temperature discontinuity so formed would be considerable. It is considered unlikely that a uniflow engine running with a volumetric efficiency as low as 54% would experience any short circuiting of air. To confirm this, however, a plot of volumetric efficiency against torque was made for all the air consumption trials. Over 95% of the results, including that of the indicated trial, lay within a straight narrow band, and since a very wide range of operating conditions were covered, it was assumed that, in general, no short circuiting occurred. The few results which did not come within this linear band were displaced towards the volumetric efficiency axis, indicating that for these isolated cases short circuiting did occur.

The evaluation of the regions containing the temperature discontinuity was not performed using the theory as developed in Section 3.7(c), instead a modified calculation as shown in Section 6.3 was used. This simplified analysis results in a difference in pressure on either side of the discontinuity, and the mean of these two values is taken.

The simplified treatment, however, considerably reduces the time of calculation, and since it introduced a maximum artificial pressure difference of only $1\frac{1}{2}$ %

across the interface, which is within the measuring accuracy of the pressure transducers used, then its use was considered to be justified.

Calculation of the cylinder boundary regions were performed in the manner described in Section 3.8(d). When using the slope equation for the transferred characteristic allowing for irreversibility in the pipe, equation (3.8-23), however, the term involving $\Delta \bar{U}_{f+g}$ was found to be only of the order of 1% of the value of the other term, and hence it was neglected. Further, the 'shift' of the boundary state point obtained by applying this equation was very small, and application of the correction was discarded after blowdown was completed. These simplifications make for a considerable reduction in the calculation time at the cylinder boundary.

The interpolation of the cylinder boundary conditions from the γ=1.3 and γ=1.4 diagrams, and the adoption of the simplified analysis for the temperature discontinuities, gives results which compare extremely well with the indicated records for both the cylinder and exhaust pipe, see Figs. 39 and 40. These show that the amplitude and timing of the pressure and rarefaction waves given by the irreversible flow analysis are in good agreement with the recorded traces, whereas, the isentropic analysis is in error.

The major temperature discontinuity increases the

peak of the blowdown pressure pulse by 0.583 psi. as compared with the isentropic value. The overall decay of this pulse for the 50 inches of pipe from the major temperature discontinuity to the point at which it meets the returning rarefaction wave is 0.368 psi. The larger amplitude pressure pulse arising in the non-isentropic flow analysis, on arriving at the open end, will give a reflected rarefaction trough which is more intense. This is, however, attenuated by the irreversibilities and the main temperature discontinuity. The net effect is that the irreversible flow theoretical rarefaction wave amplitude is comparable with the isentropic flow value at the 41 inch indicating point in the exhaust pipe, but the attenuation at the main temperature discontinuity produces an amplitude comparable with that recorded at the 11 inch indicating point.

The steep rise in pressure following the rarefaction wave at the indicating point 11 inches from the ports, as given by the irreversible flow theoretical analysis, is exaggerated through not using the full reflection treatment for the temperature discontinuity in this region. From the position diagram, Fig.38, it can be seen that if all the reflections from the temperature discontinuity had been considered, then the time taken for the pressure to rise from the lowest value to the atmospheric value would be increased, with a consequent lessening of the rate

of pressure rise.

Poor correlation is obtained for the pressures occurring in the region of the pipe open end after the passage of the pressure pulse, see Fig.38. The pressure changes are very rapid and oscillatory in nature and hence reduction of the lozenge size in this region of the position diagram would improve the accuracy of the analysis. Also, the oscillatory nature of the pressure fluctuations combined with the effect of the passage length between the transducer diaphragm and the pipe will be to produce distortion of the recorded pressure trace, this combined with the lozenge size resulting in the poor correlation shown.

The volumetric efficiency, based on ambient conditions, gives a value of 60.8% for the isentropic analysis as compared with the measured value of 53.4%. The irreversible flow analysis was not completed, but at the end of the last cylinder step calculated, i.e. 30% after B.D.C. exhaust piston, the mass of air then present represents a volumetric efficiency of 57.5%. It is not possible to estimate the air content of the cylinder at the time of exhaust port closure, without completing the analysis, but in the period between this latter event and air port closure, some air is pushed out of the cylinder by the movement of the pistons. Hence the final theoretical result would almost certainly be less than 57.5% and

probably less than the measured value due to the early arrival of the positive pressure pulse following the rarefaction wave, see the theoretical and recorded pressure traces at 11 inches from the ports, Fig.38.

The maximum particle velocity in both the isentropic and irreversible flow analyses occurs at the pipe open end, the velocities being 1000 ft/sec. and 762 ft/sec. in the regions I_6 II_6 and I_{14} II_{36}, respectively, see Fig.36 and the table of results. For both analyses, the pressure associated with these regions is atmospheric, substantiating the communication[5] on the published simulated work that a velocity squared diagram could be of great assistance in interpreting pressure diagrams as pressure and particle velocity could not be correlated directly.

The computation time involved in performing the irreversible flow analysis is considerable, the time taken to produce Fig.38 and the associated table of results being approximately 1600 hours. The approximate average times to perform the different types of calculation involved were:- 1 hour for a region in the pipe; $1\frac{1}{2}$ to 2 hours for a region containing a temperature discontinuity; 4 hours for a cylinder boundary region. In comparison, the isentropic analysis for a comparable period of crank angle took approximately 200 hours.

The allowance for the variation of specific heats with temperature in the cylinder calculations increases

the step calculation time by approximately 20%. Allowance for the γ variation, however, is considered justified since the accuracy of the result will be improved, and its inclusion only increases the computation time by approximately 40 hours.

8. Conclusions

1. The good agreement obtained between the irreversible fluid flow analysis and the indicated records for both the cylinder and the exhaust pipe shows the physical premises of the theory to be correct and sufficient. The use of the quasi-steady flow approach, i.e. the use of steady flow data for pipe friction, heat transfer, inflow at the pipe open end and flow through the cylinder ports, is shown to be justified and permissible for application, instantaneously and locally, to the kind of wave motion under consideration.

2. Accurate results are obtainable by the Method of Characteristics using finite increments of from 1 to 4 degrees of crank angle depending upon the rate of change of pressure and/or velocity at the point under consideration. During the calculation procedure the choice of the most convenient approach rests with the calculator, and typical examples are given in the thesis for guidance.

3. In addition to giving good correlation of the form of the pressure changes occurring throughout the cylinder and exhaust pipe system, the full theory gives an assessment of the mass flow which is significantly more accurate than that given by the earlier and simpler isentropic flow theory. This confirms that an accurate result for the mass flow, in addition to particle velocity and pressure,

is obtained by use of the boundary chart interpolation technique developed in this thesis. The technique allows for the specific heat variation and the flow irreversibilities at the cylinder boundary.

4. Effecting the solution by using a position diagram instead of calculated and tabulated ordinates possesses the advantage that a clear picture is presented of the development of the main wave pattern, the origins of secondary waves and reflections, and the history of the motion of gas particles.

5. In a firing engine, the temperature discontinuities produced within the exhaust pipe are very pronounced and have a marked influence on the wave motion, and the variation of specific heats is significant. These effects are absent in a motored engine using simulated release conditions.

6. Earlier workers[5] have shown that, in a motored engine, the air consumption resulting from the wave action was uniquely related to the dimensionless group $\frac{nL}{a}$ which they termed "the natural pipe length". The present work, however, shows clearly that no such relationship exists when the engine is firing, and that the results of simulated work are of no real practical value.

7. Since the present work demonstrates that the exhaust pipe wave motion and mass flow can be predicted theoretically with considerable accuracy for a single cylinder firing

engine, future developments will probably be as follows:-

(a) Use of digital computors to remove the tedium and slowness of manual computation.

(b) Steady flow or single-pulse experiments on pipe enlargements, contractions, junctions, and other elements of practical exhaust systems. These would provide the data necessary for the construction of boundary charts for such elements and permit the extension of the present treatment to the case of the firing engine with more than one cylinder exhausting into a common manifold.

9. Appendices

9.1. Solution of three partial differential equations.

The fundamental equations defining the flow of a fluid in a pipe are those of mass continuity, momentum and energy. In order to obtain a general solution of these equations, it is convenient to consider three partial differential equations in purely mathematical terms which will be appropriate to any condition of flow.

Consider the following three general partial differential equations:

$$L_1 \equiv A_1\left(\frac{\partial v}{\partial x}\right) + B_1\left(\frac{\partial v}{\partial y}\right) + C_1\left(\frac{\partial w}{\partial x}\right) + D_1\left(\frac{\partial w}{\partial y}\right) + E_1\left(\frac{\partial z}{\partial x}\right) + F_1\left(\frac{\partial z}{\partial y}\right) + G_1 = 0$$

$$L_2 \equiv A_2\left(\frac{\partial v}{\partial x}\right) + B_2\left(\frac{\partial v}{\partial y}\right) + C_2\left(\frac{\partial w}{\partial x}\right) + D_2\left(\frac{\partial w}{\partial y}\right) + E_2\left(\frac{\partial z}{\partial x}\right) + F_2\left(\frac{\partial z}{\partial y}\right) + G_2 = 0$$

$$L_3 \equiv A_3\left(\frac{\partial v}{\partial x}\right) + B_3\left(\frac{\partial v}{\partial y}\right) + C_3\left(\frac{\partial w}{\partial x}\right) + D_3\left(\frac{\partial w}{\partial y}\right) + E_3\left(\frac{\partial z}{\partial x}\right) + F_3\left(\frac{\partial z}{\partial y}\right) + G_3 = 0 \qquad (9.1\text{-}1)$$

where the coefficients A_1, A_2, A_3, B_1, B_2, B_3, C_1, C_2, C_3, D_1, D_2, D_3, E_1, E_2, E_3, F_1, F_2, F_3, G_1, G_2, G_3, are functions of v, w, z, x and y, and v, w, and z are functions of the

variables x and y.

$$\text{i.e. } v = v(x,y)$$
$$w = w(x,y)$$
$$z = z(x,y)$$

The main obstacle to integration is that partial derivitives with respect to both x and y are present. To obviate this, consider any linear combination:

$$L = L_1 \lambda_1 + L_2 \lambda_2 + L_3 \lambda_3$$

where λ_1, λ_2 and λ_3 are functions of v, w, z, x and y.

$$\text{i.e. } L \equiv M \frac{\partial v}{\partial x} + N \frac{\partial v}{\partial y} + P \frac{\partial w}{\partial x} + Q \frac{\partial w}{\partial y} + R \frac{\partial z}{\partial x} + S \frac{\partial z}{\partial y} + T$$
$$= 0 \qquad (9.1\text{-}2)$$

where:

$$M = \lambda_1, A_1 + \lambda_2 A_2 + \lambda_3 A_3$$
$$N = \lambda_1, B_1 + \lambda_2 B_2 + \lambda_3 B_3$$
$$P = \lambda_1, C_1 + \lambda_2 C_2 + \lambda_3 C_3$$
$$Q = \lambda_1, D_1 + \lambda_2 D_2 + \lambda_3 D_3$$
$$R = \lambda_1, E_1 + \lambda_2 E_2 + \lambda_3 E_3$$
$$S = \lambda_1, F_1 + \lambda_2 F_2 + \lambda_3 F_3$$
$$T = \lambda_1, G_1 + \lambda_2 G_2 + \lambda_3 G_3$$

The aim now is to adjust the functions λ_1, λ_2, and λ_3, so that along some particular line in the x-y plane equation (9.1-2) becomes one relating only total differential coefficients dv, dw, dz, and dx.

In moving a short distance from (x,y) to $(x + dx, y + dy)$ along this line, let v become $v + dv$, w become $w + dw$, and z become $z + dz$.

$$\left.\begin{aligned} \text{Then: } dv &= dx\left(\frac{\partial w}{\partial x} + \frac{\partial v}{\partial y}\ \frac{dy}{dx}\right) \\ dw &= dx\left(\frac{\partial w}{\partial x} + \frac{\partial w}{\partial y}\ \frac{dy}{dx}\right) \\ dz &= dx\left(\frac{\partial z}{\partial x} + \frac{\partial z}{\partial y}\ \frac{dy}{dx}\right) \end{aligned}\right\} \qquad (9.1\text{-}3)$$

If λ_1, λ_2, and λ_3 can be so chosen that a line can be found along which:

$$\frac{dy}{dx} = \frac{N}{M} = \frac{Q}{P} = \frac{S}{R}$$

$$\text{i.e. } \left.\begin{aligned} \frac{dy}{dx} &= \frac{N}{M} = \frac{\lambda_1 B_1 + \lambda_2 B_2 + \lambda_3 B_3}{\lambda_1 A_1 + \lambda_2 A_2 + \lambda_3 A_3} \\ \frac{dy}{dx} &= \frac{Q}{P} = \frac{\lambda_1 D_1 + \lambda_2 D_2 + \lambda_3 D_3}{\lambda_1 C_1 + \lambda_2 C_2 + \lambda_3 D_3} \\ \frac{dy}{dx} &= \frac{S}{R} \quad \frac{\lambda_1 F_1 + \lambda_2 F_2 + \lambda_3 F_3}{\lambda_1 E_1 + \lambda_2 E_2 + \lambda_3 E_3} \end{aligned}\right\} (9.1\text{-}4)$$

then from equations (9.1-3) and (9.1-4)

$$\left.\begin{aligned} M\frac{\partial v}{\partial x} + N\frac{\partial v}{\partial y} &= M\frac{dv}{dx} \\ P\frac{\partial w}{\partial x} + Q\frac{\partial w}{\partial y} &= P\frac{dw}{dx} \\ R\frac{\partial z}{\partial x} + S\frac{\partial z}{\partial y} &= R\frac{dz}{dx} \end{aligned}\right\} \qquad (9.1\text{-}5)$$

Therefore, along such a line, if obtainable, equation (9.1-2) with equation (9.1-5) substituted gives:

$$Mdv + Pdw + Rdz + Tdx = 0 \qquad (9.1\text{-}6)$$

The functions M, P, R and T are algebraic functions comprising combinations of the given functions A_1, A_2, A_3, C_1, C_2, C_3, E_1, E_2, E_3, and G_1, G_2, G_3, respectively, with the unknown functions λ_1, λ_2, and λ_3.

Construction of the lines.

Writing $\frac{dy}{dx} = \emptyset$ for convenience, then from equation (9.1-4)

$$\emptyset = \frac{\lambda_1 B_1 + \lambda_2 B_2 + \lambda_3 B_3}{\lambda_1 A_1 + \lambda_2 A_2 + \lambda_3 A_3}$$

$$= \frac{\lambda_1 D_1 + \lambda_2 D_2 + \lambda_3 D_3}{\lambda_1 C_1 + \lambda_2 C_2 + \lambda_3 C_3}$$

$$= \frac{\lambda_1 F_1 + \lambda_2 F_2 + \lambda_3 F_3}{\lambda_1 E_1 + \lambda_2 E_2 + \lambda_3 E_3}$$

Therefore:

$$\left.\begin{aligned} \lambda_1 (A_1 \emptyset - B_1) + \lambda_2 (A_2 \emptyset - B_2) + \lambda_3 (A_3 \emptyset - B_3) &= 0 \\ \lambda_1 (C_1 \emptyset - D_1) + \lambda_2 (C_2 \emptyset - D_2) + \lambda_3 (C_3 \emptyset - D_3) &= 0 \\ \lambda_1 (E_1 \emptyset - F_1) + \lambda_2 (E_2 \emptyset - F_2) + \lambda_3 (E_3 \emptyset - F_3) &= 0 \end{aligned}\right\} \qquad (9.1\text{-}7)$$

or:

$$\begin{vmatrix} A_1 \phi - B_1 & A_2 \phi - B_2 & A_3 \phi - B_3 \\ C_1 \phi - D_1 & C_2 \phi - D_2 & C_3 \phi - D_3 \\ E_1 \phi - F_1 & E_2 \phi - F_2 & E_3 \phi - F_3 \end{vmatrix} = 0 \qquad (9.1\text{-}8)$$

The solution of the determinant (9.1-8) is of the form:-

$$(\phi + e)(a\phi^2 - 2b\phi + c) = 0 \qquad (9.1\text{-}9)$$

Thus the required line along which equation (9.1-6) holds has a slope $\frac{dy}{dx} = \phi$ which satisfies equation (9.1-9)

i.e. $$\frac{dy}{dx} = \phi_{I,\,II} = \frac{b \pm \sqrt{(b^2 - ac)}}{a} \qquad (9.1\text{-}10)$$

If equation (9.1-10) has two real roots, then the basic equations (9.1-1) are termed hyperbolic and characteristics can exist (see Classification of Differential Equations at the end of this section)

To eliminate the unknown functions λ_1, λ_2, and λ_3, from equation (9.1-6),

$$\text{write } \frac{\lambda_1}{\lambda_3} = m_1$$

$$\text{and } \frac{\lambda_2}{\lambda_3} = m_2$$

Then from equations (9.1-7)

$$\left.\begin{aligned} m_1 (A_1 \phi - B_1) + m_2 (A_2 \phi - B_2) + (A_3 \phi - B_3) = 0 \\ m_1 (C_1 \phi - D_1) + m_2 (C_2 \phi - D_2) + (C_3 \phi - D_3) = 0 \end{aligned}\right\} \quad (9.1\text{-}11)$$

Solving equations (9.1-11) for m_1 and m_2 gives:

$$m_1 = \frac{(A_2 \phi - B_2)(C_3 \phi - D_3) - (A_3 \phi - B_3)(C_2 \phi - D_2)}{(A_1 \phi - B_1)(C_2 \phi - D_2) - (A_2 \phi - B_2)(C_1 \phi - D_1)} \quad (9.1\text{-}12)$$

$$m_2 = \frac{(A_3 \phi - B_3)(C_1 \phi - D_1) - (A_1 \phi - B_1)(C_3 \phi - D_3)}{(A_1 \phi - B_1)(C_2 \phi - D_2) - (A_2 \phi - B_2)(C_1 \phi - D_1)} \quad (9.1\text{-}13)$$

Now $M = \lambda_1 A_1 + \lambda_2 A_2 + \lambda_3 A_3$

and substituting for λ_1 and λ_2 in terms of m_1, m_2, and λ_3 gives:

$$M = (m_1 A_1 + m_2 A_2 + A_3) \lambda_3$$

Similarly:

$$P = (m_1 C_1 + m_2 C_2 + C_3) \lambda_3$$

$$R = (m_1 E_1 + m_2 E_2 + E_3) \lambda_3$$

$$T = (m_1 G_1 + m_2 G_2 + G_3) \lambda_3$$

Hence, equation (9.1-6) becomes:

$$(m_1 A_1 + m_2 A_2 + A_3)\, dv + (m_1 C_1 + m_2 C_2 + C_3)\, dw$$

$$+ (m_1 E_1 + m_2 E_2 + E_3)\, dz + (m_1 G_1 + m_2 G_2 + G_3)\, dx = 0 \quad (9.1\text{-}14)$$

Thus the slope of the required line in the x-y plane is completely defined by equation (9.1-8) and along this line dv, dw, dz, and dx are related by equation (9.1-14) with the appropriate substitutions for m_1, m_2, and $\emptyset$ [equations (9.1-12), (9.1-13) and (9.1-10) respectively]

Classification of differential equations.

If $b^2 > a\,c$, equation (9.1-10) has two real roots and the basic equations (9.1-1) are of the hyperbolic type, i.e. two characteristic curves pass through every point of the physical plane.

If $b^2 = a\,c$, equation (9.1-10) has one real root and the equations (9.1-1) are termed parabolic and have no great practical significance.

If $b^2 < a\,c$, equation (9.1-10) has no real roots and the characteristic curves are imaginary. The basic equations (9.1.-1) are then known as elliptic.

Use of the Method of Characteristics requires the basic equations to be of the hyperbolic type, i.e. with two real roots. Then the general form of the resultant diagram is as shown in Fig.41.

The I characteristics are based on:

$$\emptyset_I = \frac{b + \sqrt{(b^2 - ac)}}{a}$$

each member of the family corresponding to a given value of the integration constant.

The II characteristics are based on:

$$\phi_{II} = \frac{b - \sqrt{(b^2 - ac)}}{a}$$

each member of the family corresponding to a given value of the integration constant.

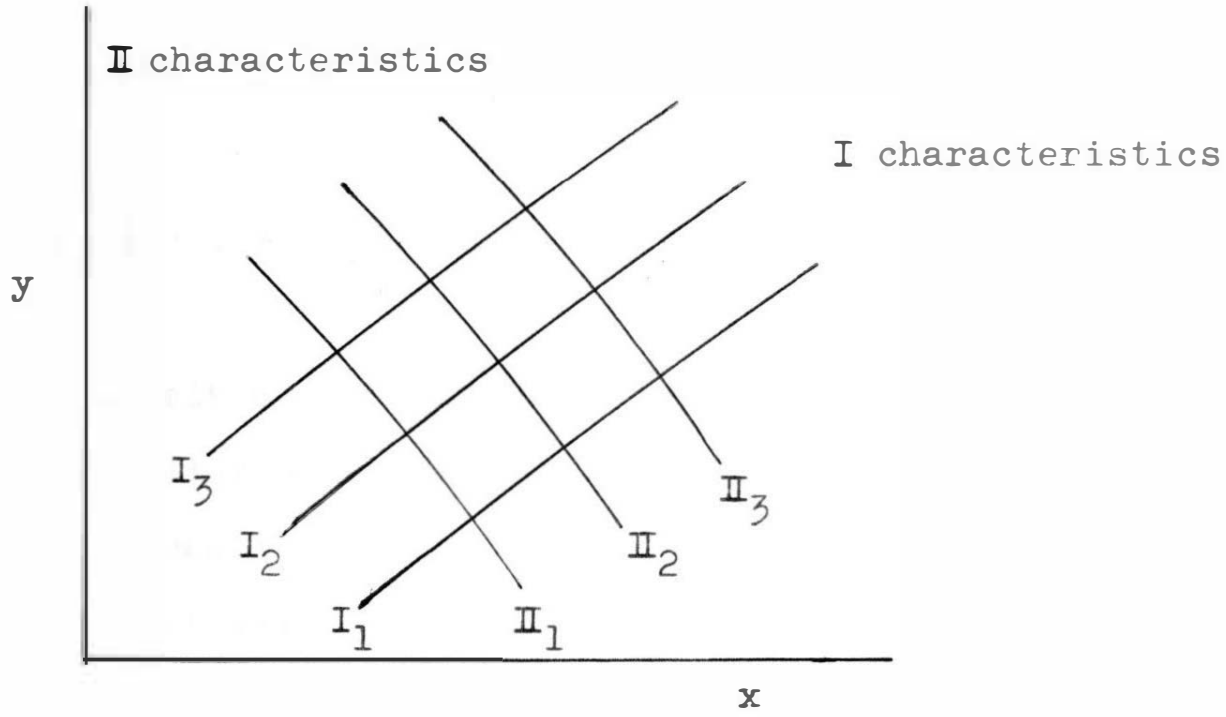

Fig.41

9.2 Solution of two partial differential equations.

When the flow of a fluid along a pipe is considered to be isentropic, the state parameters are completely defined by two partial differential equations (see Section 3.3)

The solution of two partial differential equations of the form:

$$\left.\begin{aligned} L_1 \equiv A_1\left(\frac{\partial v}{\partial x}\right) + B_1\left(\frac{\partial v}{\partial y}\right) + C_1\left(\frac{\partial w}{\partial x}\right) + D_1\left(\frac{\partial w}{\partial y}\right) + G_1 = 0 \\ L_2 \equiv A_2\left(\frac{\partial v}{\partial x}\right) + B_2\left(\frac{\partial v}{\partial y}\right) + C_2\left(\frac{\partial w}{\partial x}\right) + D_2\left(\frac{\partial w}{dy}\right) + G_2 = 0 \end{aligned}\right\} \qquad (9.2\text{-}1)$$

is completely analogous to the method given in Section 9.1. The full solution, therefore, will not be repeated, and only the result will be stated.

The partial differential equations (9.2-1) can be transformed into total differentials along two paths in the x-y plane, the slopes of which are given by:

$$\begin{vmatrix} A_1 \phi - B_1 & A_2 \phi - B_2 \\ C_1 \phi - D_1 & C_2 \phi - D_2 \end{vmatrix} = 0 \qquad (9.2.2)$$

where $\phi = \frac{dy}{dx}$

The relationship between dv, dw, and dx along these lines in the x-y field is given by:

$$(m_1 A_1 + A_2)dv + (m_1 C_1 + C_2)dw + (m_1 G_1 + G_2)dx = 0 \quad (9.2\text{-}3)$$

$$\text{where} \quad m_1 = \frac{B_2 - A_2 \phi}{A_1 \phi - B_1} \quad (9.2\text{-}4)$$

9.3. Application of the Method of Characteristics to isentropic flow.

The basic equations which define the flow parameters for isentropic flow in a pipe of constant cross-sectional area are those of mass continuity (3.3-1) and momentum (3.3-7) repeated below.

$$\rho \frac{\partial u}{\partial x} + u \frac{\partial \rho}{\partial x} + \frac{\partial \rho}{\partial t} = 0 \qquad (3.3\text{-}1)$$

$$\rho u \frac{\partial u}{\partial x} + \rho \frac{\partial u}{\partial t} + a^2 \frac{\partial \rho}{\partial x} = 0 \qquad (3.3\text{-}7)$$

The general solution of two partial differential equations of this form is given in Section 9.2, the equations therein being of the form:

$$\left.\begin{aligned} L_1 \equiv A_1\left(\frac{\partial v}{\partial x}\right) + B_1\left(\frac{\partial v}{\partial y}\right) + C_1\left(\frac{\partial w}{\partial x}\right) + D_1\left(\frac{\partial w}{\partial y}\right) + G_1 &= 0 \\ L_2 \equiv A_2\left(\frac{\partial v}{\partial x}\right) + B_2\left(\frac{\partial v}{\partial y}\right) + C_2\left(\frac{\partial w}{\partial x}\right) + D_2\left(\frac{\partial w}{\partial y}\right) + G_2 &= 0 \end{aligned}\right\} \qquad (9.3\text{-}1)$$

It is also established in Section 9.2 that the partial differential equations (9.3-1) can be transformed into total differentials along two paths, the slopes of which are given by:

$$\begin{vmatrix} A_1 \phi - B_1 & A_2 \phi - B_2 \\ C_1 \phi - D_1 & C_2 \phi - D_2 \end{vmatrix} = 0 \qquad (9.3\text{-}2)$$

where $\phi = \frac{dy}{dx}$

Comparison of equations (3.3-1) and (3.3-7) with equations (9.3-1) yields the following identities:

A_1	B_1	C_1	D_1	G_1
ρ	0	u	1	0

(9.3-3)

A_2	B_2	C_2	D_2	G_2
ρu	ρ	a^2	0	0

where $v \equiv u$; $w \equiv \rho$; $x \equiv x$; $y \equiv t$.

Substitution of these identities in (9.3-2) gives the result:

$$\begin{vmatrix} \rho\,\emptyset & \rho(u\,\emptyset - 1) \\ u\,\emptyset - 1 & a^2\,\emptyset \end{vmatrix} = 0$$

where $\emptyset = \frac{dt}{dx}$

Expansion of this determinant gives:

$$(a^2 - u^2)\,\emptyset^2 - 2u\,\emptyset - 1 = 0$$

which has the following roots:

$$\left(\frac{dx}{dt}\right)_{I\,II} = u \pm a \quad \text{(Mach lines)} \qquad (9.3\text{-}4)$$

Equation (9.3-4) signifies that disturbances are propagated either rightward or leftward with the local acoustic velocity relative to the fluid. Thus the absolute

propagation velocity of a disturbance is the algebraic sum of the local acoustic velocity and the particle velocity at the point under consideration.

The general solution obtained in Section 9.2 gives the differential equations of the Mach lines in terms of the state parameters on substitution of the identities given by (9.3-3)

From Section 9.2:

$$(m_1 A_1 + A_2)\, dv + (m_1 C_1 + C_2)\, dw + (m_1 G_1 + G_2)dx = 0 \quad (9.3\text{-}5)$$

$$\text{where } m_1 = \frac{B_2 - A_2 \emptyset}{A_1 \emptyset - B_1} \quad (9.3\text{-}6)$$

Substitution of the values for the coefficients given by (9.3-3) in equation (9.3-6) yields the result:

$$m_1 = \frac{1 - u \emptyset}{\emptyset}$$

and equation (9.3-5) becomes:

$$\left[(1 - u \emptyset)\, \rho + \rho u \emptyset \right] du + \left[(1 - u\emptyset)\, u + a^2 \emptyset \right] d\rho = 0$$

Substitution of $\emptyset = \frac{dt}{dx}$

$$= \frac{1}{u \pm a} \quad \text{from equation (9.3-4)}$$

then gives:

$$(u \pm a)\, du + (a \pm u)\, a\, d\rho = 0$$

which reduces to:

$$du = \mp \frac{a}{\rho}\, d\rho \quad (9.3\text{-}7)$$

Since isentropic conditions are assumed, then:

$$\rho = \rho_o \left(\frac{a}{a_o}\right)^{\frac{2}{\gamma-1}}$$

$$\text{and } d\rho = \rho_o \frac{2}{\gamma-1} \left(\frac{a}{a_o}\right)^{\frac{3-\gamma}{\gamma-1}} d\left(\frac{a}{a_o}\right)$$

and substituting for ρ and $d\rho$ in equation (9.3-7) gives the result:

$$d\left(\frac{u}{a_o}\right) = \mp \frac{2}{\gamma-1} d\left(\frac{a}{a_o}\right) \qquad (9.3\text{-}8)$$

Hence writing $\bar{U}$ for $\left(\frac{u}{a_o}\right)$ and $\bar{X}$ for $\left(\frac{P}{P_o}\right)^{\frac{\gamma-1}{2\gamma}} = \left(\frac{a}{a_o}\right)$

equation (9.3-8) becomes:

$$(d\,\bar{U})_{I,\,II} = \mp \frac{2}{\gamma-1} (d\,\bar{X})_{I,\,II} \qquad (9.3\text{-}9)$$

This equation completely defines the change in state along any characteristic in the x-t or physical plane.

Page 196 inserted after page 201

having slopes given by:

$$\left(\frac{d\bar{X}}{d\bar{U}}\right)_{I,\,II} = \mp \frac{\gamma-1}{2} \qquad (9.4\text{-}2)$$

Each characteristic line in the state diagram represents the change of state when following a particular wave point in the position diagram.

Thus the position diagram consists of lines which are the boundaries of regions within which the state of the fluid is represented by a point in the state diagram.

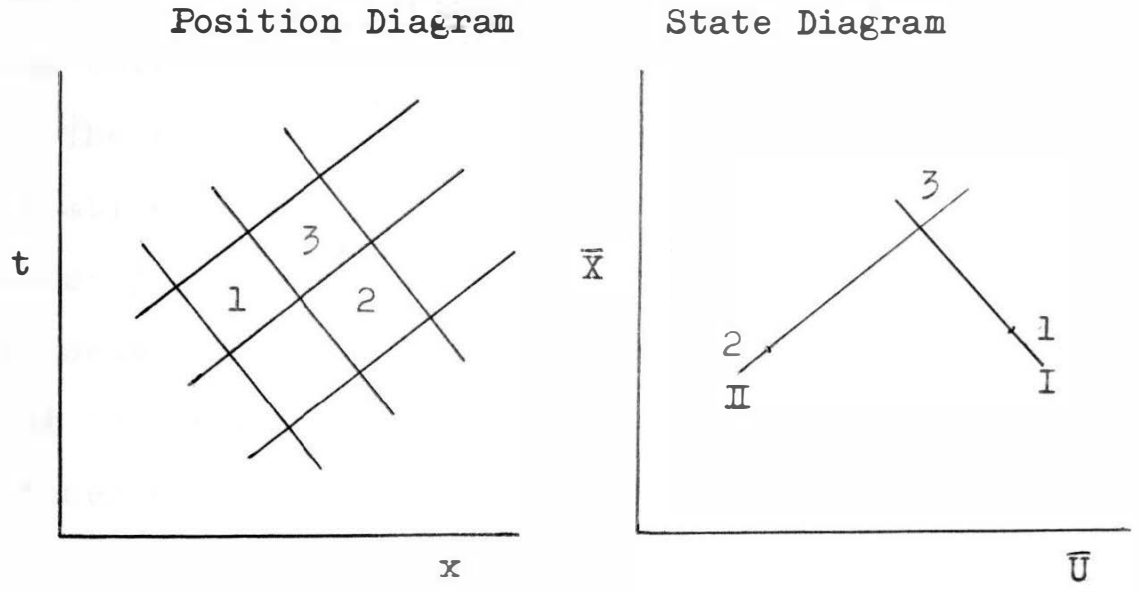

Fig. 42

Consider the position and state diagrams, Fig. 42, in which the regions 1 and 2 are known. The state in region 3 results from the superimposition of the rightward moving wave through 1 and the leftward moving wave through 2. The rightward moving wave from region 1 can only change its state along a line of

slope $-\frac{(\gamma-1)}{2}$ through point 1 in the state diagram. Similarly, the leftward moving wave from region 2 can only change its state along a line of slope $+\frac{(\gamma-1)}{2}$ through point 2 in the state diagram. Construction of these two characteristics in the state diagram results in their intersection at point 3, which completely defines the state in region 3 of the position diagram.

The wave path boundaries in the position diagram between regions 1 and 3, and regions 2 and 3 can now be constructed, their slopes being given by equation (9.4-1) in which the values used for u and a are the means between the respective states.

The position and state diagrams defining the initiation of the fundamental pulse in an engine exhaust pipe are shown in Fig. 43 . The state 1.1 represents the stagnation conditions in the pipe prior to discharge from the cylinder commencing and is taken as the origin of the state diagram. This implies the use of a_o, the datum condition, as that defined by the state of the gas in the exhaust pipe.

At the instant of port opening, an acoustic wave, o b, in the position diagram, is generated in the exhaust pipe, the slope of which is given by $\frac{dt}{dx} = \frac{1}{a_o}$.

The state of region 2.1 is obtained from a consideration of the boundary conditions at the engine ports. In the state diagram, 2.1 lies on a II

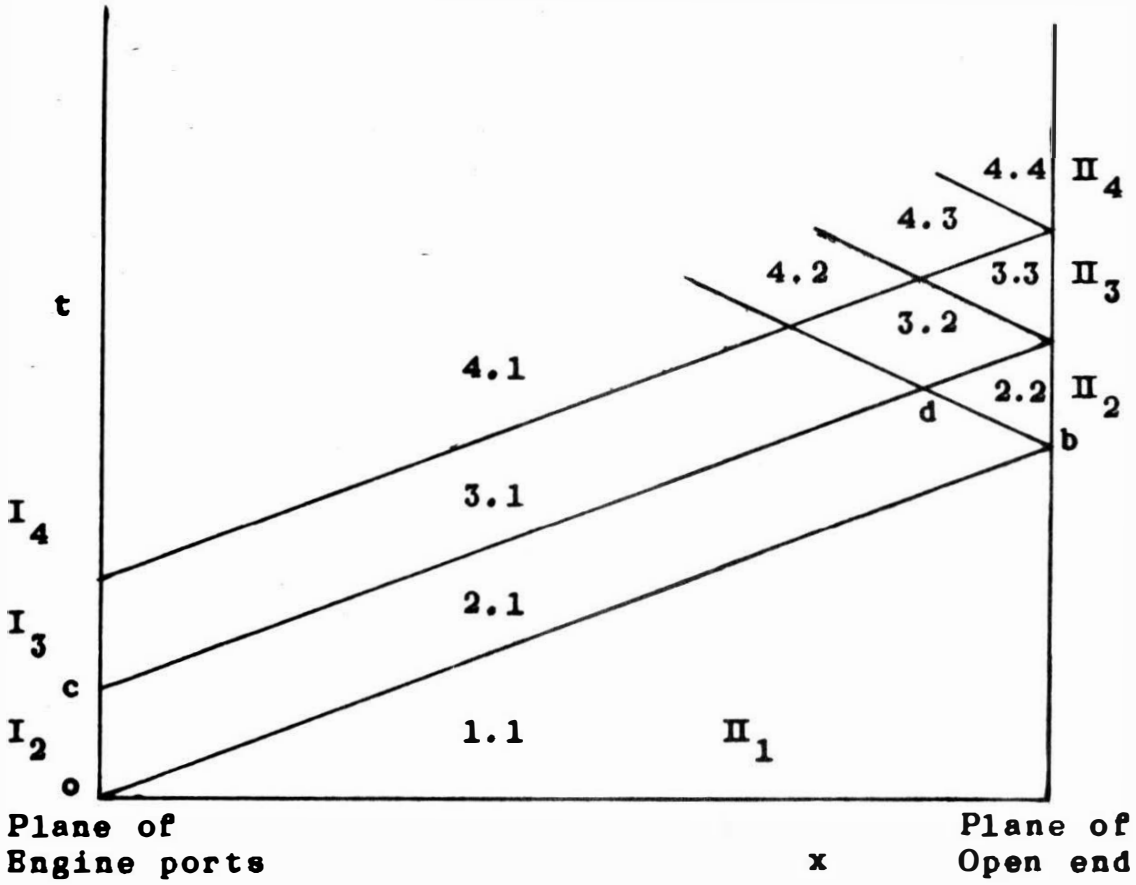

Position Diagram

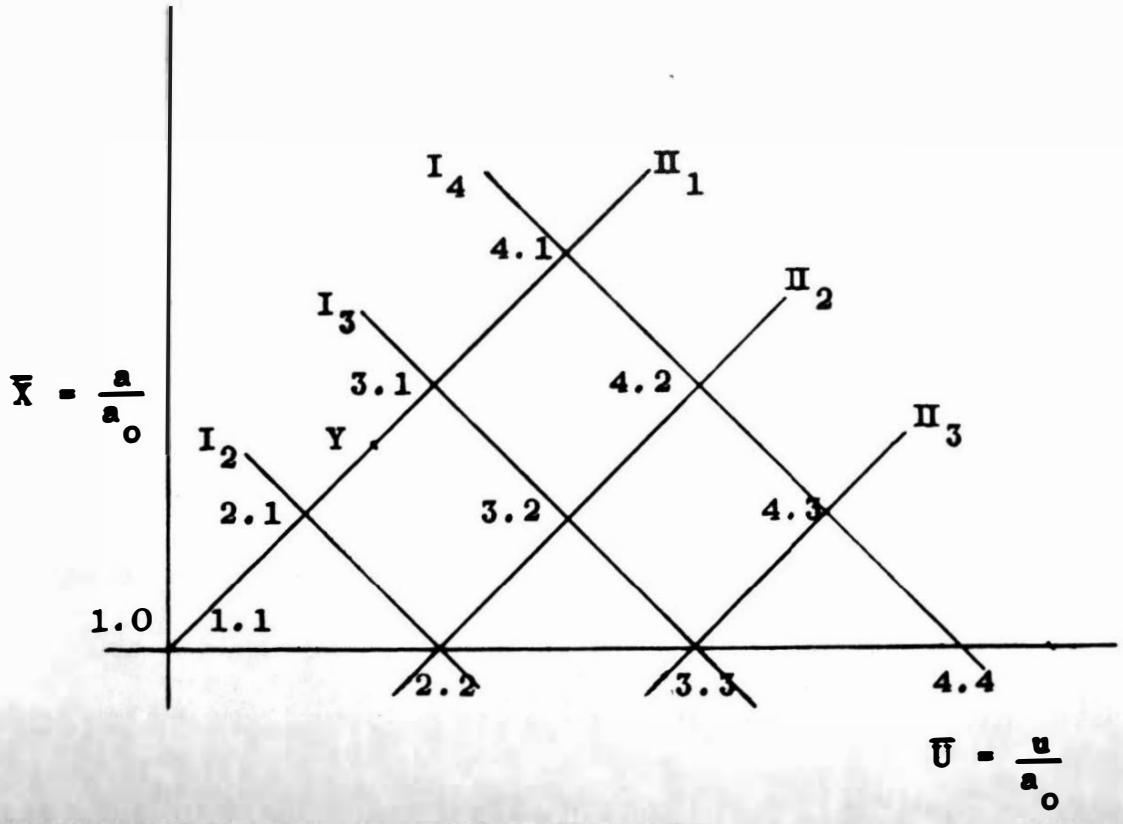

State Diagram

Fig.43.

characteristic of slope + $\frac{(\gamma-1)}{2}$ which passes through the origin $\frac{a}{a_o} = 1$. Similarly, state 3.1 can be obtained which again lies on the II_1 characteristic of slope + $\frac{(\gamma-1)}{2}$ through the origin 1.1.

The slope of the propagation path c d in the position diagram can now be obtained from equation (9.4-1) using the mean values for u and a between the states 2.1 and 3.1, as given by the point Y in the state diagram.

On reaching the open end of the pipe, the flow must satisfy the local boundary conditions, i.e. the pressure in region 2.2 is atmospheric, and therefore $\frac{a}{a_o} = 1$. The change of state between 2.1 and 2.2 is along a rightward path and can only take place along the I_2 characteristic of slope $-\frac{(\gamma-1)}{2}$ through 2.1. Therefore state 2.2 is located on the abscissa of the state diagram. The slope of the propagation path b d in the position diagram can now be obtained from equation (9.4-1), using the appropriate mean values between the states 2.1 and 2.2.

Proceeding in this manner, the complete network can be completed, and the next few steps in the analysis are shown in Fig. 43.

The value of a_o in the pipe is a constant for the isentropic analysis, hence axes of a as ordinate and u

as abscissa can be used for the state diagram. This is more convenient, since the mean values of a and u between two regions can be obtained directly from the state diagram.

9.4. Graphical Solution for Isentropic Flow Using the Method of Characteristics.

The nature of the characteristic equations (9.3-4) and (9.3-9) necessitates the use of a step-by-step integration in which the pressure profile is considered to be of a stepped form, the accuracy of the result depending upon the step duration. From a consideration of these equations, the solution for a pressure wave propagated in a pipe can be obtained by the simultaneous construction of two diagrams, a position diagram and a state diagram.

The position diagram has lines or characteristics of position which represent changes in position with time of the particular wave point considered. Using axes of time as ordinate and distance as abscissa, from equation (9.3-4), the slopes of the position lines are given by:

$$\left(\frac{dt}{dx}\right)_{I,\,II} = \frac{1}{u \pm a} \qquad (9.4\text{-}1)$$

Along any line of position, the change of state of the fluid is given by equation (9.3-9), i.e.:

$$(d\,\bar{U})_{I,\,II} = \mp \frac{2}{\gamma-1} (d\,\bar{X})_{I,\,II}$$

Hence, the state diagram with axes of $\bar{X}$ as ordinate and $\bar{U}$ as abscissa gives a network of characteristic lines

9.5. References.

1. KADENACY, M.E. (1936)
   Patent Specifications.
   Nos. 473684 and 473686.

2. DAVIES, S.J. (1940)
   An analysis of certain characteristics of the Kadenacy engine.
   Engineering. Vol. 149.

3. BANNISTER, F.K. and MUCKLOW, G.F. (1948)
   Wave action following sudden release of compressed gas from a cylinder.
   Proc.I.Mech.E. Vol.159, p.269.

4. WALLACE, F.J. and STUART MITCHELL, R.W. (1952)
   Wave action following sudden release of air through an engine port system.
   Proc.I.Mech.E. Vol.1B, No.8, p.343.

5. WALLACE, F.J. and NASSIF, M.H. (1954)
   Air flow in a naturally aspirated two-stroke engine.
   Proc.I.Mech.E. Vol.168, p.515.

6. JENNY, E. (1949)
   Berechnungen und modelversuche uber druckenwellen grosser amplituden in suspuff-leitengen.
   E.T.H.Z.(Zurich). Doctors Thesis.

7. KEENAN, J.H. and KAYE, J. (1948)
   Gas Tables.
   J. Wiley and Sons, Inc., N.Y.

8. McADAMS, W.H. (1942)
   Heat Transmission.
   McGraw Hill Book Co., N.Y.

9. BROWN, A.I. and MARCO, S.M. (1942)
   Introduction to Heat Transfer.
   McGraw-Hill Book Co., N.Y.

10. COLEBROOK, C. and WHITE, C.M. (1937)
    Experiments with fluid friction in Roughened Pipes.
    Proc.Roy.Soc.(A). Vol.161, p.367.

11. MOODY, L. (1947)
    An approximate formula for pipe friction factors.
    Mechanical Engineering. Vol.169, p.1005.

9.6. Bibliography

BINDER, R.C. (1943)
The Damping of Large Amplitude Vibrations of a Fluid in a Pipe.
Journ. of the Acoustical Society of America. vol. 15, page 41.

BELILOVE, S. (1943)
Improving Two-Stroke Cycle Engine Performance by Exhaust Pipe Tuning.
Diesel Power, vol. 21, page 608.

BODEN, R.H. and SCHEOTER, H. (1944)
Dynamics in the Inlet System of a Four-Stroke Engine.
NACA TN 935.

BANNISTER, F.K. and MUCKLOW, G.F. (1948)
Wave action following sudden release of compressed gas from a cylinder.
Proc.I.Mech.E. Vol. 159, p.269.

BENSON, R.S. (1955)
The effect of excess scavenge air on the pressure drop in the cylinder of a two-stroke cycle engine during exhaust blowdown.
J.Roy.Aero.Soc. Vol.59. p.773.

BENSON, R.S. (1957)
A method for calculating exhaust-port area for two-stroke cycle engines.
J.Roy.Aero.Soc. Vol.61. p.127.

BENSON, R.S. (1958)
The effect of variation in cylinder length on the exhaust port timing of a two-stroke cycle engine.
J.Roy.Aero.Soc. Vol.62. p.382.

BENSON, R.S. (1957)
The application of modern gas dynamic theories to exhaust systems of internal combustion engines.
Trans. Liverpool Engineering Soc. Vol.76. p.88.

BROWN, A.I. and MARCO, S.M. (1942)
Introduction to Heat Transfer.
McGraw-Hill Book Co., N.Y.

COURANT, R. and FRIEDRICHS, K. (1948)
Supersonic Flow and Shock Waves. New York.

CARRIERE, P. (1948)
The Method of Characteristics Applied to Problems of Internal Ballistics.
Proceedings 7th International Congress Applied Mechanics. London. vol.3. p.139.

CALLAGHAN, E.E. and BOWDEN, D.T. (1949)
Investigation of flow coefficient of circular, square and elliptical orifices at high pressure ratios.
N.A.C.A. Tech.Note. 1947.

COLEBROOK, C. and WHITE, C.M. (1937)
Experiments with fluid friction in Roughened Pipes.
Proc.Ray.Soc.(A), vol. 161.

DAWIDSON, I.M. (1949)
Some Properties of the Compression Shock as in Turbine and Compressor Blade Passages.
Proc.Inst.Mech.Eng. vol. 161, p.187.

DENNISON, E.S. (1933)
Inertia Supercharging of Engine Cylinders.
Trans. ASME, vol. 55, p.53.

DAVIES, S.J. (1940)
An analysis of certain characteristics of the Kadenacy Engine.
Engineering. vol. 149.

EARNSHAW. (1860)
On the mathematical theory of sound.
Trans. of the Royal Soc. of London. vol.150.

FARMER, H.O. (1938)
Exhaust Systems of Two-stroke Engines.
Proc.Inst.Mech.Eng. vol.138. p.367.

FERGUSSON, D.F. and LIGHTHILL, M.J. (1947)
The hodograph transformation in transonic flow.
Proc.Roy.Soc. vol.A192. p.135.

GUDERLEY, G. (1942)
Non-steady gas flows in thin tubes of variable cross-section.
NACA translation. Technical Memoranda.

GEYER, E.W. (1941)
Theory of Kadenacy system.
Engineering. vol.151. p.463.

HENDERSON, J.B. (1939)
Phenomena of the exhaust of Internal Combustion Engines.
Engineering. vol.148. p.378.

HALL, W.B. and ORME, E.M. (1955)
Flow of a compressible fluid through a sudden enlargement in a pipe.
Proc.I.Mech.E. vol.196, p.1007.

JENNY, E. (1949)
Berechnungen und modelversuche uber druckenwellen grosser amplituden in suspuff-leitengen.
E.T.H.Z. (Zurich). Doctor's Thesis.

JACKSON, P. (1956)
Recent developments in marine diesels (Doxford engine).
Trans.I.Mar.E. vol.68. p.373.

JENNY, E. (1950)
The utilization of exhaust-gas energy in the supercharging of the four-stroke diesel engine.
The Brown Boveri Review. vol.37. p.433.

KASTNER, L.J. (1940)
Exhaust pipe pressure waves.
Engineering. vol.150. p.301.

KAHANE, E. and LEES, L. (1948)
Unsteady one-dimensional flows with heat addition or entropy gradients.
Aeronautical Sciences. vol.15. p.665.

KESTIN, J. (1949)
Application of the Method of Characteristics to the transient flow of gases.
Proc.Inst.Mech.Eng. vol.161. p.250.

KADENACY, M.E. (1936)
Patent Specifications.
Nos. 473684 and 473686.

KEENAN, J.H. and KAYE, J. (1948)
Gas Tables.
J. Wiley and Sons, N.Y.

LEADBETTER, R.L. (1944)
Exhaust and intake systems for best performance and quiet operation.
Proc.Nat.Conf.Oil and Gas Power Dir.ASME, Tulsa.

LIGHTHILL, M.J. (1953)
The hodograph transformation.
Modern developments in fluid dynamics. High speed flow.
(Ed. L. Howarth) vol.1. p.222.
Oxford University Press.

MUCKLOW, G.F. (1940)
Exhaust pipe effects in a single-cylinder four-stroke engine.
Proc.Inst.Mech.Eng. vol.143. p.109.

MUCKLOW, G.F. (1943)
Exhaust pipe phenomena.
Motorship.

MEYER, R.E. (1948)
The Method of Characteristics for problems of compressible flow involving two independent variables.
Quarterly Mechanics, Applied Mathematics.
vol. 1. p.196-215.

McADAMS, W.H. (1942)
Heat transmission.
McGraw Hill Book Co. N.Y.

PETTER, B.W. (1944)
Induced Air Scavenge for two-stroke engines.
Engineer. vol.158. p.157.

KECKSTEIN. (1940)
Messungen u. Berechnungen des Liefergrades an einem Einzylinder-Viertaktmotor mit Aufladesaugrohr.
Diss.T.H. Graz.

RUDINGER, G. (1955)
On the reflection of shockwaves from an open end of a duct.
J.Appl.Phys. vol.26. p.981.

RUDINGER, G. (1957)
The reflection of pressure waves of finite amplitude from an open end of a duct.
J.Fluid Mech. vol.3. p.48.

SHEPHERD, F.H. (1932)
Correct Exhaust Piping Improves Engine Performance.
Power. vol.75. p.401.

SCHWEITZER, P.H. (1944)
Improving engine performance by exhaust pipe tuning.
Journal Am.Soc.Naval Engineers. vol.56. p.185.

STANITZ, J.D. (1951)
Analysis of the exhaust process in four-stroke reciprocating engines.
Trans.Amer.Soc.Mech.Engrs. p. 319-329.

SCHWEITZER, P.H. (1949)
Scavenging of two-stroke diesel engines.
Macmillan and Co.Ltd. London.

SCHWEITZER, P.H., OVERBEKE, C.W.Van., and MANSON, L. (1945)
The Kadenacy effect.
Engineering. vol.160. p.241.

SCHWEITZER, P.H., OVERBEKE, C.W.Van., and MANSON, L. (1946)
Taking the mystery out of the Kadenacy system of scavenging diesel engines.
Trans. A.S.M.E. Vol68. p.729.

SHAPIRO, A.H. (1954)
The dynamics and thermodynamics of compressible fluid flow.
The Ronald Press Co., New York.

STANTON, T.E. (1926)
On the flow of gases at high speeds.
Proc.Roy.Soc. vol.Alll. p.306.

TEMPLE, G. (1944)
The Method of Characteristics in supersonic flow.
Tech. Report of the Aeronautical Research Committee.

TSAI, D.H. (1952)
A study of the dynamics in the inlet system of a four-stroke, single cylinder engine with inlet pipes of different lengths and diameters.
Sc.D.Thesis, Course XVI, Massachusetts Inst. of Technology, Cambridge.

TSAI, D.H. (1956)
Effect of size on the inlet system dynamics in four-stroke, single cylinder engines.
Trans.ASME, p.197-210.

TSIEN, H.S. (1939)
Two-dimensional subsonic flow of compressible fluids.
J.Aero.Sci. vol.6. p.399.

VON KÁRMÁN, TH. (1941)
Compressibility effects in aerodynamics.
J.Aero.Sc. vol.8. p.337.

WHITEFIELD, K.C. (1933)
Improving diesel engine operation by the selection of proper exhaust pipe length.
Power. vol.77. p.695.

WARMING, T. (1946)
Polar diagram for tuning exhaust pipes.
ASME Trans. vol.68.

WALLACE, F.J. (1956)
Wave action in diffusers for exhaust pipe systems.
Proc.Inst.Mech.Eng. vol.170.

WEAVING, J.H. (1949)
Discharge of exhaust gases in two-stroke engines.
Proc.Inst.Mech.Eng. vol.161. p.98.

WALLACE, F.J. and STUART MITCHELL, R.W. (1952)
Wave action following sudden release of air through an engine port system.
Proc.Inst.Mech.Eng. vol.1.B. No.8. p.343.

WALLACE, F.J. and NASSIFF, M.H. (1954)
Air flow in a naturally aspirated two-stroke engine.
Proc.Inst.Mech.Eng. vol.168. p.515.

WOODS, W.A. (1957)
Pressure wave phenomena in the exhaust system of a supercharged two-stroke cycle engine model.
Ph.D. Thesis. University of Liverpool.